UNIVERSITY OF CALIFORNIA SAN DIEGO

Mechanisms in bacterial utilization of cellular debris in the ocean

A dissertation submitted in partial satisfaction of the requirements for the degree

Doctor of Philosophy

in

Marine Biology

by

Ryan Paul Guillemette

Committee in charge:

Professor Farooq Azam, Chair
Professor Lihini Aluwihare
Professor Douglas Bartlett
Professor Lin Chao
Professor John Mekalanos
Professor Forest Rohwer

2018

The Dissertation of Ryan Paul Guillemette is approved, and it is acceptable in quality and form for publication on microfilm and electronically:

_____

_____

_____

_____

_____

_____

Chair

University of California San Diego
2018

DEDICATION

To my parents, Roger & Jacqueline – Thank You

EPIGRAPH

"If I could do it all over again, […] I would be a microbial ecologist. I would […] travel in an imagined submarine through drops of water proportionately the size of lakes, and track predators and prey in order to discover new life ways and alien food webs"

-E.O. Wilson

TABLE OF CONTENTS

LIST OF SUPPLEMENTARY FILES

Supplementary Table 2.1: Data for all molecular formulas identified by FT-ICR-MS analysis

LIST OF FIGURES

LIST OF TABLES

ACKNOWLEDGMENTS

I express sincere gratitude to my committee chair, Dr. Farooq Azam, for his sustained guidance over the past six years. His ‘open door policy’ encouraged regular science discussions that undeniably changed my perception of aquatic systems and the microbes that reside within them. Thank you for accepting my desire to collaborate with a number of scientists from a broad range of disciplines and for supporting my travel so that I could interact with them. I aspire to share your degree of accessibility and open-mindedness with my own future students and colleagues. I extend this appreciation to my committee members: Drs. Lihini Aluwihare, Douglas Bartlett, Lin Chao, John Mekalanos, and Forest Rohwer. I thank them for listening to my frequent questions and for their patience in helping me understand the answers. I also thank my past mentors, Drs. Andrei Alyokhin and Jose Pruneda-Paz, for their encouragement.

To my collaborators: B. Koch, J. Blanton, T. Samo, X. Mayali, P. Weber, M. Medina, K. Hamasaki, R. Kaneko, and B. Ushijima—thanks for the opportunity to work and learn together. I’m also grateful to the talented undergraduate students that I mentored: J. Tan, M. Jalan, and N. Lee. I wish you all a successful future. I’ll give a shout–out here as well to the instructors and participants of the 2017 Advanced Bacterial Genetics course at Cold Spring Harbor Laboratory.

My lab and cohort mates have been invaluable to my happiness at SIO. Jessica Blanton is the first friend that I made at Scripps and has been there for me through many of the fun and challenging times, thank you. Nirav, Logan, & Marco—thanks for the comradery. Mike and Dan, it’s been all laughs and good memories. Julie and Yosuke, thanks for the fellowship. Ty, Byron, Ryan P., & Francesca welcomed me to the lab and taught me the ropes. Francesca in particular took me under her wing and helped me through the first year, thank you.

Katie, Tim, & Gabriel–thanks for all of the fun and laughs. To Julie Chippendale and her late husband, Tom, I sincerely appreciate the kindness and support that you provided me with when I moved to San Diego. I thank my Mom & Dad, Kristyn, Katelynn, Ethan, and Fish for visiting and being available to talk. It hasn't been easy being 3,000 miles away. And finally, for her love, wisdom, and support, I thank my best friend, Aisha.

Chapter 2, in full, is a reprint of the material. Guillemette, R., Kaneko, R., Blanton, J., Tan, J., Witt, M., Hamilton, S., Allen, E.E., Medina, M., Hamasaki, K., Koch, B.P., Azam, F. 2018. Bacterioplankton drawdown of coral-mass spawn organic matter off Bocas del Toro, Panama. The ISME Journal: 12; 2238-2251. The dissertation author was the primary investigator and author of this material.

Chapter 3, in full, has been submitted for publication of the material. Guillemette, R., Ty J. Samo, Xavier Mayali, Peter K. Weber, John J. Mekalanos, and Farooq Azam. The bacterial Type Six Secretion System enables intraguild predation. The dissertation author was the primary investigator and author of this material.

Chapter 4, in full, has been submitted for publication of the material. Guillemette, R., Ushijima B., Jalan M., Hase C., and Farooq Azam. Insight into the resilience and susceptibility of marine bacteria to T6SS attack by *Vibrio cholerae* and *Vibrio coralliilyticus*. The dissertation author was the primary investigator and author of this material.

VITA

2004	High School Diploma. Sanford High School, Sanford, Maine
2008 – 2009	Bingham Undergraduate Research Fellow, Climate Change Institute, University of Maine, Orono
	Margaret Chase Smith Public Affairs Scholar, Margaret Chase Smith Policy Center, University of Maine, Orono
2009	Bachelor of Science in Biology & Ecology, University of Maine, Orono
2010	Research Associate, Maine Institute for Human Genetics & Health, The Jackson Laboratory, Bar Harbor, Maine
2011	Research Associate, Division of Biological Sciences, University of California San Diego
2017	Advanced Bacterial Genetics course participant, Cold Spring Harbor Laboratory, Cold Spring Harbor, New York
2018	Doctor of Philosophy in Marine Biology, Scripps Institution of Oceanography, University of California San Diego

PUBLICATIONS

Guillemette, R., Kaneko, R., Blanton, J., Tan, J., Witt, M., Hamilton, S., Allen, E.E., Medina, M., Hamasaki, K., Koch, B.P., Azam, F. 2018. Bacterioplankton drawdown of coral-mass spawn organic matter off Bocas del Toro, Panama. The ISME Journal: (12): 2238-2251

Nakajima, R., Tanaka, Y., Guillemette, R., Kurihara, H. 2017. Effects of coral-derived organic matter on the growth of bacterioplankton and heterotrophic nanoflagellates. Coral Reefs: DOI:10.1007/s00338-017-1608-3

Mitulla, M., Dinasquet, D., Guillemette, R., Simon, M., Azam, F., Wietz, M. 2016. Response of bacterial communities from California coastal waters to alginate particles and an alginolytic *Alteromonas macleodii* strain. Environmental Microbiology: (18): 4369 - 4377

Gong, M., Ma, J., Guillemette, R., Zhou, M., Yang., Y, Yang, Y., Hock, J.M., Yu, X. 2013. miR-335 inhibits small cell lung cancer bone metaseses via IGF-1R and RANKL pathways. Molecular Cancer Research: (13): 01-36

Alyokhin, A., R. Guillemette, and R. Choban. 2009. Stimulatory and Suppressive Effects of Novaluron on the Colorado Potato Beetle Reproduction. Journal of Economic Entomology: (6): 2078-2083

SUBMITTED

Guillemette, R., Ty J. Samo, Xavier Mayali, Peter K. Weber, John J. Mekalanos, and Farooq Azam. The bacterial Type Six Secretion System enables intraguild predation.

Guillemette R., B. Ushijima, M. Jalan, C. Häse, and F. Azam. Insight into the resilience and susceptibility of marine bacteria to T6SS attack by *Vibrio cholerae* and *Vibrio coralliilyticus*.

ABSTRACT OF THE DISSERTATION

Mechanisms in bacterial utilization of cellular debris in the ocean

by

Ryan Paul Guillemette

Doctor of Philosophy in Marine Biology

University of California San Diego, 2018

Professor Farooq Azam, Chair

This dissertation investigates the mechanisms in bacterial utilization of cells and cellular debris in the ocean. Bacteria are key members of marine ecosystems. They serve as the predominant biotic force acting on marine biogeochemical cycling of organic matter and exert a strong influence on marine microbial community dynamics via their cell-cell interactions. While scientists have begun to untangle the web of seemingly intractable mechanisms that marine bacteria use to acquire and consume organic matter, many unknowns still remain.

This research implements a number of techniques including bacterial production measurement, mass spectrometry, single-cell analyses, and genetics to test two hypotheses: (1) that bacteria can readily respond to a natural pulse of cellular debris from coral mass-spawning, and (2) that contact-dependent predatory bacteria can kill and consume their bacterial prey.

Studies conducted off coastal Panama found that coral gametes elevated the organic matter concentration of the surrounding seawater by ~5-fold after a mass spawning event. Bacterial production measurements and 454 pyrosequencing of bromodeoxyuridine-labeled 16S bacterial rRNA genes showed that it was primarily active Rhodobacteraceae, Flavobacteriaceae, and Saprospiraceae taxa that degraded the coral gametes. High resolution mass spectrometry analysis supported this hypothesis, showing trends that indicated microbial alteration of the organic matter pool. This study demonstrated that coastal marine bacteria can readily respond to a large input of autochthonous cellular debris.

Contact-dependent bacterial predation was tested by using bacteria with a type 6 secretion system ($T6SS^+$) as model predators in competition assays. Nanoscale secondary ion mass spectrometry analysis showed that $T6SS^+$ *Vibrio cholerae* utilized carbon from its bacterial prey. *V. cholerae* also exhibited the ability to utilize DNA and ribosomes from lysed bacteria as nutrients. Additionally, independent competition assays between $T6SS^+$ *V. cholerae* and 15 different marine bacterial isolates showed that *V. cholerae* and/or the challenged isolate were killed in 12 out of the 15 assays. The experiments also revealed that the coral and shellfish pathogen, *Vibrio coralliilyticus*, has a functional T6SS. Collectively, these results demonstrate that bacterial antagonism often ends in carnage for one or both of the competing species, and suggest that the susceptible prey are fresh fodder for the victorious bacterium.

CHAPTER 1

Introduction

INTRODUCTION

Consider that the average milliliter of seawater contains approximately 10^7 viruses, 10^6 bacteria, 10^4 phytoplankton, 10^8 colloids and particles, and an astounding $10^{12\text{-}15}$ *different* dissolved organic molecules (as reviewed in Azam and Malfatti 2007)[1]. These constituents of seawater—especially the microbes—intimately interact with each other and the environment to shape the marine ecosystems that we so cherish and rely upon (Figure 1)[1]. Bacteria in particular are major players in the ocean, as they are believed to consume up to 50% of marine primary production[2]. Marine bacteria are also of importance due to their prevalence as pathogens. However, the mechanisms that bacteria implement to survive in the ocean are not fully understood. In this dissertation, I primarily aim to understand the mechanisms in bacterial response to—and creation of—energy rich pulses of organic matter. I also explore the role of contact-dependent bacterial predation on marine bacteria and discuss the relevance of these findings to marine ecology.

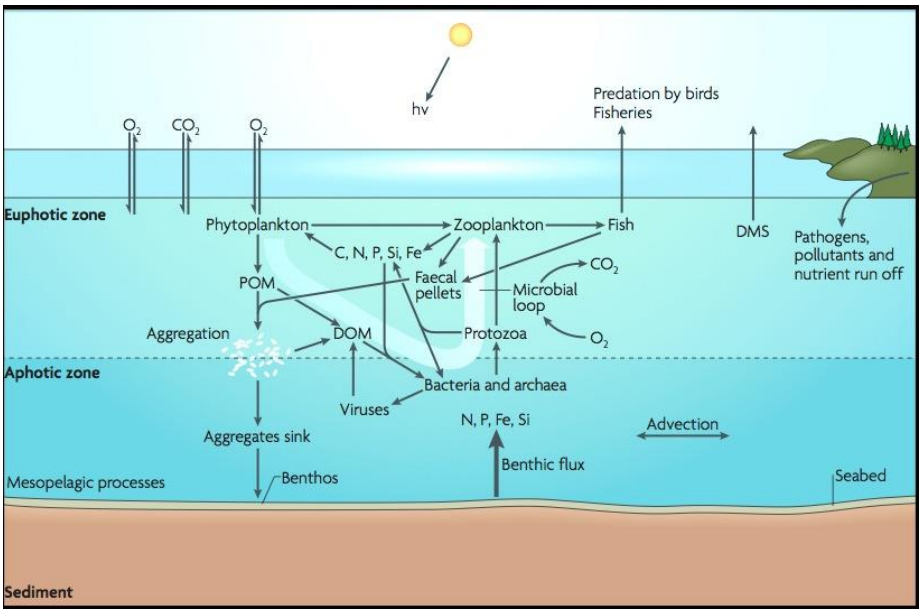

Figure 1.1 Microbial structuring of marine ecosystems. (Azam & Malfatti, 2007)[1]

Marine organic matter

Marine organic matter is generally categorized into two operationally defined fractions based on 0.7 µm-nominal-pore-size filtration: > 0.7µm, particulate organic matter (POM) and < 0.7 µm, dissolved organic matter (DOM). This organic matter is perhaps better conceptualized as a continuum of biologically labile, semi-labile, and refractory material that is comprised of truly dissolved molecules, colloids, gels, large particles and aggregates, and cells (Figure 2)[3]. Importantly, the age of marine organic matter also varies extensively, ranging from newly produced (~10% of the pool) to 100s or even 1000s of years old (~90% of the pool), with the latter fraction being predominantly refractory to bacteria[4, 5]. In trying to better understand bacterial utilization of organic matter in the ocean, it is imperative to study how bacteria degrade and consume newly derived, nascent organic matter.

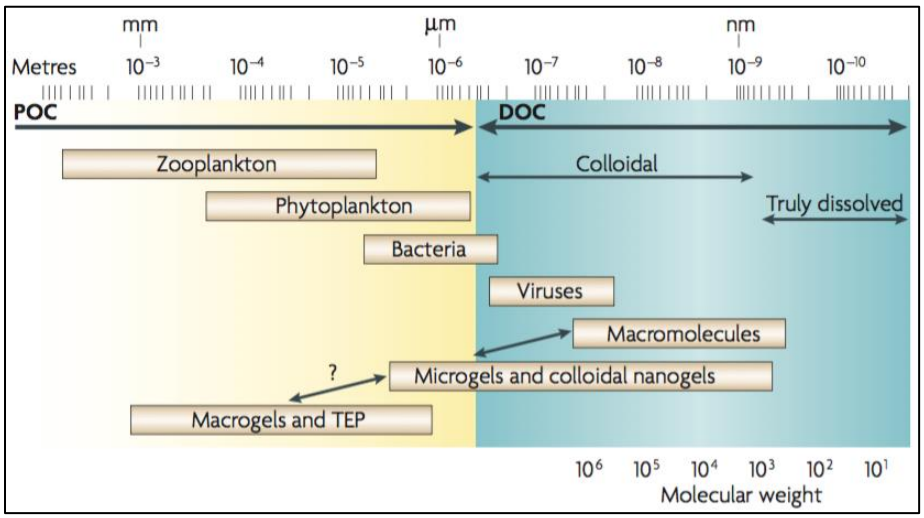

Figure 1.2 Conceptual diagram of marine organic matter continuum (Verdugo et al., 2004)[3]

Bacterial response to pulses of organic matter

The estimated ~10^{29} phylogenetically and metabolically diverse heterotrophic bacteria that reside in the sea[6, 7] rely upon a broad suite of hydrolytic enzymes[8], membrane transporters[9], and other mechanisms such as the recently discovered DNA-harnessing pili[10] to utilize the dynamic constituents of the marine organic matter pool. Bacterial response to the varying classes organic matter largely influence the alteration and removal of this material[11-13] and plays a role in the shaping of marine microbial community structure[14, 15]. However, the majority of studies on the nature and mechanisms of such organic matter utilization have largely taken place in the form of controlled laboratory amendment experiments, with few studies investigating the bacterial response to natural resource pulses in environment (see review in Pedler 2014)[16]. How bacteria respond to an input of natural organic matter, as well as the possible fates of such inputs, remains to be better understood.

Bacterial utilization of nutrient rich "hotspots"

In addition to understanding bacterial response to organic matter at the macro-scale, it has been postulated that bacterial interaction with nutrients at the nano- to micro-scale plays a large role in marine biogeochemical cycling and the structuring of microbial communities[17]. For example, such "hotspots" of organic matter can be created via lysis of single-cell organisms during a phytoplankton bloom crash, "sloppy feeding" by grazers, host-cell viral lysis, and bacterial-lysis of prey bacteria (as reviewed in Azam 1998)[18]. However, there have been relatively few studies on the specific fractions of cell lysate that bacteria can utilize[19, 20], and *in situ* mechanistic studies are rare. One mechanism that is ripe for testing bacterial utilization of organic matter hotspots is the highly prevalent bacterial type 6 secretion system (T6SS)[21]. The

T6SS is a nanomachine that is capable of injecting toxic effector proteins into adjacent bacterial target cells via a needle-like apparatus (Figure 3; as reviewed in Ho et al. 2014)[22]. The effector

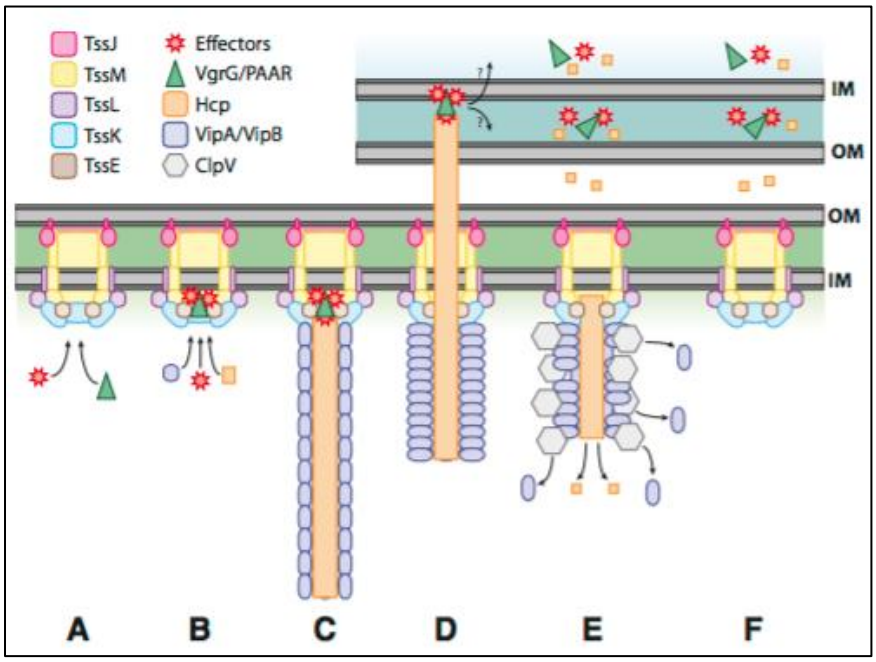

Figure 1.3 Model for T6SS assembly, effector translocation, and component recycling. (A) formation of a membrane baseplate; (B) recruitment and assembly of effector proteins; (C) polymerization of a Hcp tube with VipA/VipB sheath proteins; (D) sheath contraction and launch of the Hcp tube from the host inner membrane which delivers the effector proteins into the target cell's membrane; (E) disassembly of the sheath and tube; (F) recycling or disassembly of the baseplate complex (reproduced from Ho et al., 2014; with modified legend summary)[22].

proteins have a variety of lethal functions[23] which can lead to the lysis of susceptible prey[24]. T6SS-enabled bacterivorous bacteria may (1) gain an advantage in the form of nutrients from lysed bacterial prey, in addition to (2) eliminating bacterial competitors—both scenarios have been relatively unexplored for marine bacteria.

In this work, I aim to better understand the mechanisms in bacterial utilization of cells and cellular debris in the ocean. Chapter 2 takes advantage of a field sampling opportunity during a highly predictable coral mass-spawning event to determine the bacterial response to a pulse of nascent organic matter entering the coastal marine environment. Using a series of microcosm studies, I quantify the degradation rate of the coral gametes and ascribe the transformation and removal of the gametes' POM to active bacterial taxa. In Chapter 3, I transition into controlled laboratory experiments that focus on bacterial use of prey bacteria as nutrients. Lysate amendments to artificial seawater cultures of bacteria demonstrate that bacterial cellular debris, including the DNA and ribosome fractions are readily consumed by bacteria. Furthermore, nanoscale secondary ion mass spectrometry (NanoSIMS) analysis is used to show that the bacterial T6SS is an effective method for generating utilizable cellular debris from lysed bacterial prey *in situ*. In Chapter 4, I investigate the killing efficacy of *Vibrio cholerae's* T6SS and highlight the resistance and susceptibility of marine bacterial isolates to *V. cholerae* T6SS attack. In this chapter, I also provide the first report of a functional T6SS in *Vibrio coralliilyticus* which is shown to kill *V. cholerae*.

References

[1]Azam, F. & Malfatti F. Microbial structuring of marine ecosystems. Nature Reviews Microbiology. 2007;5:782-91.

[2]Fuhrman, J. & Azam F. Thymidine incorporation as a measure of heterotrophic bacterioplankton production in marine surface waters: evaluation and field results. Marine biology. 1982;66:109-120.

[3]Verdugo, P., Alldredge A. L., Azam F., Kirchman D. L., Passow U. & Santschi P. H. The oceanic gel phase: a bridge in the DOM–POM continuum. Marine Chemistry. 2004;92:67-85.

[4]Williams & Druffel. Radiocarbon in dissolved organic matter in the central North Pacific Ocean. Nature. 1987;330:246 - 248.

[5]Bauer, Williams & Druffel. 14C activity of dissolved organic carbon fractions in the north-central Pacific and Sargasso Sea. Nature 1992;357:667 - 670.

[6]Whitman, W., Coleman D. & Wiebe W. Prokaryotes: the unseen majority Proceedings of the National Academy of Sciences. U. S. A. 1998;95:6578–6583.

[7]Sogin, M., Morrison H., Huber J., Welch D., Huse S., Neal P., Arrieta J. & Herndl G. Microbial diversity in the deep sea and the underexplored 'rare biosphere' Proceedings of the National Academy of Sciences of the United States of America. 2006;103:12115–12120.

[8]Martinez, J., Steward G. & Azam F. Variability in ectohydrolytic enzyme activities of pelagic marine bacteria and its significance for substrate processing in the sea. Aquatic Microbial Ecology. 1996;10:223-230.

[9]Poretsky, R., Sun S., Mou X. & Moran M. Transporter genes expressed by coastal bacterioplankton in response to dissolved organic carbon. Environmental Microbiology. 2010.;12:616-627.

[10]Ellison, C. K., Dalia T. N., Ceballos A. V., Wang J. C.-Y., Biais N., Brun Y. V. & Dalia A. B. Retraction of DNA-bound type IV competence pili initiates DNA uptake during natural transformation in Vibrio cholerae. Nat Microbiol. 2018;3:773-780.

[11]Pedler, B. E., Aluwihare L. I. & Azam F. Single bacterial strain capable of significant contribution to carbon cycling in the surface ocean. Proceedings of the Academy of Natural Sciences. 2014;111:7202–7207.

[12]Azam, F. & E. H. R. Size distribution and activity of marine microheterotrophs. Limnology and Oceanography. 1977;22:492-501.

[13]Ammerman, J. W., A. F. J., Å. H. M. & F. A. Bacterioplankton growth in seawater: 1. Growth kinetics and cellular characteristics in seawater cultures. Marine Ecology Progress Series. 1984;18:31-39.

[14]Pinhassi, J., Azam F., Hemphala J., Long R. & Martinez J. Coupling between bacterioplankton species composition, population dynamics, and organic matter degradation. Aquatic Microbial Ecology. 1999;17:13-26.

[15]Riemann, L., Steward G. & Azam F. Dynamics of bacterial community composition and activity during a mesocosm diatom bloom. Applied and Environmental Microbiology. 2000;66:578–587.

[16]Sherwood, B. P. Bacterial Alteration and Removal of Dissolved Organic Matter in the Surface Ocean. 2014.

[17]Azam, F., Smith D., Steward G. & Hagstrom A. Bacteria-organic matter coupling and its significance for oceanic carbon cycling. Microbial Ecology. 1993;28:167-179.

[18]Azam, F. Microbial control of oceanic carbon flux: The plot thickens. Science. 1998;280:694-696.

[19]Mayali, X., Stewart B., Mabery S. & Weber P. K. Temporal succession in carbon incorporation frommacromolecules by particle-attached bacteria inmarine microcosms. Environmental Microbiology. 2016;8:68-75.

[20]Smriga, S., Fernandez V. I., Mitchell J. G. & Stocker R. Chemotaxis toward phytoplankton drives organic matter partitioning among marine bacteria. Proceedings of the Academy of Natural Sciences. 2016;6:1576-1581.

[21]Pukatzki, S., Ma A., Sturtevant D., Krastins B., Sarracino D., Nelson W. & Al E. Identification of a conserved bacterial protein secretion system in Vibrio cholerae using the Dictyostelium host model system. Proceedings of the National Academy of Sciences of the United States of America. 2006;103:1528–1533.

[22]Ho, B. T., Dong T. G. & Mekalanos J. J. A View to a Kill: The Bacterial Type VI Secretion System. Cell Host & Microbe. 2014;15:9-21.

[23]Macintyre, D. L., Miyata S. T., Kitaoka M. & Pukatzki S. The Vibrio cholerae type VI secretion system displays antimicrobial properties. Proc. Natl. Acad. Sci. 2010;107:19520–19524.

[24]M. Basler, Ho B. T. & Mekalanos J. J. Tit-for-tat: type VI secretion system counterattack during bacterial cell-cell interactions. Cell. 2013;152:884-94.

CHAPTER 2

Bacterioplankton drawdown of coral mass-spawned organic matter

The ISME Journal
https://doi.org/10.1038/s41396-018-0197-7

ARTICLE

Bacterioplankton drawdown of coral mass-spawned organic matter

Ryan Guillemette[1] · Ryo Kaneko[2] · Jessica Blanton[1] · Jasmine Tan[1] · Matthias Witt[3] · Samantha Hamilton[4] · Eric E. Allen[1] · Mónica Medina[5] · Koji Hamasaki[6] · Boris P. Koch[7] · Farooq Azam[1]

Received: 6 June 2017 / Revised: 23 March 2018 / Accepted: 12 April 2018

Abstract

Coral reef ecosystems are highly sensitive to microbial activities that result from dissolved organic matter (DOM) enrichment of their surrounding seawater. However, the response to particulate organic matter (POM) enrichment is less studied. In a microcosm experiment, we tested the response of bacterioplankton to a pulse of POM from the mass-spawning of *Orbicella franksi* coral off the Caribbean coast of Panama. Particulate organic carbon (POC), a proxy measurement for POM, increased by 40-fold in seawater samples collected during spawning; 68% degraded within 66 h. The elevation of multiple hydrolases presumably solubilized the spawn-derived POM into DOM. A carbon budget constructed for the 275 µM of degraded POC showed negligible change to the concentration of dissolved organic carbon (DOC), indicating that the DOM was readily utilized. Fourier transform ion cyclotron resonance mass spectrometry shows that the DOM pool became enriched with heteroatom-containing molecules, a trend that suggests microbial alteration of organic matter. Our sensitivity analysis demonstrates that bacterial carbon demand could have accounted for a large proportion of the POC degradation. Further, using bromodeoxyuridine immunocapture in combination with 454 pyrosequencing of the 16S ribosomal RNA gene, we surmise that actively growing bacterial groups were the primary degraders. We conclude that coral gametes are highly labile to bacteria and that such large capacity for bacterial degradation and alteration of organic matter has implications for coral reef health and coastal marine biogeochemistry.

Introduction

Marine organic matter can be conceptualized as a size continuum of biochemically diverse particles and molecules in labile, semi-labile, and refractory states [1–3]. Given its diverse and dynamic nature, organic matter has the ability to shape marine microbial communities [4, 5] including those associated with coral reefs [6, 7], which largely drive reef biogeochemical cycling [8–10] and can influence coral susceptibility to disease [11]. With the global health of coral reefs on a continued decline [12] it is imperative to better understand the microbial dynamics resulting from organic matter perturbation, which can directly influence these highly productive and bio-diverse marine habitats [13].

Studies of bacterial utilization of organic matter in coral reefs have primarily focused on dissolved organic matter (DOM), operationally defined as the organic matter within seawater filtrate from GF/F (glass fiber, 0.7 µm nominal-pore-size), 0.45 µm, or 0.2 µm filtration. Reports show that DOM composition, specifically of the mucus and sugars from coral and algal exudates, respectively, can affect bacterial specific growth rate, growth efficiency, and community composition [6, 7]. However, little is known about coral reef-associated microbial utilization of particulate organic matter (POM), operationally defined as the organic matter retained by GF/F filtration. Bacterial interaction with POM in the ocean is important for carbon cycling since

Electronic supplementary material The online version of this article (https://doi.org/10.1038/s41396-018-0197-7) contains supplementary material, which is available to authorized users.

✉ Ryan Guillemette
rpguille@ucsd.edu

[1] Scripps Institution of Oceanography, UC San Diego, San Diego, CA, USA

[2] National Institute of Polar Research (NIPR), Tokyo, Japan

[3] Bruker Daltonik GmbH, Bremen, Germany

[4] Smithsonian Tropical Research Institute, Bocas del Toro, Panama

[5] Pennsylvania State University, University Park, PA, USA

[6] Atmosphere and Ocean Research Institute, The University of Tokyo, Tokyo, Japan

[7] Alfred Wegener Institute Helmholtz Centre for Polar and Marine Research, Bremerhaven, Germany

Published online: 08 June 2018

POM can be transformed into DOM and subsequently respired by microbes [14]. Additionally, POM composition and concentration can influence microbial community dynamics [4, 5, 15], including the ability to select for virulence factors and pathogenic bacteria [16]. The few studies on POM degradation in coral reefs have suggested that it can be a highly labile nutrient source to microbes as indicated by dissolved oxygen depletion [17–19].

One particularly tractable, natural system for investigating microbial response to an influx of POM is coral mass-spawning. Through expulsion of gametes, vast amounts of organic matter are released that have been reported to produce slicks up to 5 km in length and 10 m in width [20]. On rare occasions, such events have caused severe hypoxia resulting in massive death for millions of fish and large areas of coral [21]. Conversely, less dramatic mass-spawning events are thought to provide nutrients to the generally oligotrophic reef waters [18].

A study off Heron Island, Great Barrier Reef in 2001 estimated that over 300 tons of particulate organic carbon (POC) was released during a mass-spawn event; the authors concluded that such episodic pulses of POM were important for fueling benthic microbial communities [19]. A series of studies conducted in 2005 found 3-fold to 11-fold increases in the concentration of POC in the water column, and increased oxygen consumption rates lasting for at least 1 week [18]. Primary production in the water column increased fourfold, likely a result of the observed increase in inorganic nutrients [22, 23]. Bacterial abundance in the field samples increased 2-fold [24], while laboratory experiments showed POC degradation rates of ~15% h^{-1} in seawater incubations that were enriched with filtered and killed gametes [18]. A study at Kaneohe Bay, Hawaii found a slight correlation of bacterial taxa to the presence of coral eggs [25]. While these studies have shown that coral gametes degrade in the sediment and water column, direct evidence that specifically links bacteria to gamete degradation has not been empirically demonstrated.

We designed a microcosm experiment to quantify the degradation of spawn-derived POM and investigated the bacterioplankton response to coral mass-spawning. Bacterial response was determined from bacterial production (BP) measurements based on incorporation rates of the thymidine analog, bromodeoxyuridine (BrdU), combined with 454 pyrosequencing of the BrdU-labeled 16S ribosomal RNA (rRNA) gene to estimate the bacterial carbon demand (BCD) of actively growing bacterial groups. Additionally, proxy measurements for POM degradation were determined by quantifying carbon flux through POC, colloidal organic carbon (colloidal carbon), and dissolved organic carbon (DOC) pools, along with the hydrolytic enzyme activities that we hypothesized would degrade the organic matter. Furthermore, via Fourier transform ion cyclotron resonance mass spectrometry (FT-ICR MS) we tested the hypothesis that the extracellular DOM (hereafter DOM) pool would contain a modified molecular composition as the organic matter moved between reservoirs.

Materials and methods

Study design

This study took place in 2014 at the Smithsonian Tropical Research Institute, Bocas del Toro, Panama, where each year coral of the genus *Orbicella* engage in well documented mass-spawn reproductive events [26]. Seawater was collected from within the 100×30 m transect of a long-term *Orbicella franksii* monitoring site (9° 19' 38" N, 82° 12' 14" W) to initiate three independent microcosm experiments, each conducted in triplicate. The field sampling was performed with an 80-liter carboy 3 days prior to spawning (September 8), during spawning while gametes were highly abundant in the water column (September 14), and 3 days after spawning (September 17). Microcosm experiments commenced within 8 h of sample collection and were sub-sampled at 0, 24, 44, and 66 h (Fig. 1). Additional field samples were taken for analysis 1 h before and 1 day after spawning (Table 1). All carboys were acid washed, MilliQ water-rinsed, and sample-rinsed prior to use.

Seawater samples from microcosms starting on September 8 and September 17 contained no gametes. These collections had ~40-fold less POC and ~15-fold less particulate organic nitrogen (PON) than the seawater collected during spawning on September 14. Additionally, these collections had comparable POC:PON ratios of 5.5 and 3.9, respectively, in comparison to 13.0 on the night of spawning (Table 1). Therefore, we combined data from these two microcosms and reported them together as "Non-spawn" microcosm throughout the manuscript. Seawater collected for the microcosm on September 14 did contain gametes and is referred to as "Spawn" microcosm.

Particulate organic carbon and nitrogen analysis

Sample volumes of 500 ml were filtered onto pre-combusted 47 mm GF/F filters (Whatman, GE Life Sciences, Marlborough, MA) and frozen at −20 °C until processed (Supplementary Methods).

Total, dissolved, and colloidal organic carbon

Seawater samples were each independently size fractionated through a pre-combusted GF/F filter and a 0.2 µm pore-size polytetrafluoroethylene filter (MilliporeSigma, Burlington,

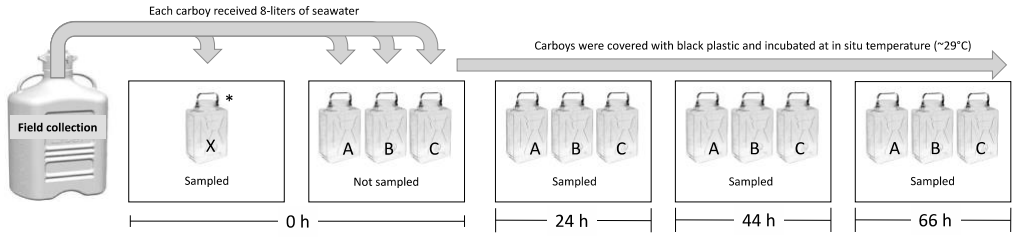

Fig. 1 Microcosm sampling. Spawn and Non-spawn microcosm experiments were independently conducted in triplicate 10-liter polycarbonate carboys in the dark. Samples were taken at all time points for bacterial production, microbial abundance, and enzyme activities; the 0 and 66 h time points were also sampled for 16S rRNA sequencing, FT-ICR MS analysis, organic carbon and nitrogen concentration, and inorganic nutrient concentration. Carboys were well mixed by 5-times inversion before sampling with sterile-glass serological pipettes or a peristaltic pump. *One sampling was conducted at the 0 h time point; an 8-liter aliquot from the field sampling carboy was transferred into carboy "X" and then sampled to ensure that the seawater had been exposed to the same container composition and surface area

MA). A 40 ml aliquot from each fraction was separately collected into pre-combusted borosilicate vials and immediately acidified to pH 2 with hydrochloric acid (HCl). Each sample was quantified with a Shimadzu 500 V-CSN/TNM-1 analysis system (minimum limit of detection = 2.0 µM C) using a seven-point carbon standard with five sample injections (100 µl) per sample.

Organic carbon concentration in the 0.2 µm filtrate is reported as DOC. Colloidal carbon was calculated as the difference between organic carbon concentration in the GF/F (0.7 µm) filtrate and 0.2 µm filtrate. Total organic carbon (TOC) was calculated as the sum of POC, DOC, and colloidal carbon.

Fourier transform ion cyclotron mass spectrometry

A peristaltic pump was used to filter each seawater sample (500 ml) through a GF/F filter then 0.2 µm pore-size polytetrafluoroethylene (PTFE) filter in sequence. The filters were each independently housed in a 47 mm filter-holder and were conjoined by polytetrafluoroethylene tubing. The 0.2 µm filtrate from each sample was independently collected into a polycarbonate bottle, acidified to pH 2 with HCl, then stored at −20 °C. DOM was extracted from the thawed 0.2 µm filtrate (320 ml per sample) using solid-phase extraction (SPE) cartridges (PPL, BondElut, 0.2 g). The cartridges were eluted with ~1 ml methanol. The exact volume of the extract was weighed and recalculated to volume (0.6–0.68 ml; equivalent to an enrichment factor of ~500). The DOC concentration in the extract [$DOC_{extract}$] was determined with a Shimadzu analysis system as described above, and the carbon-based extraction efficiency (%) was calculated as 100 × [$DOC_{extract}$]/enrichment factor × [DOC]. The average extraction efficiency for DOC was 47 ± 8%. FT-ICR MS analysis of the DOM was carried out as described previously [27] (Supplementary Methods).

Bacterial production and loss

Triplicate samples were incubated with 20 nM BrdU, a thymidine analog. After incubation, BrdU incorporation was stopped by adding 100 µM thymidine, flash frozen, and stored at −80 °C until processed [28–30]. BrdU incorporation rates were converted to BP rates using an empirically derived conversion factor of 2×10^{18} bacterial cells produced per mole of incorporated-thymidine [31] and an applied linear regression of $y = 0.69 \times -0.81$ for BrdU to thymidine incorporation rates [30]. Calculations for integrated BP rates, bacterial carbon production, and bacterial loss are detailed in the Supplementary Methods.

Modeled apportionment of TOC drawdown

Refer to Supplementary Methods for terminology and equations used to calculate TOC drawdown; hypothetical bacterial growth efficiency (BGE); and estimation of BCD, bacterial respiration (BR), community respiration (CR), and non-bacterial respiration (NBR).

Microbial cell enumeration

Seawater samples were fixed with 0.5% glutaraldehyde and stored at −80 °C until processed. Samples (1–2 ml) were filtered onto 0.2 µm pore-size polycarbonate filters and stained with DAPI Vectashield (Vector Labs., Burlingame, CA) for bacteria and sperm cell counts [32]. Samples (1 ml) were filtered onto 0.02 µm pore-size Anodisc filters (Whatman) then stained with SYBR Green I (Invitrogen, Carlsbad, CA) for virus-like-particle (VLP) counts [33]. Samples (5 ml) were filtered onto black 0.8 µm pore-size polycarbonate membranes and stained with DAPI Vectashield for protist enumeration. At least 200 cells from ten or more fields of view were counted by epifluorescence microscopy for bacteria and

Table 1 Concentrations of particulate, dissolved, and colloidal organic carbon; particulate organic nitrogen; and inorganic nutrients in field-collected seawater

Date (2014)	Field sample	POC¶ (>0.7 µm)	PON¶ (>0.7 µm)	POC:PON† (ratio)	Colloidal carbon† (0.2–0.7 µm)	DOC¶ (<0.2 µm)	TOC† (µm)	Phosphate¶ (µm)	Silicate¶ (µm)	Nitrate¶ (µm)	Nitrite¶ (µm)	Ammonium¶ (µm)
September 8	**6 d pre-spawn**	12	2	5.5	BD	90	102	0.04	10.4	0.13	0.02	BD
September 14	1 h pre-spawn	11	2	5.3	BD	94	105	NS	NS	NS	NS	NS
September 14	**Spawn**	403 ± 7[a]	31 ± 2[a]	13.0	BD	112 ± 3[a]	515 ± 10	0.24	0.5	BD	0.04	BD
September 15	24 h post-spawn	6	2	2.8	BD	94	100	NS	NS	NS	NS	NS
September 17	**3 d post-spawn**	11	3	3.9	BD	96	107	0.4	0.4	BD	0.07	2.16

Values (in µM) were measured (¶) or calculated (†) from a single sample unless otherwise denoted

Sampling dates in bold indicate collections that were used to start a microcosm

NS not sampled, *BD* below detection

[a]SD calculated from two technical replicates of a single-biological replicate

VLPs, while entire filters were examined for enumeration of protists.

Bacterial cell size

DAPI fluorescence was used to measure the length and width of 100–600 individual bacterial cells per sample. An area cutoff of 0.1–2.0 µm^2 was implemented to exclude VLPs and protists. Cell area was converted to biovolume (µm^3 cell^{-1}) based on the equation $V = (\pi/4) \times W^2 \times (L - W/3)$ [34]. Biovolumes were converted to protein content cell^{-1} using the power law function $P = 88.6^{*V0.59}$ and multiplied by 0.86 [35] to calculate cell-specific bacterial carbon (cell-specific BC) (fgC cell^{-1}) [36].

Hydrolytic enzyme activities

Hydrolytic enzyme activities were assayed using fluorogenic substrates derived from 7-amino-4-methyl- coumarin (AMC) and 4-methyl-umbelliferone (MUF) [37, 38]. Protease activity was assayed as the hydrolysis rate of leucine-AMC. α-D-glucosidase, β-D-glucosidase, lipase, alkaline phosphatase, and chitinase activities were assayed as the hydrolysis rates of MUF labeled- α-D-glucoside, β-D-glucoside, oleate, phosphate and N-acetyl-β-D-glucosamine, respectively.

Combined BrdU immunocapture and 454 pyrosequencing

Sample volumes (3 or 5-liter) were taken for BrdU labeling and processing [39]. Incubation details and genomic DNA extraction methods are contained in the Supplementary Methods. BrdU-incorporated DNA represented the actively growing bacterial fraction (AGB) and was isolated from 1 µg of the Total DNA pool by immunocapture as previously described [39, 40]. DNA in both the Total and BrdU-labeled pools were processed and sequenced.

The hypervariable V1–V3 region of bacterial 16S rRNA gene sequences were amplified for 454 pyrosequencing with universal bacterial primers 27F (5'- AGAGTTTGATCMTGGCTCAG -3') [41] and 519R (5'- GWATTACCGCGGCKGCTG -3') [42]. Refer to the Supplementary Methods for detailed PCR amplification, pyrosequencing, data processing, and analysis methods. The average 454 pyrosequencing read length in our study was 388 base pairs. High confidence taxonomic assignments were made for 16S rRNA gene OTUs at family-level resolution. A small proportion of BrdU-labeled OTUs went undetected in the Total DNA pool, likely due to their relatively low abundance [43]. These OTUs are referred to as "active-but-rare" (ABR) [43].

Sequence data have been submitted to the NCBI Sequence Read Archive and are available under BioProject

PRJNA388504. FASTA sequences for the reported AGB in Fig. 5c are available in Table S4.

Inorganic nutrient analyses

Inorganic nutrient analyses (phosphate, silicic acid, nitrate + nitrite, nitrite, and ammonium) were performed on a Seal Analytical continuous-flow AutoAnalyzer 3 by the ODF Chemistry Laboratory (Scripps Institution of Oceanography, San Diego, CA).

Statistical analysis

Statistics were conducted using GraphPad Prism version 7.0 (GraphPad Software, Inc.). A Shapiro–Wilk test of normality was implemented for each data set. Significant difference between treatments was evaluated with an unpaired *t*-test (two-tailed) for normally distributed data or a Mann–Whitney *U* test for data that was not normally distributed.

Results

Organic carbon concentration and POC:PON ratio

Seawater collected during spawning on September 14 was elevated approximately 5-fold in TOC in comparison to field samples collected during non-spawning conditions (Table 1). While POC constituted the predominant fraction of TOC in the September 14 spawning samples, insufficient replication precluded statistical evaluation for determining significant difference in POC concentration between field collections. However, the POC concentration during spawning (403 ± 7 μM) versus non-spawning conditions (6–12 μM) (Table 1) was substantial in comparison to a published compilation of global data that evaluated over 45 000 marine POC measurements (median POC = 7.36 μM) (Figure S1) [44]. Samples collected during spawning also had approximately threefold higher POC:PON ratio in comparison to samples from non-spawning conditions (Table 1). The calculated colloidal carbon concentration in all field-collected samples was below detection (Table 1).

The TOC concentration in microcosm $Spawn_{0h}$ samples (515 ± 10 μM) was comprised of (403 ± 7 μM POC) + (112 ± 3 μM DOC) and colloidal carbon was below detection (Table 1, Fig. 2a). The observed TOC drawdown in microcosm Spawn (258 ± 42 μM) primarily resulted from a 68% reduction in POC, as colloidal carbon increased by 13 ± 2 μM, and the increase in DOC (4 ± 5 μM) was on the order of the error in our measurements (Fig. 2a). By comparison, microcosm Non-spawn TOC concentration underwent little change during incubation; the decrease in POC (5 ± 5 μM) and increase in DOC (3 ± 11 μM) remained within the error observed between replicates, and colloidal carbon remained undetectable (Fig. 2a). This resulted in a negligible drawdown of 2 ± 5 μM TOC in microcosm Non-spawn. The difference between TOC drawdown observed in microcosm Spawn and Non-spawn was significant ($p < 0.0001$) (Fig. 2a).

Bacterial production and loss

Bacterial production rates were ~50-fold higher in microcosm $Spawn_{0h}$ ($p < 0.01$), $Spawn_{24h}$ ($p < 0.0001$), and $Spawn_{66h}$ ($p < 0.05$) samples in comparison to Non-spawn (Fig. 2b). The BP rate in $Non\text{-}spawn_{44h}$ samples exceeded those in $Spawn_{44h}$, but the difference was not statistically significant. Integration of BP rates shows that microcosm Spawn produced approximately 6-fold more bacterial cells and biomass in comparison to Non-spawn ($p < 0.0001$), and that a large proportion of bacterial cells were lost during incubation (Spawn, 50 ± 18%; Non-spawn, 42 ± 16%) (Table 2). Cell-specific BC measured at each respective time point showed no statistical difference between treatments (Table 2).

Modeled apportionment of the observed TOC drawdown

Our sensitivity analysis shows an estimated range of BCD (33–196 μM) for microcosm Spawn (Fig. 2c). Under the assumptions used, this model demonstrates that the TOC drawdown in microcosm Spawn could have been satisfied by a broad range of combined BR (23–186 μM) and NBR (71–234 μM) (Fig. 2c) (further discussed below).

Microbial abundance

Bacterial abundance was 1.3-fold to 2.6-fold higher ($p < 0.0001$) in microcosm $Spawn_{24h}$, $Spawn_{44h}$, and $Spawn_{66h}$ samples in comparison to Non-spawn samples at the same time points (Fig. 3a). VLP abundance in microcosm Spawn was elevated at each sampling time point in comparison to Non-spawn, however only the $Spawn_{24h}$ and $Spawn_{66h}$ samples were significantly higher ($p < 0.0001$) (Fig. 3b). Interestingly, the VLP abundance at $Spawn_{0h}$ decreased 3-fold within 24 h (Fig. 3b) suggesting that the VLPs were consumed or degraded. We also note that the virus-to-bacteria ratio (VBR) was higher at all time points for microcosm Spawn samples in comparison to Non-spawn, however there was no significant difference between treatments (Fig. 3c). Protist abundance was approximately 2-fold higher ($p < 0.01$) in microcosm Spawn samples ($Spawn_{0h}$, $3.6 \pm 0.6 \times 10^6$ cells l^{-1}; $Spawn_{66h}$, $2.2 \pm 0.3 \times 10^6$ cells l^{-1}) in comparison to microcosm Non-spawn

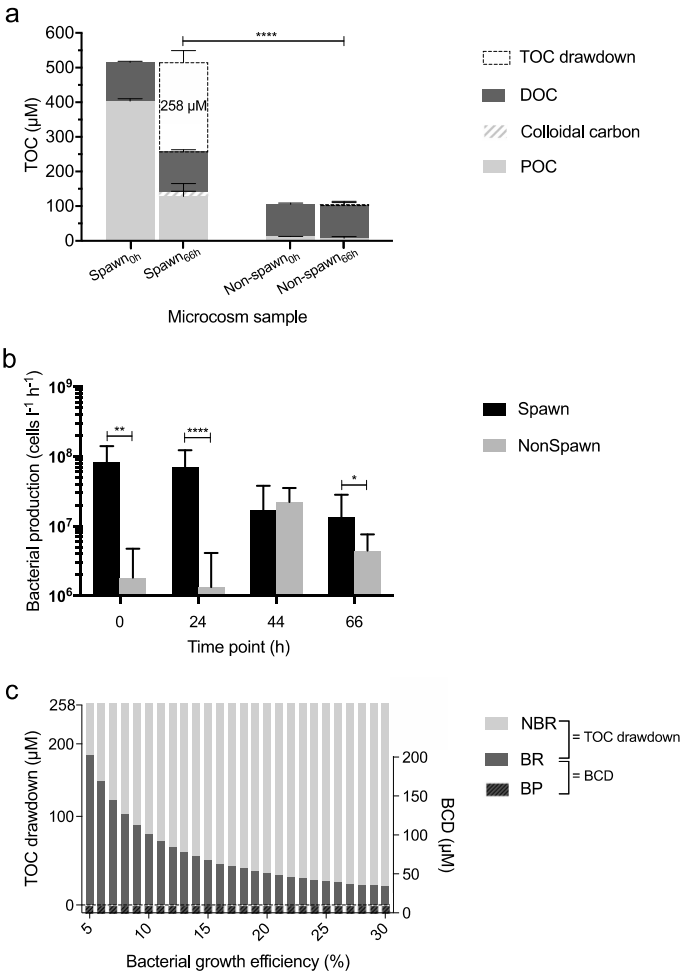

Fig. 2 **a** Total organic carbon (TOC) concentration in microcosms Spawn and Non-spawn. TOC = particulate organic carbon (POC) + dissolved organic carbon (DOC) + colloidal carbon. For each fraction the error is represented by the mean ± SD of technical replicates ($spawn_{0h}$, $n = 2$) or by single measurements of multiple biological replicates ($Spawn_{66h}$, $n = 3$; $Non\text{-}spawn_{0h}$, $n = 2$; $Non\text{-}spawn_{66h}$, $n = 6$). Asterisks indicate significant difference in TOC drawdown (TOC_{0h}–TOC_{66h}) between treatments: ****$p < 0.0001$. **b** Bacterial production. Error bars represent ± SD of the mean ($Spawn_{0h}$, $n = 3$; $Spawn_{66h}$, $n = 6$; $Non\text{-}spawn_{0h}$, $n = 6$; $Non\text{-}spawn_{66h}$, $n = 18$). Asterisks indicate significant difference between treatments for each time point: *$p < 0.05$; **$p < 0.01$; ****$p < 0.0001$. **c** A range of bacterial carbon demand (BCD) (right *y*-axis) was estimated for microcosm Spawn on the basis of integrated BP rate measurements and a hypothetical range (5–30%) of bacterial growth efficiency. BCD = BP + bacterial respiration (BR). The model indicates that a broad range of BR and non-bacterial respiration (NBR) could have satisfied the observed TOC drawdown in microcosm Spawn (left *y*-axis)

samples at the same time point ($Non\text{-}spawn_{0h}$, $1.8 \pm 0.7 \times 10^6$ cells l^{-1}; $Non\text{-}spawn_{66h}$ $1.1 \pm 0.5 \times 10^6$ cells l^{-1}). At $Spawn_{0h}$, the sperm cell abundance was $3.9 \pm 0.9 \times 10^7$ cells l^{-1}. No sperm cells were detected in the subsequent microcosm Spawn samples or in any of the Non-spawn samples.

Hydrolytic enzyme activities

Hydrolytic enzyme activities in microcosm Spawn samples were greater than Non-spawn at each time point for all measured enzymes (Fig. 4). Protease activity was particularly elevated (up to 19-fold) ($p < 0.0001$) (Fig. 4a) and lipase activity was 1.5-fold to 11-fold higher ($p < 0.01$) in Spawn versus Non-spawn samples (Fig. 4b).

Actively growing bacterial community analysis

Microcosm Spawn and Non-spawn samples contained a large number of unique taxa relative to their specific treatment, however in terms of mean relative abundance the vast majority of sequences in the 0 h samples (>97%) (Figure S2 a) and 66 h samples (>91%) (Figure S2 b) were assigned to taxa found in both treatments.

Over 75% of the summed mean relative abundances from the sequenced Total DNA and BrdU-labeled DNA pools of

Table 2 Cell-specific bacterial carbon, integrated bacterial production and bacterial loss in microcosm samples

		Cell-specific BC	Bacterial production[¶]		Bacterial loss[¶]		
Microcosm	Time (h)	(fgC cell^{-1})	(10^9 cells × l^{-1})	(μM C)	(10^9 cells × l^{-1})	(μM C)	(%)
S	0	42.7 ± 18.3[†]	**3.0 ± 0.62**	**9.8 ± 2.1**	**2.2 ± 0.99**	**7.0 ± 3.3**	50 ± 18
	24	31.8 ± 1.32					
	44	38.3 ± 4.06					
	66	47.8 ± 2.22					
NS	0	40.1 ± 0.94	0.57 ± 0.30	1.6 ± 0.86	0.70 ± 0.47	1.8 ± 1.3	42 ± 16
	24	28.8 ± 1.10					
	44	30.2 ± 2.31					
	66	36.6 ± 3.32					

Cell-specific bacterial carbon (cell-specific BC) is represented by the mean ± SE of 406 to 2408 single-cell measurements per biological replicate unless otherwise denoted ($Spawn_{0h}$, $n = 1$; $Spawn_{66h}$, $n = 3$; $Non\text{-}spawn_{0h}$, $n = 2$; $Non\text{-}spawn_{66h}$, $n = 6$)

Insufficient replication precluded statistical evaluation between treatments for cell-specific BC at the 0 h time point

Bacterial production and bacterial loss are reported as the mean ± SD (spawn, $n = 3$; Non-spawn, $n = 6$)

Values in bold denote significant difference between treatments: bacterial production ($p < 0.0001$); bacterial loss ($p < 0.01$)

[†]SD calculated from single-cell measurements in one biological replicate

[¶]Integrated rates (66 h)

microcosm Spawn samples were assigned to common OTUs (Fig. 5a,b). Taxa that were not BrdU-labeled, but were present in the Total DNA pool comprised much of the remaining mean relative abundance for $Spawn_{0h}$ samples (23.3%) (Fig. 5a) and $Spawn_{66h}$ samples (17.8%) (Fig. 5b). We also found OTUs in the BrdU-labeled DNA pools that went undetected in the Total DNA. These ABR bacterial groups had mean relative abundances of ~2% in the $Spawn_{0h}$ samples and ~2% in the $Spawn_{66h}$ samples (Figure S3).

Eight OTUs were the most abundant AGB in microcosm Spawn samples, which included members of the families *Rhodobacteracea*, *Saprospiraceae*, *Flavobacteriaceae*, and *Alteromonadaceae* (Fig. 5c). The AGB in $Spawn_{66h}$ samples included five OTUs that arose from below detection at $Spawn_{0h}$, including additional members of the *Rhodobacteracea*, *Flavobacteriaceae*, and *Alteromonadaceae*. Eleven OTUs that were present as AGB at $Spawn_{0h}$ fell below detection in the $Spawn_{66h}$ samples, including OTUs of the *Rhodobacteracea*, *Saprospiraceae*, *Flavobacteriaceae*; as well as the only members of the *OM1*, *SAR116*, *Cryomorphaceae*, and *SAR86 clades*. The abundance of AGB represented by OTUs in the $Spawn_{66h}$ samples shifted, as total *Rhodobacteracea* dropped from 80.0 to 49.1%, while *Saprospiraceae* increased from 2.6 to 12.2%, and *Flavobacteriaceae* increased from 8.5 to 11.8%. The fourth most abundant OTU, an *Alteromonadacea*, increased slightly from 0.27 to 0.33%. These four dominant families also represented the highly abundant AGB that were particle-associated in the microcosm $Spawn_{66h}$ samples (Figure S4). Further taxonomic classification of differentially abundant OTUs at the genus or species level did not resolve with high confidence suggesting novel groups of marine bacteria, specifically Alphaproteobacteria (*Rhodobacteraceae*) and Bacteroidetes (*Flavobacteriaceae* and *Saprospiraceae*), were associated with Spawn samples.

FT-ICR MS analysis of dissolved organic matter

Cluster analysis of the relative spectral peak-heights for all molecular formulas identified in the microcosms (Table S1) shows that $Spawn_{66h}$ samples clustered together, and distinct from, $Spawn_{0h}$ and all Non-spawn samples (Fig. 6a). The most marked differences between identified molecular formulas in $Spawn_{0h}$ and $Spawn_{66h}$ samples was represented by the formulas unique to $Spawn_{66h}$ ($n = 532$). Most of these unique formulas ($n = 404$) contained nitrogen or sulfur atoms (heteroatoms) (Table S2). Additionally, the weighted-means of the elemental ratios (O/C, H/C) for these unique formulas shows a relative decrease in oxygen content, and a slight decrease in saturation, when compared to the weighted-mean for all of the molecular formulas present in $Spawn_{66h}$ samples (Fig. 6b).

The color density scale (±20%) (Fig. 6b) and the weighted-means of the elemental ratio (O/C) (Table S2) shows that slightly less oxidized formulas remained after 66 h incubation for the molecular formulas ubiquitously identified in all microcosm Spawn samples (at 0 and 66 h). There were also five molecular formulas ubiquitously present in all microcosm Spawn samples that were not present

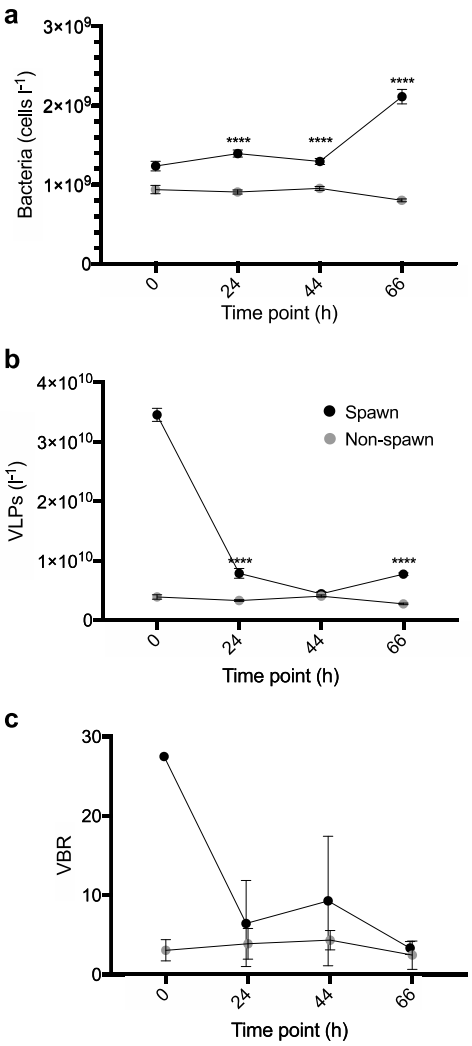

Fig. 3 Bacterial abundance (**a**) and virus-like-particle (VLP) abundance (**b**) in microcosm Spawn (black) and Non-spawn (gray) samples. At least 20 fields of view were enumerated for each microscopy sample ($Spawn_{0h}$, $n = 1$; $Spawn_{66h}$, $n = 3$; $Non\text{-}spawn_{0h}$, $n = 2$; $Non\text{-}spawn_{0h}$, $n = 6$). Error bars represent the standard error of the mean. **c** Virus-to-bacteria ratio (VBR). Error is represented by ± SD of the mean. Asterisks indicate significant difference between treatments for each time point: $****p < 0.0001$. Insufficient replication precluded statistical evaluation between treatments at the 0 h time point for data in (**a**–**c**)

in any of the microcosm Non-spawn samples (Table S3), which suggests that there were unique formulas to the mass-spawning event.

Discussion

Increased POC and PON concentration during mass-spawning

We hypothesize that coral gametes, primarily the eggs, were responsible for the ~40-fold increase in POC and ~15-fold increase in PON of seawater samples collected during spawning (Table 1). When spawning commenced, clouds of released gametes were observed by SCUBA and the samples contained eggs that were visibly abundant. Furthermore, the POC:PON ratio in microcosm Spawn was approximately 3-fold higher than Non-spawn samples (Tables 1) and approximately 2-fold higher than the median POC:PON ratio (6.6) of over 45,000 global samples [44]. Previous studies have reported that lipid-rich coral eggs [45] elevated the POC:PON ratio of post-spawn seawater to levels comparable to those in our study [18] (Table 1), further supporting our hypothesis.

It is noteworthy that seawater samples collected 1 d and 3 d post-spawning had POC and DOC concentrations that were similar to pre-spawning samples (Table 1). The current at our study site may have displaced spawn-derived organic matter from the reef proper, particularly the gametes and developing larvae, which are buoyant and can remain in the surface-water for days [19, 20, 45]. Advection implies that metabolic signatures of the mass-spawning event were not confined exclusively to the sampling location and that any impacts on the carbon cycle may also have influenced water masses away from our site. Future studies might consider sampling away from the reef to assess the broader impacts that spawning may have on the surrounding coastal marine ecosystem.

POC degradation and TOC drawdown in microcosm Spawn

The observed degradation of 275 ± 36 µM POC in microcosm Spawn (Fig. 2a) may have resulted from enzymatic hydrolysis of gametes. We found significantly elevated lipase and protease activity (Fig. 4a, b), and further note that coral eggs and sperm are largely comprised of lipid and protein [45]. While the source of enzymes was not determined, it is well known that marine bacteria are capable of high enzymatic hydrolysis rates [37, 38], and to our knowledge no enzymes have been found directly associated with coral gametes.

The majority of degraded POC was presumably respired by bacteria and non-bacteria (e.g., zooplankton and protists) resulting in the observed TOC drawdown (Fig. 2a). As shown in Fig. 2a, the increase in DOC was on the order of the error in our measurements and can be considered negligible. Additionally, only a small quantity of carbon

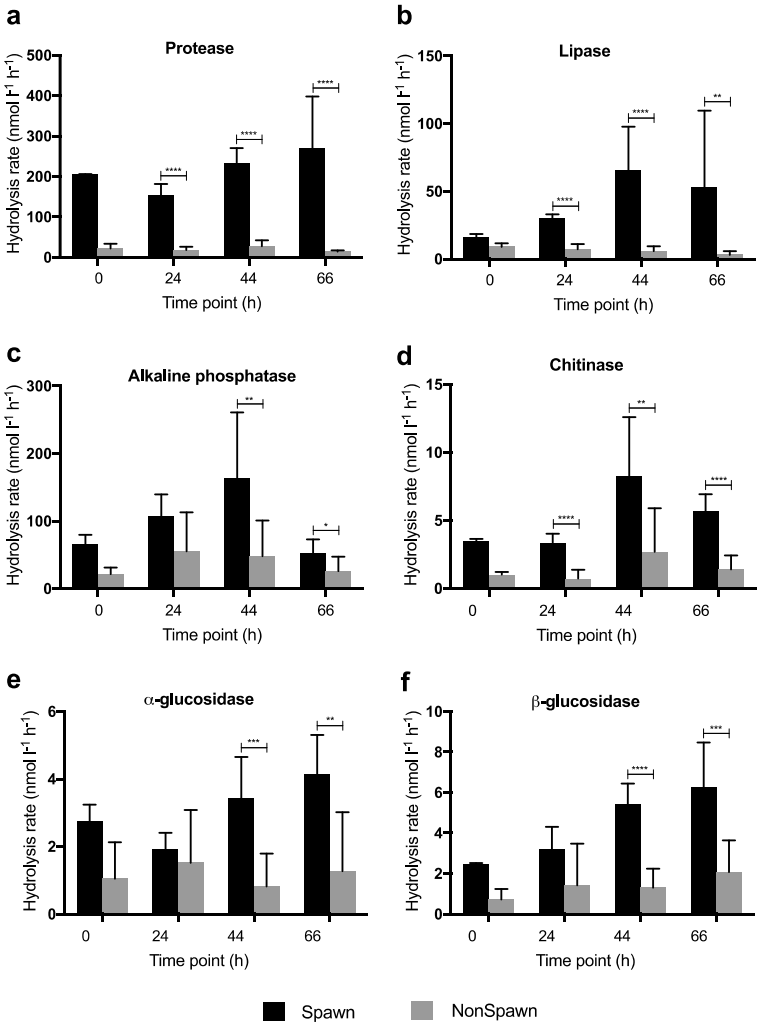

Fig. 4 Hydrolysis rates of enzyme substrates for microcosm Spawn samples (black) and Non-spawn samples (gray). **a** Protease; **b** Lipase; **c** Alkaline phosphatase; **d** Chitinase; **e** α-glucosidase; and **f** β-glucosidase. Error bars represent ± SD of the mean ($Spawn_{0h}$, $n = 2$; $Spawn_{24,44,66h}$, $n = 6$; $Non\text{-}spawn_{0h}$, $n = 4$; $Non\text{-}spawn_{24,44,66h}$, $n = 12$). Asterisks indicate significant difference between treatments for each time point: $*p < 0.05$; $**p < 0.01$; $***p < 0.001$; $****p < 0.0001$. Insufficient replication precluded statistical evaluation between treatments for the 0 h time point

appeared in the colloidal fraction (Fig. 2a). This suggests that consumers of the degraded POM readily utilized it through tight-coupling mechanisms [46, 47].

Our model shows that BCD (primarily BR) could theoretically account for a large proportion of the TOC drawdown (Fig. 2c). To be conservative, we used a range of BGE (5–30%) that is commonly reported in marine studies [14, 48] to estimate BR. However, the literature shows that BR generally constitutes 40–80% of CR in seawater (median = 45%) [48]. Based on our model, an overall BGE of <8% would have been required for BR to have constituted at least 40% of CR (Fig. 2c). Therefore, it is possible that BGE of >8% in our model underestimates the contribution of BR.

The remaining proportion of degraded POC appears to have accumulated in the colloidal carbon pool, which may be due to a number of factors. One possibility is that a portion of the spawn-derived POM transitioned through an intermediate colloidal phase during degradation. Additionally, bacterial lysate that may have accumulated from the 7.0 ± 3.3 µM C of bacterial loss (Table 2) could have constituted a substantial proportion of the observed increase in colloidal carbon

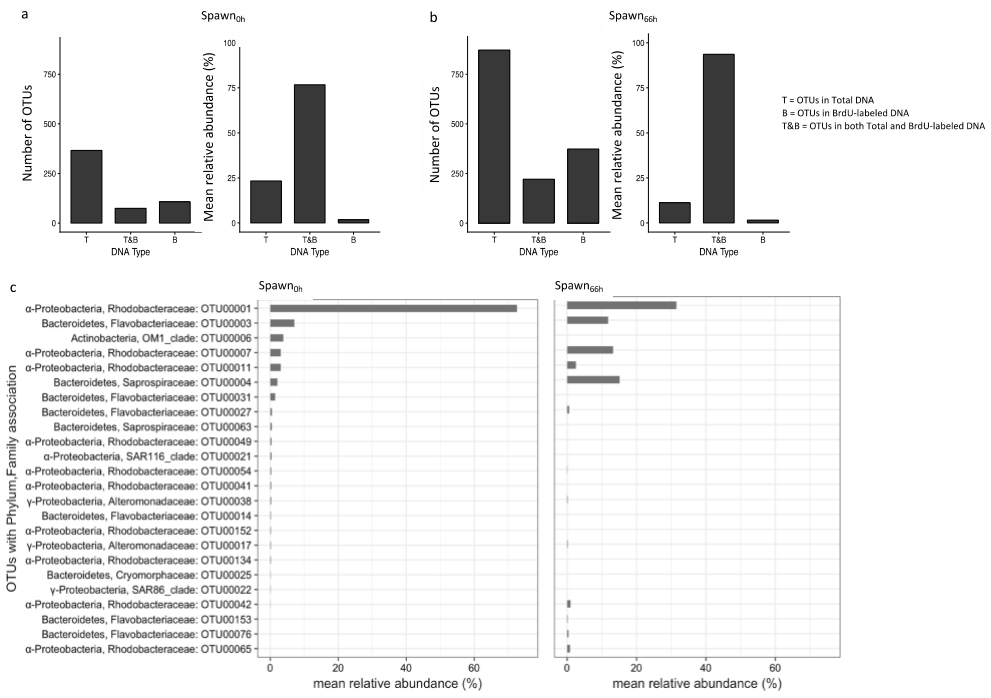

Fig. 5 Actively growing bacterial community analysis. $Spawn_{0h}$ (**a**) and $Spawn_{66h}$ (**b**) show the number of taxa and summed mean relative abundances of OTUs. T Total DNA, B BrdU-labeled DNA, T&B total & BrdU-labeled DNA. **c** Mean relative abundance of BrdU-labeled taxa in microcosm Spawn samples ($Spawn_{0h}$, $n = 1$; $Spawn_{66h}$, $n = 3$). BrdU-labeled OTUs that have ≥0.1% relative abundance are shown, and taxa from $Spawn_{66h}$ samples had to be found in at least two of the three replicates. Class designations: α, Alphaproteobacteria; γ, Gammaproteobacteria

(Fig. 2a). It is also possible that a portion of the DOM underwent spontaneous assembly into colloids [49, 50].

Colloids have been reported at concentrations of up to 10^8 ml^{-1} in seawater samples [51, 52] and may comprise ~10% of the total DOM pool [53]. Organic matter within the colloidal size range could be directly consumed by protists or further degraded and taken up by bacteria. It has been suggested that colloidal particles are a significant source of nutrient to bacteria [54]. Future studies might consider colloids when quantifying carbon flux, as marine bacteria likely use different mechanisms for processing truly dissolved versus colloidal organic matter—both contained in operationally defined DOM samples of GF/F filtrate.

Actively growing bacteria as the primary degraders

Given that BrdU was used as the tracer for BP rate measurements and the AGB community analysis, the AGB found in microcosm Spawn samples (Fig. 5c) were presumably responsible for the greatest proportion of our estimated BCD (Fig. 2c). AGB community analysis revealed Bacteriodetes and Proteobacteria (class Alphaproteobacteria) as the dominant phyla in microcosm Spawn (Fig. 5c). Both phlya have been reported as actively growing via BrdU incorporation in a previous study [55], and are known responders to organic matter enrichment by coral- and algal-reef-associated bacteria [6, 11]. The dominant AGB in microcosm $Spawn_{0h}$ and $Spawn_{66h}$ samples were comprised of *Rhodobacteraceae*, *Flavobacteriaceae*, and *Saprospiraceae* families, and were specifically represented by OTUs 001, 003, 004, 007, and 011 (Fig. 5c). These OTUs were also identified in both the filtrate-associated and particle-associated fraction of $Spawn_{66h}$ samples (Figure S4). It is possible that the particle-associated taxa may have released progeny into the surrounding water to feed on energy-rich plumes of DOM generated by degraded POM [56–58], or that the existing, free-living bacteria also fed on such hydrolysate plumes [59]. It has been suggested that such strategies could account for up to 50% of global ocean BCD [59].

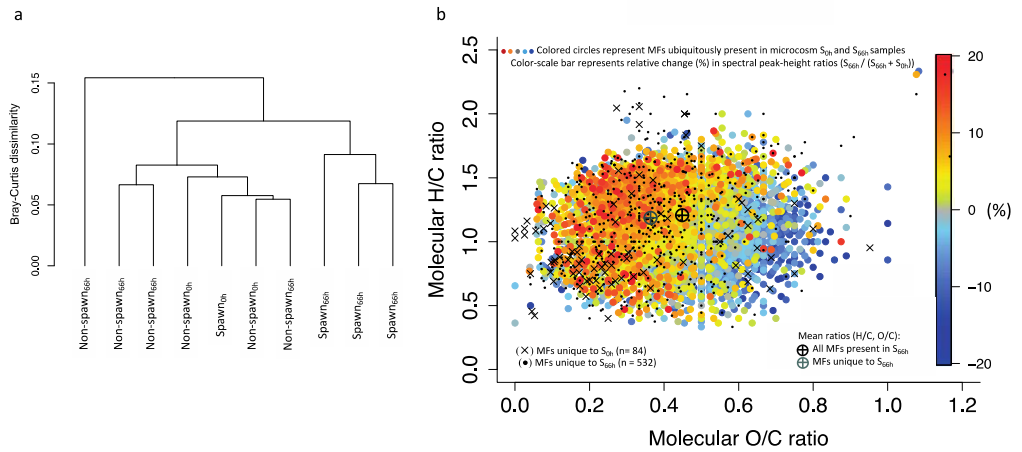

Fig. 6 FT-ICR MS analysis of dissolved organic matter (see Table S1 for sample details; Table S2 for data summary). **a** Cluster dendrogram based on the relative spectral peak-heights of all molecular formulas (MFs) identified in microcosm samples. Distance calculated by Bray–Curtis measure and the complete-linkage method. **b** Van Krevelen diagram showing identified MFs in microcosm Spawn samples ($Spawn_{0h}$, $n = 1$; $Spawn_{66h}$, $n = 3$). Black crosses ($n = 82$), MFs unique to microcosm $Spawn_{0h}$; black dots ($n = 532$), MFs unique to $Spawn_{66h}$. Colored dots ($n = 3\ 007$), MFs ubiquitously identified in both $Spawn_{0h}$ and $Spawn_{66h}$ samples (all replicates). Color scale represents relative change from $Spawn_{0h}$ to $Spawn_{66h}$, derived by calculating relative peak-height ratios for each molecular formula ($Spawn_{66h}$/($Spawn_{66h}$ + $Spawn_{0h}$)). Ratios as "percent relative change" are shown: red, 20% relative increase; gray, no change; blue, 20% relative decrease. Black crosshair, weighted-mean element ratio of all MFs detected in microcosm $Spawn_{66h}$ samples ($n = 16{,}907$); gray crosshair, weighted-mean element ratio of the unique MFs ($n = 532$) in the same samples. S, microcosm Spawn.

The overwhelmingly abundant OTU in microcosm Spawn, OTU 001 (*Rhodobacteraceae*), constituted 72.5 and 31.5% of the relative abundances for AGB in $Spawn_{0h}$ and $Spawn_{66h}$ samples, respectively (Fig. 5c). This sustained dominance, particularly at 0 h when BP was the highest (Fig. 2b), suggests that OTU 001 may have been responsible for the greatest proportion of BCD. As the AGB community composition shifted from microcosm Spawn 0 to 66 h (Fig. 5c) there was a concomitant reduction in BP (Fig. 2b). At 66 h, the relative abundance of OTU 001 dropped by over 50%, and OTUs 003 (*Flavobacteriaceae*), 007 (*Rhodobacteraceae*), and 004 (*Saprospiraceae*) increased by 2-fold to 5-fold, while BP dropped by approximately 4-fold . This may have led to a shift in the BGE of specific taxa, and/or in the overall BGE of the bacterial community, but these possibilities were not investigated. We acknowledge that the use of universal primers does not necessarily mean that all taxa contained in microcosm Spawn were detected, therefore no attempt was made to quantitatively apportion BP or BCD to specific taxa.

Active-but-rare bacterial taxa in microcosm Spawn

Active-but-rare bacterial taxa have been previously described as OTUs that are either found at the tail-end of the rank-abundance curve for the sequenced Total DNA pool, but make-up a large proportion of the OTUs in the BrdU-labeled DNA pool; or they emerge in samples where bacteria are rapidly dividing, but their abundances are kept in check by tight predatory controls [43, 60]. The observation of significantly elevated BP rates during microcosm Spawn (Fig. 2b), coupled with our finding that ~50% of bacteria were lost during incubation (Table 2), seems to support the latter scenario for the ABR taxa found in our study (Figure S3). Although the ABR OTUs never reached high relative abundance, they could have made significant contributions to carbon flux as their rapidly assimilated cell carbon could have been lysed or consumed by grazers and cycled into the microbial loop.

Protist grazing, viral lysis, and bacterial antagonism are considered to be the primary predatory controls that regulate bacterial abundance [61]. The VBR of 28 in the microcosm $Spawn_{0h}$ sample was approximately three fold higher than all other Spawn samples, but insufficient replication precluded statistical evaluation for determining significant differences between treatments (Fig. 3c). However, we note that this value is approximately 4-fold higher than the mean VBR reported in a study of 223 global coral reef samples (range, 2–25; mean, 7.4) [62]. The high VBR at $Spawn_{0h}$ may suggest that bacteria were subject to viral infection early in the microcosms when BP rates were the highest.

We also found highly abundant families of *Saprospiraceae* in the microcosm Spawn samples (Fig. 5c), which are known to prey on other bacteria using a method known as 'ixotrophy' [63]. Additionally, the protists that were present in microcosm Spawn likely contributed to the regulation of bacterial abundance. Protist communities are reported to ingest ~5×10^7 bacteria l^{-1} h^{-1} [64].

Alteration of DOM in microcosm Spawn revealed by FT-ICR MS analysis

Ultrahigh resolution FT-ICR MS analyses have been applied to characterize the molecular composition of complex DOM samples [65, 66] including the alteration of DOM pools by microbial activity [67, 68]. We predicted that the DOM composition in our microcosm Spawn samples would differ after incubation due to bacterial degradation of gametes. The molecular formulas unique to microcosm $Spawn_{66h}$ samples (Fig. 6b) were dominated by heteroatom-containing (sulfur and nitrogen) formulas (Table S2), which are likely to be metabolized faster than the refractory DOM background [69]. Our finding is similar to the mesocosm results of a previous DOM study where nitrogen and sulfur heteroatom-containing compounds were generated via microbial alteration of organic matter [68]. Metabolic processes associated with the AGB in our study, along with the elevation of multiple hydrolases likely contributed to the observed alteration of the DOM pool.

Lastly, we note that our analysis which identified the five molecular formulas unique to microcosm Spawn samples (Table S3) did not consider the entirety of molecules present, as there are biases inherent to DOM size fractionation, electrospray ionization, and DOM extraction methods [70]. However, we suggest that given the conservative criteria used (formulas had to be found in all replicates of all Spawn samples and not present in any of the Non-spawn samples), these molecular formulas may be a good starting point for future research related to: (1) signaling molecules for coral to synchronously release mass-spawn; (2) molecular settling cues for developing larvae; or (3) molecular indicators that corals have spawned.

Conclusion

Our microcosms study showed that the microbial community in the water overlying coral reef could readily respond to spawn input even though this input was mainly comprised of particulate phase. While the underlying mechanisms were not fully examined here, the elevation of multiple hydrolases was presumably responsible for the transition of the particulate phase into DOM to meet the large estimated BCD and an impressive magnitude of carbon flux into the microbial loop. Our study of the AGB community dynamics via BrdU incorporation led to the finding that *Rhodobacteraceae*, *Flavobacteriaceae*, and *Saprospiraceae* taxa were capable of utilizing the episodic organic matter input. Further, we suggest these AGB played a major role in the degradation of POM and likely contributed to the alteration of DOM as identified by high resolution mass spectrometry (FT-ICR MS) analysis. These findings of tight coupling between bacteria and organic matter are highly relevant to coral reef health and to the broader biogeochemical dynamics of coastal marine systems subject to large episodic input of organic matter.

Acknowledgements We thank the Lihini Aluwihare Lab and Yanyan Zhou for assistance. We are grateful to three anonymous reviewers for substantially improving this manuscript. This work was supported by the Gordon and Betty Moore Foundation, Marine Microbial Initiative (grant 4827) to (FA); CREST, Japan Science and Technology Agency to (KH); and NSF (OCE 1442206) to (MM).

Funding Gordon and Betty Moore Foundation (grant 4827) to FA; CREST, Japan Science and Technology Agency to KH, NSF (OCE 1442206) to MM.

Compliance with ethical standards

Conflict of interest The authors declare that they have no conflict of interest.

References

1. Verdugo P, Alldredge AL, Azam F, Kirchman DL, Passow U, Santschi PH. The oceanic gel phase: a bridge in the DOM–POM continuum. Mar Chem. 2004;92:67–85.
2. Azam F. Microbial control of oceanic carbon flux: the plot thickens. Science. 1998;280:694–6.
3. Azam F, Smith D, Steward G, Hagstrom A. Bacteria-organic matter coupling and its significance for oceanic carbon cycling. Microb Ecol. 1993;28:167–79.
4. Riemann L, Steward G, Azam F. Dynamics of bacterial community composition and activity during a mesocosm diatom bloom. Appl Environ Microbiol. 2000;66:578–87.
5. Pinhassi J, Azam F, Hemphala J, Long R, Martinez J. Coupling between bacterioplankton species composition, population dynamics, and organic matter degradation. Aquat Microb Ecol. 1999;17:13–26.
6. Nelson CE, Goldberg SJ, Wegley Kelly L, Haas AF, Smith JE, Rohwer F, et al. Coral and macroalgal exudates vary in neutral

sugar composition and differentially enrich reef bacterioplankton lineages. ISME J. 2013;7:962–79.
7. Haas AF, Nelson CE, Wegley Kelly L, Carlson CA, Rohwer F, Leichter JJ, et al. Effects of coral reef benthic primary producers on dissolved organic carbon and microbial activity. PLoS ONE. 2011;6:e27973.
8. Van Duyl FC, Gast GJ. Linkage of small-scale spatial variations in DOC, inorganic nutrients and bacterioplankton growth with different coral reef water types. Aquat Microb Ecol. 2001;24:17–26.
9. Torreton J, Dufour P. Bacterioplankton production determined by DNA synthesis, protein synthesis, and frequency of dividing cells in Tuamotu Atoll lagoons and surrounding ocean. Microb Ecol. 1996;32:185–202.
10. Torreton J, Dufour P. Temporal and spatial stability of bacterioplankton biomass and productivity in an atoll lagoon. Aquat Microb Ecol. 1996;11:251–61.
11. Haas AF, Fairoz MF, Kelly LW, Nelson CE, Dinsdale EA, Edwards RA, et al. Global microbialization of coral reefs. Nat Microbiol. 2016;1:16042.
12. Jackson J, Donovan MK, Cramer KL, Lam VV (eds). Status and trends of caribbean coral reefs: 1970–2012. Gland, Switzerland: Global Coral Reef Monitoring Network, IUCN; 2014.
13. Knowlton N, Brainard RE, Fisher R, Moews M, Plaisance L, Caley MJ. Coral reef biodiversity. In: Mcintyre AD, editor. Life in the World's oceans: diversity, distribution, and abundance.. Oxford, UK: Wiley-Blackwell; 2010. 65–79.
14. Del Giorgio P, Cole J. Bacterial growth efficiency in natural aquatic systems. Annu Rev Ecol Evol Syst. 1998;29:503–41.
15. Delong EF, Franks DG, Alldredge AL. Phylogenetic diversity of aggregate-attached vs. free-living marine bacterial assemblages. Limnol Oceanogr. 1993;38:924–34.
16. Fontanez KM, Eppley JM, Samo TJ, Karl DM, Delong EF. Microbial community structure and function on sinking particles in the North Pacific Subtropical Gyre. Front Microbiol. 2015;6:469.
17. Wild C, Huettel M, Klueter A, Kremb SG, Rasheed MYM, Jørgensen BB. Coral mucus functions as an energy carrier and particle trap in the reef ecosystem. Nature. 2004;428:66–70.
18. Wild C, Jantzen C, Struck U, Hoegh-Guldberg O, Huettel M. Biogeochemical responses following coral mass spawning on the Great Barrier Reef: pelagic–benthic coupling. Coral Reefs. 2008;27:123–32.
19. Wild C, Tollrian R, Huettel M. Rapid recycling of coral mass-spawning products in permeable reef sediments. Mar Ecol Prog Ser. 2004;271:159–66.
20. Oliver JK, Willis BL. Coral-spawn slicks in the Great Barrier Reef: preliminary observations. Mar Biol. 1987;94:521–9.
21. Simpson CJ, Cary JL, Masini RJ. Destruction of corals and other reef animals by coral spawn slicks on Ningaloo Reef, Western Australia. Coral Reefs. 1993;12:185–91.
22. Glud R, Eyre B, Patten N. Biogeochemical responses to mass coral spawning at the Great Barrier Reef: effects on respiration and primary production. Limnol Oceanogr. 2008;53:997–1013.
23. Eyre B, Glud R, Patten N. Mass coral spawning: a natural large-scale nutrient addition experiment. Limnol Oceanogr. 2008;53:997–1013.
24. Patten N, Mitchell J, Middelboe M, Eyre B, Seuront L, Harrison P et al. Bacterial and viral dynamics during a mass coral spawning period on the Great Barrier Reef. Aquat Microb Ecol. 2008;50:209–20.
25. Apprill A, Rappé MS. Response of the microbial community to coral spawning in lagoon and reef flat environments of Hawaii, USA. Aquat Microb Ecol. 2011;62:251–66.
26. Levitan DR, Fogarty ND, Jara J, Lotterhos KE, Knowlton N. Genetic, spatial, and temporal components of precise spawning synchrony in reef building corals of the *Montastraea annularis* species complex. Evolution. 2011;65:1254–70.
27. Lechtenfeld OJ, Koch BP, Gašparovi´C B, Frka S, Witt M, Kattner G. The influence of salinity on the molecular and optical properties of surface microlayers in a karstic estuary. Mar Chem. 2013;150:25–38.
28. Hamasaki K. Comparison of bromodeoxyuridine immunoassay with tritiated thymidine radioassay for measuring bacterial productivity in oceanic waters. J Oceanogr. 2006;62:793–9.
29. Nelson CE, Carlson CA. A nonradioactive assay of bacterial productivity optimized for oligotrophic pelagic environments. Limnol Oceanogr Methods. 2005;3:211–20.
30. Steward G, Azam F. Bromodeoxyuridine as an alternative to 3H thymidine for measuring bacterial productivity in aquatic samples. Aquat Microb Ecol. 1999;19:57–66.
31. Fuhrman J, Azam F. Thymidine incorporation as a measure of heterotrophic bacterioplankton production in marine surface waters: evaluation and field results. Mar Biol. 1982;66:109–20.
32. Porter K, Feig Y. The use of DAPI for identifying and counting aquatic microflora. Limnol Oceanogr. 1980;25:943–8.
33. Noble R, Fuhrman J. Use of SYBR Green I for rapid epifluorescence counts of marine viruses and bacteria. Aquat Microb Ecol. 1998;14:113–8.
34. Bratbak G. Bacterial biovolume and biomass estimations. Appl Environ Microbiol. 1985;49:1488–93.
35. Simon M, Azam F. Protein content and protein synthesis rates of planktonic marine bacteria. Mar Ecol Prog Ser. 1989;51:201–13.
36. Samo TJ, Pedler BE, Ball GI, Pasulka AL, Taylor AG, Aluwihare LI, et al. Microbial distribution and activity across a water mass frontal zone in the California Current Ecosystem. J Plankton Res. 2012;34:802–14.
37. Martinez J, Steward G, Azam F. Variability in ectohydrolytic enzyme activities of pelagic marine bacteria and its significance for substrate processing in the sea. Aquat Microb Ecol. 1996;10:223–30.
38. Hoppe H. Significance of exoenzymatic activities in the ecology of brackish water: measurements by means of methylumbelliferyl-substrates. Mar Ecol Prog Ser. 1983;11:299–308.
39. Hamasaki K, Taniguchi A, Tada Y, Long RA, Azam F. Actively growing bacteria in the Inland Sea of Japan, identified by combined bromodeoxyuridine immunocapture and denaturing gradient gel electrophoresis. Appl Environ Microbiol. 2007;73:2787–98.
40. Urbach E, Vergin KL, Giovannoni SJ. Immunochemical detection and isolation of DNA from metabolically active bacteria. Appl Environ Microbiol. 1999;65:1207–13.
41. Lane DJ. 16S/23S rRNA sequencing. In: Stackebrandt E, Goodfellow M, editors. Nucleic acid techniques in bacterial systematics.. New York, NY: John Wiley and Sons; 1991. p. 115–75.
42. Turner S, Pryer KM, Miao VPW, Palmer JD. Investigating deep phylogenetic relationships among cyanobacteria and plastids by small subunit rRNA sequence analysis. J Eukaryot Microbiol. 1999;46:327–38.
43. Hamasaki K, Taniguchi A, Tada Y, Kaneko R, Miki T. Active populations of rare microbes in oceanic environments as revealed by bromodeoxyuridine incorporation and 454 tag sequencing. Gene. 2016;576:650–6.
44. Martiny AC, Vrugt JA, Lomas MW. Global ocean POM data ratios from 1971-2014 (Biological C:N:P ratios project, Global POM project). Biological and Chemical Oceanography Data Management Office (BCO-DMO). Dataset version 2014-06-09. Scientific Data. 2014. https://www.bco-dmo.org/dataset/526747/data. Accession date was 10/30/2017
45. Arai T, Kato M, Heyward A, Ikeda Y, Iizuka T, Maruyama T. Lipid composition of positively buoyant eggs of reef building corals. Coral Reefs. 1993;12:71–5.

46. Smith D, Steward G, Long R, Azam F. Bacterial mediation of carbon fluxes during a diatom bloom in a mesocosm. Deep Sea Res Part II. 1995;42:75–97.
47. Kirchman DL, Suzuki Y, Garside C, Ducklow HW. High turnover rates of dissolved organic carbon during a spring phytoplankton bloom. Nature. 1991;352:612–4.
48. Robinson C. Heterotrophic bacterial respiration. In: Kirchman DL, editor. Microbial ecology of the oceans. Hoboken, NJ: John Wiley & Sons, Inc.; 2008. pp. 299–334.
49. Verdugo P. Marine Microgels. Annu Rev Mar Sci. 2012;4:375–400.
50. Chin W-C, Orellana MV, Verdugo P. Spontaneous assembly of marine dissolved organic matter into polymer gels. Nature. 1998;391:568–72.
51. Wells ML, Goldberg ED. Occurrence of small colloids in sea water. Nature. 1991;353:342–4.
52. Isao K, Hara S, Terauchi K, Kogure K. Role of sub-micrometre particles in the ocean. Nature. 1990;345:242–4.
53. Sharp JH. Size classes of organic carbon in seawater. Limnol Oceanogr. 1973;18:441–7.
54. Passow U, Alldredge A. A dye-binding assayfor the spectrophotometric measurement of transparent exopolymer particles (TEP). Limnol Oceanogr. 1995;40:1326–35.
55. Tada Y, Taniguchi A, Nagao I, Miki T, Uematsu M, Tsuda A, et al. Differing growth responses of major phylogenetic groups of marine bacteria to natural phytoplankton blooms in the Western North Pacific Ocean. Appl Environ Microbiol. 2011;77:4055–65.
56. Azam F, Malfatti F. Microbial structuring of marine ecosystems. Nat Rev Microbiol. 2007;5:782–91.
57. Smith DC, Simon M, Alldredge AL, Azam F. Intense hydrolytic enzyme activity on marine aggregates and implications for rapid particle dissolution. Nature. 1992;359:139–42.
58. Azam F, Smith DC. Bacterial influence on the variability in the ocean's biogeochemical state: a mechanistic view. In: Demers S, editor. Particle analysis in oceanography.. Berlin: Springer-Verlag; 1991. 213–36.
59. Kiorboe TJ, Jackson GA. Marine snow, organic solute plumes, and optimal chemosensory behavior of bacteria. Limnol Oceanogr. 2001;46:1309–18.
60. Suttle CA. Marine viruses — major players in the global ecosystem. Nat Rev Microbiol. 2007;5:801–12.
61. Fuhrman JA, Hagstrom A. Bacterial and acrhaeal community structure and its patterns. In: Kirchman DL, editor. Microbial ecology of the oceans. Hoboken, NJ:John Wiley & Sons, Inc.; 2008. 299–334.
62. Knowles B, Silveira CB, Bailey BA, Barott K, Cantu VA, Cobián-Güemes AG, et al. Lytic to temperate switching of viral communities. Nature. 2016;531:466–70.
63. Lewin R. *Saprospira grandis*: A flexibacterium that can catch bacterial prey by "Ixotrophy". Microb Ecol. 1997;34:232–6.
64. Jurgens K, Massana R. (2008). Protistan grazing on marine bacterioplankton. In: Kirchman DL, editor. Microbial ecology of the oceans. Hoboken, NJ:John Wiley & Sons, Inc.; 2008. 383–424.
65. Stenson AC, Landing WM, Marshall AG, Cooper WT. Ionization and fragmentation of humic substances in electrospray ionization Fourier transform-ion cyclotron resonance mass spectrometry. Anal Chem. 2002;74:4397–409.
66. Kujawinski EB. Electrospray ionization fourier transform ion cyclotron resonance mass spectrometry (ESI FT-ICR MS): characterization of complex environmental mixtures. Environ Forensics. 2002;3:207–16.
67. Sherwood BP, Shaffer EA, Reyes K, Longnecker K, Aluwihare LI, Azam F. Metabolic characterization of a model heterotrophic bacterium capable of significant chemical alteration of marine dissolved organic matter. Marine Chem. 2015;177:357–65.
68. Koch BP, Kattner G, Witt M, Passow U. Molecular insights into the microbial formation of marine dissolved organic matter: recalcitrant or labile? Biogeosciences. 2014;11:4173–90.
69. Ksionzek KB, Lechtenfeld OJ, Mccallister SL, Schmitt-Kopplin P, Geuer J, Geibert W, et al. Dissolved organic sulfur in the ocean: Biogeochemistry of a petagram inventory. Science. 2016;354:456–9.
70. Johnson WM, Soule MCK, Kujawinski EB. Extraction efficiency and quantification of dissolved metabolites intargeted marine metabolomics. Limnol Oceanogr Methods. 2017;15:417–28.

APPENDIX 2.1: SUPPORTING INFORMATION (SI)

SI METHODS

Particulate organic carbon and nitrogen analysis

The thawed GF/F filters were placed in a desiccator in the presence of concentrated HCl vapor (12 M) to remove inorganic carbonates and then dried at 50 °C. Carbon and nitrogen was analyzed by high-temperature combustion using an organic elemental analyzer (model CEC 440HA; Control Equipment Corp.) by the Marine Science Institute Analytical Laboratory (University of California, Santa Barbara, CA). Duplicate filters with no sample were handled, stored, and processed in tandem and used as procedural blanks. Duplicate filters receiving MilliQ water were used as operational blanks. Blank values were subtracted from the field and experimental sample measurements. The limit of detection for carbon and nitrogen ranged from 0.1 to 0.4 µM with precision of ± 0.3 wt% and an accuracy of ± 0.3 wt%.

Bacterial production

Bacterial production (BP) rates at the 0, 24, 44, and 66 h time points were integrated to estimate the total number of bacteria produced per unit volume over the microcosm duration, BP_{Total}.

$$BP_{Total} = \int_{t=0}^{t=66} BP(t)\,dt = \sum_{n=1}^{n=3} \left(\frac{(BP(t_n)+BP(t_{n+1})}{2}\right) * (t_{n+1} - t_n) \qquad (1)$$

Terms: BP_{Total} = cells l^{-1}; BP = cells l^{-1} h^{-1}; $t_{1,2,3,4}$ = 0, 24, 44, and 66 h time points, respectively.

BP_{Total} (Eq. 1) was then multiplied by cell-specific bacterial carbon (cell-specific BC) to determine the total production of bacterial carbon, BP_{Total_Carbon}.

$$BP_{Total\_Carbon} = BP_{Total} * Cell\text{-}specific\ BC \quad (2)$$

Terms: BP_{Total_Carbon} = µM C; BP_{Total} = cells l^{-1}; Cell-specific BC = fgC $cell^{-1}$

Calculation of bacterial carbon demand and bacterial respiration

We aimed to estimate the proportion of organic carbon that was utilized in the microcosms to support bacterial carbon demand (BCD); carbon consumed for bacterial production (BP) and bacterial respiration (BR).

$$BCD = BP + BR \quad (3)$$

Given the methodological limitations of measuring BR in natural assemblage [1], we used a sensitivity analysis to estimate BCD based on our calculated BP (Eq. 2) and a hypothetical range of bacterial growth efficiency (BGE). BGE is defined as the proportion of BCD that is used for BP.

$$BGE = BP / BCD \quad (4)$$

The range of BGE (5–30%) was selected as input into our model based on previously reported BGE values for coastal seawater bacteria [2]. This type of analysis has been applied in several studies [2-5].

$$BCD_{Max} = BP / .05 \quad (5)$$

$$BCD_{Min} = BP / .30 \quad (6)$$

We then used BCD_{Max} (Eq. 5) and BCD_{Min} (Eq. 6) to estimate the maximum and minimum range of BR.

$$BR_{Max} = (BP / .05) - BP \quad (7)$$

$$BR_{Min} = (BP / .30) - BP \quad (8)$$

Modeled apportionment of the observed total organic carbon (TOC) drawdown to BR and non-bacterial respiration (NBR)

The difference between TOC concentration at 0 h and 66 h was reported as TOC drawdown for each microcosm.

$$TOC\ drawdown = (TOC_{0h} - TOC_{66h}) \quad (9)$$

Since all of the organic carbon (including biomass) in the microcosm samples was accounted for in the TOC, then the respiration of the entire heterotrophic community, community respiration (CR), was effectively responsible for the observed TOC drawdown. Community respiration can also be conceptualized as the sum of BR and NBR. Therefore, we hypothesized that the observed TOC drawdown in our study resulted from combined BR and NBR. We used our estimated BR_{Max} (Eq. 7) and BR_{Min} (Eq. 8) to estimate NBR_{Max} and NBR_{Min}.

$$NBR_{Min} = TOC\ drawdown - BR_{Max} \quad (10)$$

$$NBR_{Max} = TOC\ drawdown - BR_{Min} \quad (11)$$

Thus, our modeled apportionment of the observed TOC drawdown was partitioned to a broad range of combined BR (Eq. 7, 8) and NBR (Eq. 10, 11) estimates.

Bacterial loss

Bacterial loss was calculated as the difference between bacterial abundance at the 66 h time point (BA_{66h}) and the sum of BP_{Total} (Eq. 1) plus bacterial abundance at the 0 h time point (BA_{0h}) [5].

$$Bacterial\ loss = (BP_{Total} + BA_{0h}) - BA_{66h} \quad (12)$$

Terms: Bacterial loss, BP_{Total}, BA_{0h}, BA_{66h} = cells l^{-1}

Bacterial loss (Eq. 12) was multiplied by the mean cell-specific BC to estimate bacterial carbon loss during the 66 h incubation.

$$Bacterial\ carbon\ loss = Bacterial\ loss * Cell\text{-}specific\ BC \quad (13)$$

Terms: Bacterial carbon loss= µMC; Bacterial loss= cells l^{-1}; Cell-specific BC= fgC $cell^{-1}$

Fourier transform ion cyclotron mass spectrometry (FT-ICR MS)

Prior to analysis the DOM extracts were diluted with methanol:water (1:1, v:v) to reach a final concentration of 2 µmol $DOC_{extract}$ / mL MeOH. Samples were ionized by electrospray ionization (ESI, Apollo II electrospray ionization source, Bruker Daltonik, Bremen, Germany) in negative mode at an infusion flow rate of 120 µl h^{-1} with a Fourier transform ion cyclotron resonance mass spectrometer (SolariX, Bruker Daltonik, Bremen, Germany) equipped with a 12

T refrigerated, actively shielded, superconducting magnet (Bruker Biospin, Wissembourg, France). Two hundred scans were added to one mass spectrum. The magnitude threshold for the peak detection was set to a signal-to-noise ratio of > 4. Mass spectra were recalibrated internally with compounds that have been repeatedly identified in marine DOM samples (Koch et al., 2008; Flerus et al., 2011; m/z: 339.10854, 369.15549, 411.12967, 469.13515, 541.15628, 595.23962, 611.19814, 651.22944). The average mass accuracy of the internal calibrants was below 0.1 ppm.

FT-ICR MS data evaluation

All ions were singly charged as confirmed by the spacing of the related $^{12}C_n$ and $^{13}C^{12}C_{n-1}$ mass peaks. The spectra were evaluated in the mass range of 200–650 m/z. The base peak (either 407.1348 or 411.1296 m/z for all samples) was defined as 100% and relative intensities for all other peaks were calculated accordingly. Molecular formulas were calculated from m/z values allowing for elemental combinations $^{12}C_{0-\infty}$ $^{13}C_{0-1}$ $^{1}H_{0-\infty}$ $^{14}N_{0-6}$ $^{15}N_{0-1}$ $^{16}O_{0-\infty}$ $^{32}S_{0-3}$ $^{34}S_{0-1}$ $^{31}P_{0-3}$ and a mass accuracy threshold of $|\Delta m| \leq 0.2$ ppm. The double bond equivalent (DBE) of a valid neutral formula had to be an integer value and the "nitrogen rule" was applied [6]. Formulas which were either detected in two process blanks (PPL extraction of ultrapure water) or contained in the list of potential surfactants [7] were removed from the entire data set. Formulas containing a ^{13}C, ^{15}N or ^{34}S isotopes that did not correspond to a parent formula (^{12}C, ^{14}N, ^{32}S) were also removed from the data set. Two samples in the original analysis (from microcosm Non-spawn$_{66h}$) were excluded due to a disproportionately lower number of spectral peaks in comparison to all other samples, a trend that suggested contamination by salt remnants.

As an additional level of formula validation, all formulas were sorted according to DBE and ppm. A small proportion of formulas corresponded to very high DBE values, many of which

were false assignments of sulfur containing compounds (as identified by the peak ratio of the parent and daughter ions). We therefore used DBE ≤ 30 as an additional cut-off which resulted in an unambiguous assignment for the complete data set. The distribution of mass accuracy also showed that the majority of the assigned formulas were well within the 0.2 ppm threshold. After these validation steps, we excluded the stable isotopes ^{13}C, ^{15}N, and ^{34}S because they only represented duplicates of the parent formulas for subsequent sample comparisons. Intensity weighted average (wa) molecular masses and element ratios were calculated from the base-peak normalized peak-heights. For formulas with a very high relative intensity, the isotope ratio provided an additional level of formula validation [6]. It should also be considered that the solid-phase extraction method applied in this study does not cover the entirety of chemical compounds in the samples. Therefore, a focus of our evaluation procedure was on formulas that ubiquitously occurred in the control and treatment samples, and their relative peak-height changes. This excludes the possibility that differences between samples were caused by a shift of the analytical window.

Combined BrdU immunocapture and 454 pyrosequencing

BrdU incubation took place for ~6 h before the samples were filtered through 0.22 µm pore-size filters (Sterivex, EMD Millipore, Billerica, MA, USA) to collect bacteria. An additional size fractionation was performed with 8 µm pore-size polycarbonate filters (EMD Millipore) to include 16S rRNA sequencing analysis of particle attached bacteria in microcosm Spawn samples. Samples were immediately flash frozen in liquid nitrogen and stored frozen until processed.

Genomic DNA extraction was carried out using a ChargeSwitch Forensic DNA purification Kit (Invitrogen, Carlsbad, CA, USA). The extraction step was performed twice on the

same sample to maximize DNA yield. The extracted DNAs were concentrated using Amicon Ultra-15 centrifugal filter units, 30K (EMD Millipore). The concentrated DNA solutions were purified with a NucleoSpin gDNA Clean-up Kit (Macherey-Nagel, Düren, Germany) in accordance with manufacturer's instructions.

PCR amplification was carried out in triplicate using Ex Taq HS DNA Polymerase (TaKaRa Bio., Shiga, Japan). The denaturation step was done at 94 °C for 3 minutes, followed by 25 or 30 cycles at 98 °C for 10 seconds. Primer annealing took place for 30 seconds at 55 °C. Extension took place at 72 °C for 1 minute, followed by a final extension at 72 °C for 3 minutes. The PCR products were purified with Agencourt Ampure XP Kit (Beckman Coulter, Brea, CA, USA) in accordance with the manufacturer's instructions. Equal amounts of the PCR amplicons from different samples were mixed. Pyrosequencing of the amplicon mixture was performed using a GS Junior Titanium emPCR Lib-L Kit (Roche Diagnostics, Branford, CT, USA) and a 454 GS Junior system (Roche Diagnostics).

Processing and analyses of the pyrosequencing data were performed using mothur v 1.35.1 [8]. Sequencing errors and low-quality sequences in the raw sequencing data were removed in accordance with the standard 454 operating procedure [9]. A distance matrix was constructed for the remaining sequences, and the sequences were clustered into operational taxonomic units (OTUs) at 97% similarity level with average neighbor clustering. Representative sequences within each OTU were classified with a *k*-mers nearest neighbor searching method [10] against SILVA 119 reference database [11] at 80% threshold. Unknown sequences, as well as sequences affiliated to Eukaryotes, Chloroplast, and Mitochondria were eliminated. Read lengths ranged from 350 to 449 base pairs (bp) after quality filtering (average read length = 388 bp) and there were 10,419 ± 6825 reads sample^{-1}.

The resulting OTU table was imported to R using the Phyloseq package version 1.19.1 (McMurdie and Holmes, 2013) and normalized using the cumulative-sum scaling method with the MetagenomeSeq package version 1.16.0 [12]. Normalized OTU counts were transformed to represent percentages of each sample's total in order to perform comparisons of relative abundance. To calculate taxa consistently found in BrdU-labeled DNA from the Spawn microcosms, Phyloseq scripts were used to subset the data to only $Spawn_{0h}$ and $Spawn_{66h}$ samples; as well as to filter out rare OTUs of < 0.1% mean relative abundance across samples, and/or found only in a single replicate for each time point. To evaluate the contribution of taxa which were observed only in the BrdU-labled DNA and not the Total DNA, Phyloseq and base R commands were similarly used to identify those taxa unique to the BrdU-labeled samples and to determine their mean relative abundance in each subset. The MetagenomeSeq-normalized count table served as direct input to differential abundance analysis with DESeq2 version 1.14.1 [13] to identify OTUs enriched in the particle-associated fraction. P-values were corrected for multiple testing using the Benjamini-Hochberg method [14]. Output statistics of the DESeq2 analysis were filtered to include only those for taxa which were enriched or depleted in the particle fraction by log2-fold-change $\geq$ 2 (4-fold change), and with corrected p-values < 0.05. The results of these analyses were plotted using ggplot2 version 2.2.1[15].

SI REFERENCES

[1]Robinson, C. In: Kirchman, D (ed). Microbial Ecology of the Oceans. John Wiley & Sons, Inc., 299-334(2008).

[2]Del Giorgio, P. & Cole J. Bacterial growth efficiency in natural aquatic systems. Annual Review of Ecology, Evolution, and Systematics. 1998;29.

[3]Meyer, J. L., Edwards J. T. & Risley R. Bacterial Growth on Dissolved Organic Carbon from a Blackwater River. Microbial Ecology. 1987;13:13-29.

[4]Kirchman, D. L., Suzuki Y., Garside C. & Ducklow H. W. High turnover rates of dissolved organic carbon during a spring phytoplankton bloom. Nature. 1991;352:612-614.

[5]Smith, D., Steward G., Long R. & Azam F. Bacterial mediation of carbon fluxes during a diatom bloom in a mesocosm. Deep Sea Research Part II: Topical Studies in Oceanography. 1995;42:75-97.

[6]Koch, B. P., Dittmar T., Witt M. & Kattner G. Fundamentals of molecular formula assignment to ultrahigh resolution mass data of natural organic matter. Analytical Chemistry. 2007;79:1758–1763.

[7]Lechtenfeld, O. J., Koch B. P., Gašparovi´C B., Frka S., Witt M. & Kattner G. The influence of salinity on the molecular and optical properties of surface microlayers in a karstic estuary. Marine Chemistry. 2013;150:25-38.

[8]Scholss, P. D., Westcott S. L. & Ryabin T. Introducing mothur: open-source, platform-independent, community-supported software for describing and comparing microbial communities. Applied and Environmental Microbiology. 2009;75:7537–7541.

[9]Scholss, P. D., Gevers D., Westcott S. L. & Reducing the effects of PCR amplification and sequencing artifacts on 16S rRNA-based studies PLoS One. 2011;6.

[10]Wang, Y. & Qian P. Y. Conservative fragments in bacterial 16S rRNA genes and primer design for 16S ribosomal DNA amplicons in metagenomic studies. PLoS One. 2009;4.

[11]Yilmaz, P., Parfrey L. W., Yarza P., Gerken J., Pruesse E., Quast C., Schweer T., Peplies J., Ludwig W. & Glockner F. The SILVA and 'all-species Living Tree Project (LTP)' taxonomic frameworks. Nucleic Acids Research. 2014;42:D643–D648.

[12]Paulson, J. N., Stine O. C., Bravo H. C. & Pop M. Differential abundance analysis for microbial marker-gene surveys. Nature Methods. 2013;10:1200-1202.

[13]Love, M., Anders S., Huber W., Love M. M., Biocgenerics I., Biobase B., Rcpp L., Sequencing R. B., Chipseq R. & Sage D. Package 'DESeq2'. 2013.

[14]Benjamini, Y. & Hochberg Y. Controlling the false discovery rate: a practical and powerful approach to multiple testing. J R Stat Soc Ser B. 1995;57:289–300.

[15]Wickham, H. ggplot2: elegant graphics for data analysis. Springer. Vancuver. 2016.

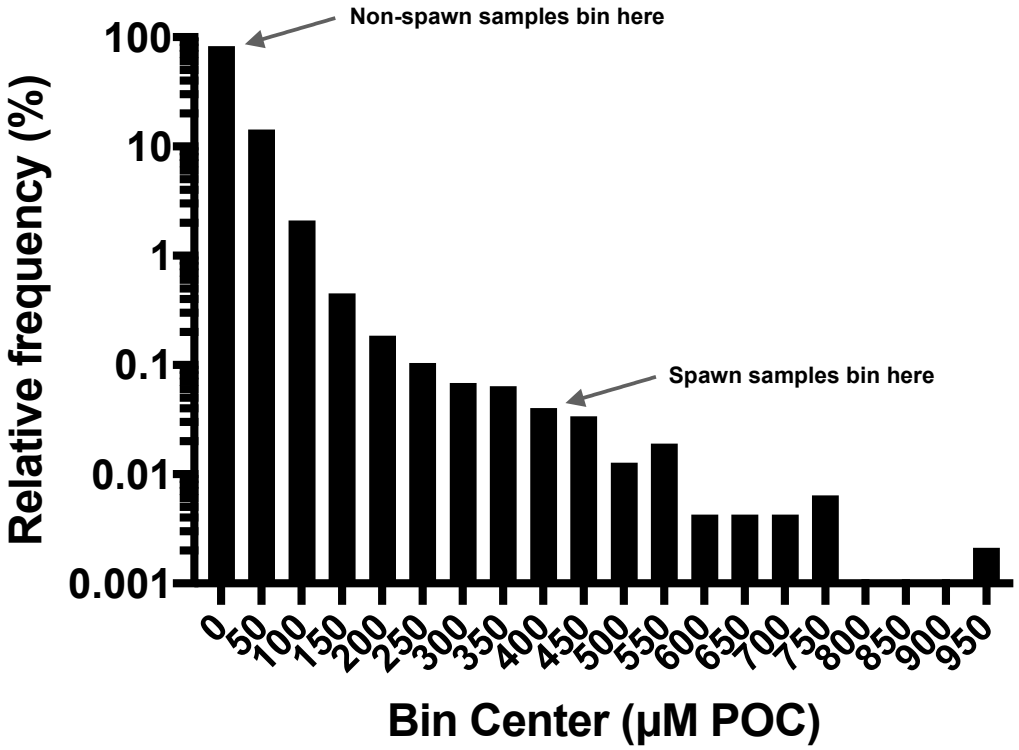

Supplementary Figure 1 Compiled POC measurements from 46 937 global samples (Martiny et al, 2014): range, 0–927.1; median, 7.4; 25% percentile, 2.8; 75% percentile, 18.1. Arrows: Non-spawn POC measurements fell within the < 25 µM POC bin, with 82.5% of the samples; Spawn POC measurements fell into the 375–425 µM POC bin. Only ~0.1% of the samples (n = 49) from the compiled data had higher POC concentration than microcosm $Spawn_{0h}$ samples. y-axis, relative frequency (%) of samples contained in bins; x-axis, histogram bin increments of 50 µM POC.

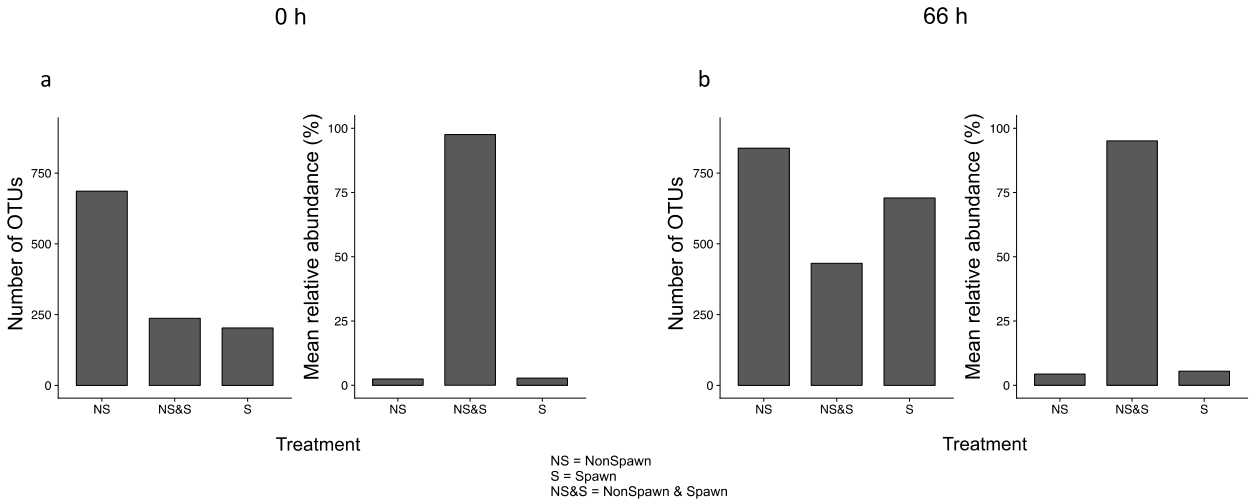

Supplementary Figure 2 Number of taxa and summed mean relative abundances of OTUs from the Total DNA in 0 h samples (a) and 66 h samples (b). S, Spawn; NS, Non-spawn; NS & S, Non-spawn and Spawn.

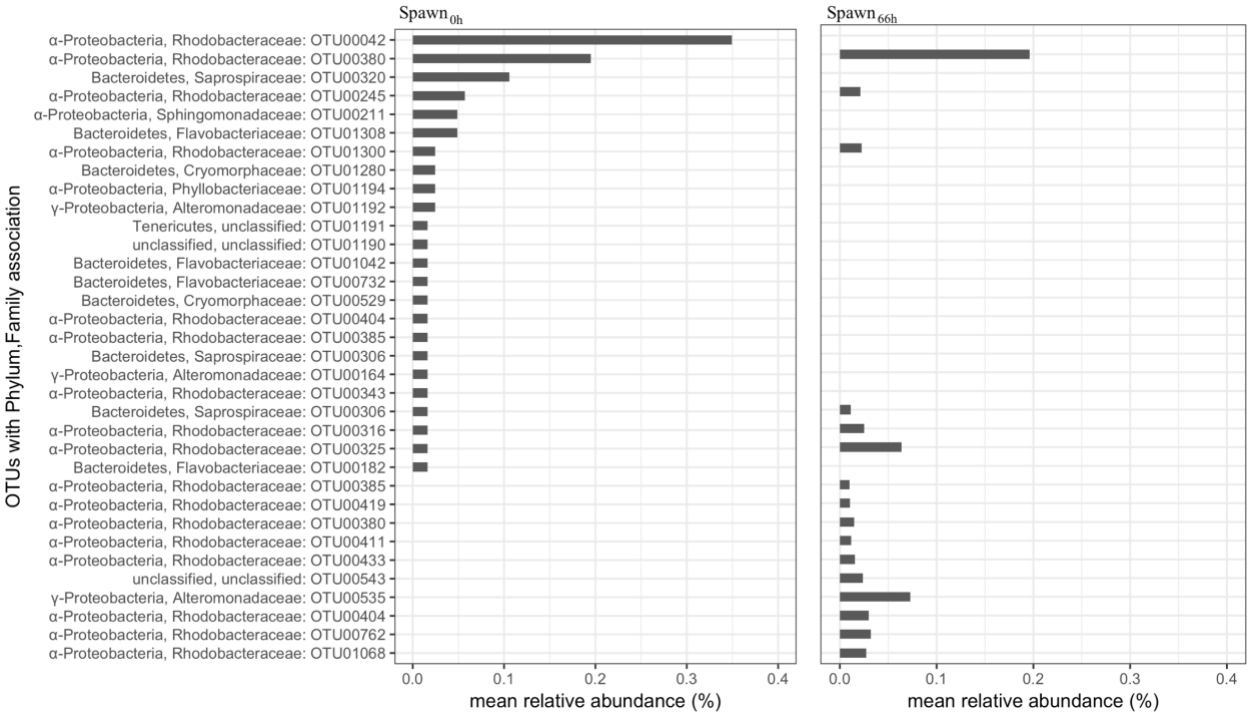

Supplementary Figure 3 Mean relative abundance (%) of active-but-rare bacterial taxa found in microcosm Spawn. Shown taxa were present in at least one biological replicate and comprised ≥ 0.01% relative abundance in the sample. Class designations: α, Alphaproteobacteria; γ, Gammaproteobacteria.

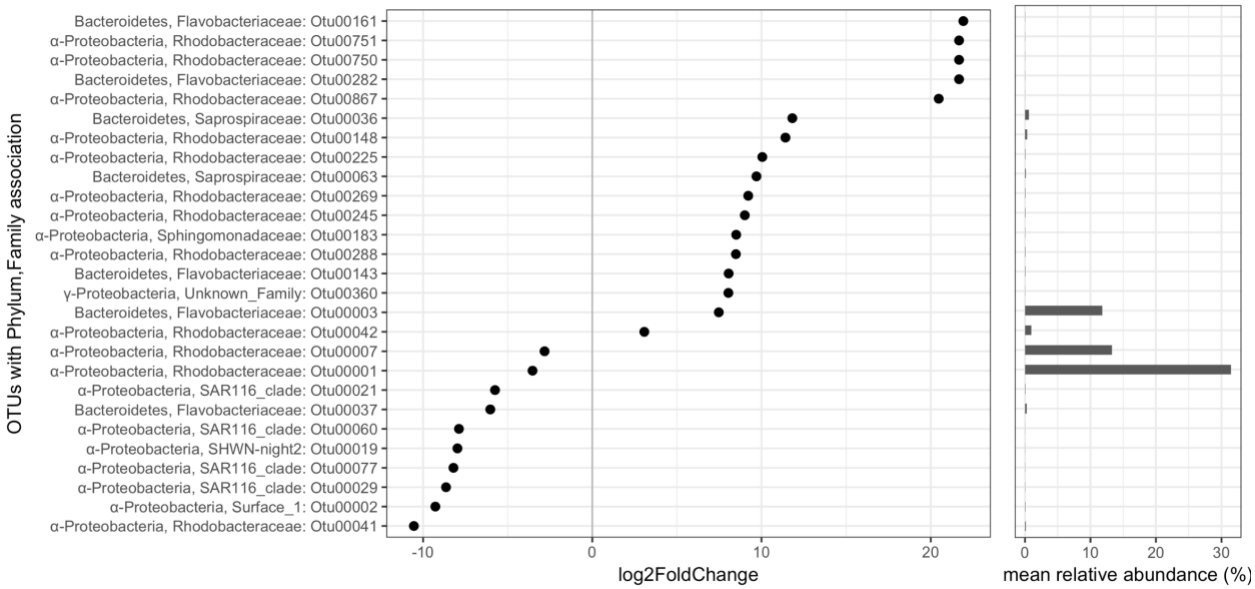

Supplementary Figure 4 Log2-fold change (left) and mean relative abundance (%) (right) for the BrdU-labeled taxa associated with > 8 µm particles from microcosm Spawn 0 h to 66 h. Class designations: α, Alphaproteobacteria; γ, Gammaproteobacteria.

Supplementary Table 2. Weighted-mean of spectral peak-heights for the molecular formulas detected by FT-ICR-MS analysis.

Sample	Treatment	No. of formulas	Mass	Double Bond Equivalent	Element (atoms formula^{-1})					Element ratio			
					C	H	O	N	S	O/C	H/C	N/C	S/C
Spawn_T0	Spawn	4702	427	9.3	20.6	24.9	9.2	0.4	0.07	0.458	1.198	0.0246	0.0042
Spawn_T66_A	Spawn	5434	423	9.3	20.6	25.1	8.9	0.5	0.09	0.442	1.210	0.0266	0.0052
Spawn_T66_B	Spawn	5695	431	9.4	20.8	25.3	9.3	0.4	0.08	0.455	1.206	0.0243	0.0049
Spawn_T66_C	Spawn	5778	426	9.3	20.7	25.1	9.1	0.4	0.09	0.448	1.206	0.0257	0.0052
PRE_Spawn_TO	NonSpawn	4865	422	9.4	20.5	24.6	9.0	0.5	0.07	0.449	1.194	0.0267	0.0040
PRE_Spawn_T66_B	NonSpawn	5541	431	9.4	20.8	25.2	9.3	0.4	0.07	0.455	1.201	0.0253	0.0040
PRE_Spawn_T66_C	NonSpawn	4848	428	9.3	20.5	24.8	9.3	0.4	0.07	0.462	1.199	0.0255	0.0040
Post_Spawn_T0	NonSpawn	5065	427	9.4	20.6	24.9	9.2	0.4	0.08	0.456	1.199	0.0249	0.0045
Post_Spawn_T66_A	NonSpawn	5505	435	9.4	20.8	25.1	9.6	0.4	0.08	0.468	1.198	0.0233	0.0045
Post_Spawn_T66_B	NonSpawn	5000	424	9.3	20.5	24.8	9.1	0.4	0.08	0.453	1.200	0.0258	0.0047

Supplementary Table 3. Molecular formulas unique to microcosm Spawn samples.

Mass	Formula	Spectral peak-heights for the molecular formulas			
nm	mf	Spawn_T0	Spawn_T60_A	Spawn_T60_B	Spawn_T60_C
393	C19H39NO5S	2.5928	16.8973	3.2509	7.0719
403	C23H33NO5	0.8177	0.7919	0.6008	0.6642
410	C16H26O10S	1.0126	1.2982	1.4754	1.3730
458	C28H42O5	0.9307	1.9907	1.1312	0.8166
484	C33H40OS	0.9064	1.3936	1.5474	8.5045

Supplementary Table 4. FASTA sequences for the OTUs presented in Figure 5c.

ID	repSeq
OTU00001	ACGAACGCTGGCGGCAGGCCTAACACATGCAAGTCGAGCGCGCCTTCGGGTGAGCGGCGGACGGGTTAGTAACGCGTGGGAACGTGCCCTTCTCTACGGAATAGCC TCTGGAAACGGAGAGTAATACCGTATACGCCCTTTGGGGGAAAGATTTATCGGAGAAGGATCGGCCCGCGTTAGATTAGGTAGTTGGTGGGGTAACGGCCTACCAA GCCTACGATCTATAGCTGGTTTTAGAGGATGATCAGCAACACTGGGACTGAGACACGGCCCAGACTCCTACGGGAGGCAGCAGTGGGGAATCTTAGACAATGGGGG CAACCCTGATCTAGCCATGCCGCGTGAGTGATGAAGGCCTTAGGGTCGTAAAGCTCTTTCGCCTGTG
OTU00003	ATGAACGCTAGCGGCAGGCCTAACACATGCAAGTCGAGGGGTAACAGGGGGTGCTTGCACTCCGCTGACGACCGGCGCACGGGTGCGTAACGCGTATACAATCTGC CTTATACTGGGGTATAGCCTTTAGAAATGAAGATTAATCCCCCATAGTCTCTAGATGTGGCATCACACTTAGAGTAAAGGTTACGGTATAAGATGAGTATGCGTTCTA TTAGTTTGTTGGTGAGGTAACGGCTCACCAAGACTACGATAGATAGGGGCCCTGAGAGGGGGATCCCCCACACTGGTACTGAGACACGGACCAGACTCCTACGGGA GGCAGCAGTGAGGAATATTGGACAATGGAGGCAACTCTGATCCAGCCATGCCGCGTGCAGGAAGACTGCCCTATGGGTTGTAAACTGCTTTTATATAGG
OTU00006	ACGAACGCTGGCGGTGCGCCTTATGCATGCAAGTCGAGCGAAGCTTTTCAGTAGTTTACTACAGAAAATGACTGAGCGGCGAACGGGTGAGTAACGCGTGAGCAAT CTACCTTAGTTACAGGGATAGCCCGAGGAAACTCGGATTAATACCTGATATTCTTTATATTTCGCATGAAATTAAAAGGAAAGGTCAGCCGAACTAAGATGAGCTCG CGTTCTATCAGCTAGTTGGTGAGGTAAAAGCTCACCAAGGCTACGACGGATAGCTGGTCTGAGAGGACGATCAGCCACACTGGGACTGAGACACGGCCCAGACTCC TACGGGAGGCTGCAGCAGGGAATATTGCGCAATGAGCGAAAGCTTGACGCAGCGACACCGCGTGTGGGATGACGGATCTAGGTTTGTAAACCACTTTCAGGAGGG
OTU00007	ACGAACGCTGGCGGCAGGCCTAACACATGCAAGTCGAACGGGATCTTCGGATCTAGTGGCGGACGGGTTAGTAACGCGTGGGAACGTACCCTTTTCTACGGAATAG CCTCGGGAAACTGAGAGTAATACCGTATACGCCCTTCGGGGAAAGATTTATCGGAGAAGGATCGGCCCGCGTAAGATTAGATAGTTGGTGGGGTAATGGCCTACCA AGTCTACGATCTTTAGCTGGTTTGAGAGGATGATCAGCAACACTGGGACTGAGACACGGCCCAGACTCCTACGGGAGGCAGCAGTGGGGAATCTTAGACAATGGGG
OTU00011	ACGAACGCTGGCGGCAGGCCTAACACATGCAAGTCGAACGGCACCTTCGGGTGTAGTGGCGGACGGGTTAGTAACGCGTGGGAACGTGCCCTTCTCTACGGAATAG CCTCGGGAAACTGAGCGTAATACCGTATACGCCCTTTGGGGGAAAGATTTATCGGAGAAGGATCGGCCCGCGTTGGATTAGGTAGTTGGTGGGGTAATGGCCTACCA AGCCTACGATCCATAGCTGGTTTGAGAGGATGATCAGCAACACTGGGACTGAGACACGGCCCAGACTCCTACGGGAGGCAGCAGTGGGGAATCTTAGACAATGGGG
OTU00004	ATGAACGCTAGCGGAAGGCCTAATACATGCAAGTCGAGGGGTAACAGGGGAGCTTGCTCCCGCTGACGACCGGCGCACGGGTGAGTAACGCGTACGTAACCTACCT TCAAGAAAGGGATAGCCCCGGGAAACTGGGATTAATACCTTATAGTATCATAAAGCCGCATGGTTTAATGATTAAAGCTCCGGCGCTTGAAGATGGACGTGCGTTCT ATTAGATAGTTGGTGAGGTAACGGCTCACCAAGTCAGCGATAGATAGGGGGCGTGAGAGCGTGGTCCCCCACACGGGTACTGAGACACGGACCCGACTCCTACGGG AGGCAGCAGTAAGGAATATTGGACAATGGGCGCAAGCCTGATCCAGCCATTCCGCGTGTAGGATGACGGCCCTCTGGGTTGTAAACTACTTTTATTTGGG
OTU00031	ATGAACGCTAGCGGCAGGCCTAACACATGCAAGTCGAGGGGTAACAGGGAAAAGCTTGCTTTTCCGCTGACGACCGGCGCACGGGTGCGTAACGCGTATGCAACCT ACCTTTTACAGGAGTATAGCCCAGAGAAATTTGGATTAATCCTCCATAATATCTTTTTCTTGCATAGGAAAAAGATTAAAGCTTCGGTGGTAAAAGATGGGCATGCG TTTTATTAGCTAGTAGGTGAGGTAACGGCTCACCTAGGCCACGATAAATAGGGGCCCTGAGAGGGGGATCCCCCACACTGGTACTGAGACACGGACCAGACTCCTA CGGGAGGCAGCAGTGAGGAATATTGGACAATGGACGAAAGTCTGATCCAGCCATGCCGCGTGCAGGATGACGGCCCTATGGGTTGTAAACTGCTTTTATACAGG
OTU00027	ATGAACGCTAGCGGCAGGCTTAACACATGCAAGTCGAGGGGCAGCGTAGATTGCTTGCAATCTGACGGCGACCGGCGAACGGGTGCGTAACGCGTATAGAACCTAC CTTATACAGAGGGATACCCCATGGAAACGTGGACTAATACCTCATAGTATAGTTGAATGGCATCGTTTAACTATTAAAGATTTATCGGTATAAGATGGCTATGCGTC CTATTAGCTAGATGGTAAGGTAACGGCTTACCATGGCGATGATAGGTAGGGGTCCTGAGAGGGAGATCCCCCACACTGGTACTGAGACACGGACCAGACTCCTACG GGAGGCAGCAGTGAGGAATATTGGTCAATGGAGGCAACTCTGAACCAGCCATGCCGCGTGCAGGAAGACTGCCCTATGGGTTGTAAACTGCTTTTATACAGG
OTU00063	ATGAACGCTAGCGGGAGGCTTAATACATGCAAGTCGAGGGGCAGCAGTTCGGCTGGCGACCGGCGCACGGGTGAGTAACGCGTACGCAATCTACCTTTAAGAGAGG GATAGCCCCGGGAAACTGGGATTAATACCTCATAGTATCATTAAATCGCATGGTTTGATGATTAAAGCTTCGGTGCTTAAAGATGAGCGTGCGTGCTATTAGCTAGTT GGTGAGGTAACGGCTCACCAAGGCTACGATAGCTAGGGGGCGTGAGAGCGTGATCCCCCACACGGGTACTGAGACACGGACCCGACTCCTACGGGAGGCAGCAGT AAGGAATATTGGACAATGGGCGCAAGCCTGATCCAGCCATCCCGCGTGCAGGATGACGGCCCTATGGGTTGTAAACTGCTTTTATTTGGG
OTU00049	ACGAACGCTGGCGGCAGGCCTAATACATGCAAGTCGAGCGCGCCCTTCGGGGTGAGCGGCGGACGGGTTAGTAACGCGTGGGAACGTGCCCTTCTCTAAGGAATAG CCACTGGAAACGGTGAGTAATACCTTATACGCCCCCAATCAAATTCCATTTGGTTGACGGAAATTCTGTTGAATGCCGGATGGCATTTGATGGGGGGGAAAGATTTA TCGGAGAAGGATCGGCCCGCGTTAGATTAGATAGTTGGTGGGGTAATGGCCTACCAAGTCTACGATCTATAGCTGGTTTTAGAGGATGATCAGCAACACTGGGACTG AGACACGGCCCAGACTCCTACGGGAGGCAGCAGTAGGGAATCTTGGACAATGGGCGCAAGCCTGATCCAGCCATGCCGCGTGAGTGAAGAAGGCCTTAGGGTCGTA
OTU00021	ACGAACGCTGGCGGCATGCTTAACACATGCAAGTCGAACGCTATTTTATAGAGTGGCGCACGGGTGAGTAACGCGTGGGAATCTGCCCTTCTGCCTGGGATAACAGC TGGAAACGGCTGCTAATACCGGATACGCCCTTCGGGGAAAGGTCCGCCGCAGAAGGAGGAGCCCGCGTCTGATTAGCTTGTTGGTAGGGTAATGGCCTACCAAGGC GACGATCAGTAGCTGGTCTGAGAGGATGATCAGCCACACTGGGACTGAGACACGGCCCAGACTCCTACGGGAGGCAGCAGTGGGGAATATTGGACAATGGGGGCA

Supplementary Table 4. FASTA sequences for the OTUs presented in Figure 5c.

ID	repSeq
OTU00054	ACGAACGCTGGCGGCAGGCCTAATACATGCAAGTCGAGCGCGCCCTTCGGGGTGAGCGGCGGACGGGTTAGTAACGCGTGGGAACGTGCCCTTCTCTAAGGAA TAGCCTCTGGAAACGGAGAGTAATACCTTATACGCCCCCAATCAAATTCCATTTGGTTGGCAAAATATTGTCAGATGCTTTGTGGCATTTGATGGGGGGGAAAG ATTTATCGGAGAAGGATCGGCCCGCGTTAGATTAGATAGTTGGTGGGGTAACGGCCTACCAAGTCTACGATCTATAGCTGGTTTTAGAGGATGATCAGCAACAC TGGGACTGAGACACGGCCCAGACTCCTACGGGAGGCAGCAGTAGGGAATCTTGGACAATGGGGGCAACCCTGATCCAGCCATGCCGCGTGAGTGATGAAGGCC
OTU00038	TTGAACGCTGGCGGCAGGCCTAACACATGCAAGTCGAACGGTAACAGGATGTGCTTGCACATCGCTGACGAGTGGCGGACGGGTGAGTAATGCTTGGGAACTT GCCTTTGCGAGGGGGATAACAGTTGGAAACGACTGCTAATACCGCATAATGTCTTCGGACCAAACGGGGCTTCGGCTCCGGCGCAGAGAGAGGCCCAAGTGAG ATTAGCTAGTTGGTAAGGTAAAGGCTTACCAAGGCGACGATCTCTAGCTGTTCTGAGAGGAAGATCAGCCACACTGGGACTGAGACACGGCCCAGACTCCTAC GGGAGGCAGCAGTGGGGAATATTGCACAATGGGGGAAACCCTGATGCAGCCATGCCGCGTGTGTGAAGAAGGCCTTCGGGTTGTAAAGCACTTTCAGTTGTG
OTU00041	ACGAACGCTGGCGGCAGGCCTAACACATGCAAGTCGAGCGCGCCTTCGGGCGAGCGGCGGACGGGTTAGTAACGCGTGGGAACGTGCCCAGATCTACGGAAT AGCCACTGGAAACGGTGAGTAATACCGTATACGCCCTTCGGGGGAAAGATTTATCGGATTTGGATCGGCCCGCGTTAGATTAGGTAGTTGGTGGGGTAACGGCC TACCAAGCCTACGATCTATAGCTGGTTTTAGAGGATGATCAGCAACACTGGGACTGAGACACGGCCCAGACTCCTACGGGAGGCAGCAGTGGGGAATCTTGGA
OTU00014	ATGAACGCTAGCGGCAGGCCTAACACATGCAAGTCGAGGGGTAACGTGAGTGCTTGCACTTGACGACGACCGGCGCACGGGTGCGGAACGCGTATGGAACCTA CCTTTATCAGGGGGATAGCCCATGGAAACGTGGATTAATACCCCATAGTATTATTTTATTGCATGATAGAATAATTAAAGAATTTCGGATAGAGATGGCCATGC GTATCATTAGCTAGTAGGCGAGGTAACGGCTCACCTAGGCGACGATGATTAGGGGTCCTGAGAGGGAGATCCCCCACACTGGTACTGAGACACGGACCAGACT CCTACGGGAGGCAGCAGTGAGGAATATTGGGCAATGGAGGCAACTCTGACCCAGCCATGCCGCGTGCAGGAAGACGGCCCTATGGGTTGTAAACTGCTTTTAT
OTU00152	ACGAACGCTGGCGGCAGGCCTAACACATGCAAGTCGAGCGCGCCCTTCGGGGTGAGCGGCGGACGGGTTAGTAACGCGTGGGAACGTGCCCTTTTCTAAGGAA TAGCCACTGGAAACGGTGAGTAATACCTTATACGCCCTTCGGGGGAAAGATTTATCGGAGAAGGATCGGCCCGCGTTAGATTAGGTAGTTGGTGGGGTAATGG CCTACCAAGCCTACGATCTATAGCTGGTTTGAGAGGATGATCAGCAACACTGGGACTGAGACACGGCCCAGACTTCTACGGAAGGCAGCAGTGGGGAATCTTG
OTU00017	TTGAACGCTGGCGGCAGGCCTAACACATGCAAGTCGAACGGTAACATTTCTAGCTTGCTAGAAGATGACGAGTGGCGGACGGGTGAGTAATGCTTGGGAACTT GCCTTTGCGAGGGGGATAACAGTTGGAAACGACTGCTAATACCGCATAATGTCTTCGGACCAAACGGGGCTTCGGCTCCGGCGCAAAGAGAGGCCCAAGTGAG ATTAGCTAGTTGGTAAGGTAACGGCTTACCAAGGCGACGATCTCTAGCTGTTCTGAGAGGAAGATCAGCCACACTGGGACTGAGACACGGCCCAGACTCCTAC GGGAGGCAGCAGTGGGGAATATTGCACAATGGGGGAAACCCTGATGCAGCCATGCCGCGTGTGTGAAGAAGGCCTTCGGGTTGTAAAGCACTTTCAGTTGTG
OTU00134	ACGAACGCTGGCGGCAGGCCTAACACATGCAAGTCGAACGAAGCCTTCGGGCTTAGTGGCGGACGGGTTAGTAACGCGTGGGAACGTACCCTTCACTACGGAA TAGTCTCGGGAAACTGGGTTTAATACCGTATACGCCCTTCGGGGAAAGAATTTCGGTGAGGGATCGGCCCGCGTTGGATTAGGTAGTTGGTGGGGTAATGGCCT ACCAAGCCTACGATCCATAGCTGGTTTGAGAGGATGATCAGCAACACTGGGACTGAGACACGGCCCAGACTCCTACGGGAGGCAGCAGTGGGGAATCTTAGAC
OTU00025	ATGAACGCTAGCGGCAGGCCTAACACATGCAAGTCGAGGGGTAACAGGAAAGCTTGCTTTCGCTGACGACCGGCGCACGGGTGCGTAACGCGTATGCAACCTA CCTCATACTGGAGAATAGCCCCTGGAAACGGGGATTAATACTCCATGGTATCATTCTTTCGCATGTTAGAATGATTAAAGAATTTCGGTATGAGATGGGCATGC GTCCCATTAGCTAGTTGGTGAGGTAACGGCTCACCAAGGCGACGATGGGTAGGGGGCCTGAGAGGGTGGTCCCCCACACTGGTACTGAGACACGGACCAGACT CCTACGGGAGGCAGCAGTGAGGAATATTGGTCAATGGAGGCAACTCTGAACCAGCCATGCCGCGTGAAGGATGACGGCCCTATGGGTTGTAAACTTCTTTTGA
OTU00022	TTGAACGCTGGCGGTAGGCCTTATACATGCAAGTCGAGCGAGAAAGTATCTTCGGATATGAGTAGAGCGGCGGACGGGTGAGTAACGCGTAGGAATCTACCTA GTAGAAGGGGATAGCCCGGGGAAACTCGGATTAATACCGTATACCTCCTTAGGGAGAAAGAGGGCCTCTCTTTGATGCTCTCGCTACTAGATGAGCCTGCGTAA GATTAGCTAGTTGGTGAGGTAATGGCTCACCAAGGCGACGATCTTTAGCTGGTCTGAGAGGACGATCAGCCACATTGGGGACTGAGACACGGCCCAGACTCC TACGGGAGGCAGCAGTAGGGAATATTGGACAATGAGCGCAAGCTTGATCCAGCCATACCGCGTGTGTGAAGAAGGCTTTCGGGTTGTAAAGCACTTTAAGCAG
OTU00042	ACGAACGCTGGCGGCAGGCCTAACACATGCAAGTCGAACGAAGTCTTCGGACTTAGTGGCGGACGGGTTAGTAACGCGTGGGAACGTGCCCTTTACTTCGGAA TAGTCCCGGGAAACTGGGTTTAATACCGAATACGCCCTTTGGGGGAAAGATTTATCGGTAAAGGATCGGCCCGCGTTGGATTAGGTAGTTGGTGGGGTAATGGC CTACCAAGCCGACGATCCATAGCTGGTTTGAGAGGATGATCAGCAACACTGGGACTGAGACACGGCCCAGACTCCTACGGGAGGCAGCAGTGGGGAATCTTAG
OTU00153	ATGAACGCTAGCGGCAGGCTTAACACATGCAAGTCGAGGGGTAACAGGAGTAGCTTGCTACTTGCTGACGACCGGCGCACGGGTGCGTAACGCGTATAGAACC TACCTTTTACAGAGGGATAGCCTTTAGAAATGAAGATTAATACCTCATAGTATTTTAGATTGGCATCGATTTAGAATTAAAGATTTATCGGTAAAAGATGGCTAT GCGTCCTATTAGCTAGATGGTAAGGTAACGGCTTACCATGGCAACGATAGGTAGGGGTCCTGAGAGGGAGATCCCCCACACTGGTACTGAGACACGGACCAGA CTCCTACGGGAGGCAGCAGTGAGGAATATTGGGCAATGGAGGCAACTCTGACCCAGCCATGCCGCGTGCAGGAAGACTGCCCTATGGGTTGTAAACTGCTTTT
OTU00076	ATGAACGCTAGCGGCAGGCTTAACACATGCAAGTCGAGGGGTAACAGGGATTGCTTGCAATCCGCTGACGACCGGCGCACGGGTGCGTAACGCGTATAGAACC TACCTTTTACTGAGGGATAGCCTTTAGAAATGAAGATTAATACCTCATGGCATCATTTAGTGGCATCACTATATGATTAAAGATTTATTGGTAAAAGATGGCTAT GCGTCCTATTAGTTAGATGGTGAGGTAACGGCTCACCATGGCATCGATAGGTAGGGGTCCTGAGAGGGAGATCCCCCACACTGGTACTGAGACACGGACCAGA CTCCTACGGGAGGCAGCAGTGAGGAATATTGGACAATGGGCGCAAGCCTGATCCAGCCATGCCGCGTGCAGGAAGACTGCCCTATGGGTTGTAAACTGCTTTT
OTU00065	ACGAACGCTGGCGGCAGGCCTAACACATGCAAGTCGAGCGCGCCCTTCGGGGTGAGCGGCGGACGGGTTAGTAACGCGTGGGAACGTGCCCAGATCTAAGGA ATAGCCACTGGAAACGGTGAGTAATACCTTATACGCCCTTCGGGGGAAAGATTTATCGGATTTGGATCGGCCCGCGTTAGATTAGGTAGTTGGTGGGGTAATGG CCTACCAAGCCTACGATCTATAGCTGGTTTTAGAGGATGATCAGCAACACTGGGACTGAGACACGGCCCAGACTCCTACGGGAGGCAGCAGTGGGGAATCTTG

Chapter 2, in full, is a reprint of the material. Guillemette, R., Kaneko, R., Blanton, J., Tan, J., Witt, M., Hamilton, S., Medina, M., Hamasaki, K., Koch, B.P., Azam, F. 2018. Bacterioplankton drawdown of coral-mass spawn organic matter off Bocas del Toro, Panama. The ISME Journal: 12; 2238-2251. The dissertation author was the primary investigator and author of this material.

CHAPTER 3

The bacterial Type Six Secretion System enables intraguild predation

Abstract

Bacteria with the Type Six Secretion System (T6SS) have been shown to kill other bacteria, but the ecological implications of these killing events have not been fully explored. Here we test the effect of T6SS on the ecological success of a *Vibrio cholerae* strain using isotopic labeling, intraguild challenges, single cell analyses and growth experiments. Our experiments with wild-type (WT) *V. cholerae* compared to mutants with an inactive T6SS confirm previously documented high mortality of competitor bacteria in intraguild challenges. Further, we show that the WT *V. cholerae* assimilated prey lysate, utilized DNA as a nutrient, and grew better with a functional T6SS in the presence of susceptible prey. These results support the hypothesis that bacterial T6SS increases the predator's success by reducing competition while providing the predator with nutrients.

Main

Bacterial population structure and function in the marine environment is controlled in part by bacteria–bacteria interactions, known metaphorically as "sideways control"[1]. While 'negative' sideways controls have been shown to reduce or eliminate bacterial competitors (e.g. antagonism)[2], little is known about bacterial antagonism as a means to consume prey bacteria. Such interactions also serve as a "bottom–up control"[1] as the prey are utilized for nutrients. Few studies on *Bdellovibrio* and like organisms (BALOs) in the marine environment have shown that BALOs invade and digest their bacterial prey[3, 4]. However, to our knowledge there are no published reports of marine bacteria using other mechanisms to kill bacteria for consumption.

One experimentally tractable mechanism that may facilitate such an interaction is the Type Six Secretion System (T6SS), a nanomachine that is harbored by ~25% of sequenced

gram–negative bacteria[5]. Capable of killing prokaryotes[6] and eukaryotes[7], T6SS injection of toxic effector proteins into neighboring cells ultimately leads to lysis of susceptible prey[8]. In a perspective article[9], authors Pukatzki and Provenzano hypothesized that the marine bacterium and human pathogen, *Vibrio cholerae*, employs its T6SS to engage in intraguild predation, whereby the predator consumes its competing prey[10]. However, this hypothesis is difficult to test given the confounding challenges inherent to distinguishing strain–specific growth and/or assimilation of prey–derived substrates, with high sensitivity, in a heterologous bacterial population.

Here we used nanoscale secondary ion mass spectrometry (NanoSIMS) to test if T6SS–harboring *V. cholerae* assimilated carbon from its prey, *Vibrio harveyi*. In a competition assay, ^{13}C–labeled *V. harveyi* was challenged against a predator strain for 8h on Zobell 2216E agar. The predator was either wild–type (WT) *V. cholerae*, which possessed a constitutively firing T6SS (WT challenge), or a T6SS–inoperable mutant, *V. cholerae ΔvipA* (*ΔvipA* challenge). In accordance with a previous study[11], we found that *V. harveyi* was indeed susceptible to *V. cholerae* T6SS–mediated toxicity. We observed an 85–fold decrease in recovered *V. harveyi* colony forming units (CFUs) in the WT challenge, in comparison to the *ΔvipA* challenge (two–tailed t–test, $p < 0.0001$; Figure 3.1a).

To trace the uptake of ^{13}C–labeled prey lysate by the predator, triplicate samples from each challenge assay, and 0h and 8h controls for all strains, were formalin fixed, filtered onto 0.2 μm polycarbonate–membrane filters, and prepared for NanoSIMS analysis (see Methods). The controls were used to determine the initial label of the predator and prey strains, and to determine the proportion of label that was retained after 8h incubation on the unlabeled media. 30 μm x 30 μm areas (n = 8–12) were analyzed for each of the three replicate filters per treatment. Single

cells (Figure 3.1b, c) were quantitatively analyzed to determine ^{13}C atom percent excess (APE), the percent enrichment of the rare isotope (^{13}C) above natural abundance (Figure 3.1d, e; Table S3.1). The predator and prey were distinguished by k–means cluster analysis[12-14], which yielded a cutoff of 0.81 ^{13}C APE (Figure 3.1d, e; Supplementary Note). This cutoff is less than the minimum enrichment observed for *V. harveyi* in the *ΔvipA* challenge, and given the average survival of *V. harveyi* in the WT challenge, this cutoff is conservative (see Supplementary Note).

Our statistical analysis of the cutoff–defined cell populations showed that *V. cholerae* was significantly enriched with ~40% more ^{13}C in the WT challenge, in comparison to the *ΔvipA* challenge (Mann–Whitney U Test, $p < 0.0001$; Kolmogorov–Smirnov Test, $p = 0.0001$; Figure 3.1f, g; Table S3.1). We calculated, that on average, 0.41% of the carbon assimilated into biomass by WT *V. cholerae* was derived from the prey, while single–cells within that population were comprised of up to 3.8% prey–carbon (see Methods). Note that these should be considered lower assimilation estimates since our cutoff excluded the possibility that WT *V. cholerae* cells had higher than 0.81 ^{13}C APE. While the cutoff was implemented to be conservative, it is reasonable to surmise that some WT *V. cholerae* cells had enrichments above that cutoff (up to a maximum observed value of 8.1 ^{13}C APE; Supplementary Note), suggesting that select single–cells may have been comprised of up to 48% prey–carbon.

Having conclusively demonstrated that WT *V. cholerae* consumed its prey *in situ*, we then designed a proof–of–concept experiment to determine the utilizability of prey lysate. Amendment of *V. harveyi*–lysate as the sole carbon source to artificial seawater (ASW) cultures of WT *V. cholerae* or *V. cholerae thyA*, a thymine auxotroph, resulted in ~140–fold increases in cell yields for both treatments, in comparison to the non–amended controls (two–tailed t–test, $p < 0.001$; Figure 3.2). These results indicate that the bacterial lysate can be readily used as a carbon

source, and furthermore, that the DNA can provide nucleic acid bases, such as thymine. We also observed that cell yields significantly increased when ASW cultures of WT *V. cholerae* were amended with purified DNA or ribosomes, in comparison to the non–amended controls (two–tailed t–test, $p < 0.01$; Figure S3.1). The apparent ability of *V. cholerae* to degrade and assimilate organic matter from DNA and ribosomes—both of which constitute a major fraction of bacterial biomass and are enriched with nitrogen and phosphorous—suggests that consumption of bacterial lysate could be advantageous in both carbon–rich and carbon–limited environments. Furthermore, studies have demonstrated that exogenous DNA, including released DNA from T6SS–killed prey can be taken up by *V. cholerae* and used for horizontal gene transfer[15-17]. Our demonstration that *V. cholerae* readily grows on the DNA from lysed bacteria supports an alternative hypothesis—that the DNA could also be used for nutrients.

Finally, we tested if T6SS functionality provided the predator with a growth advantage. Competition assays with unlabeled predator and prey were run in otherwise identical conditions to those described in our NanoSIMS experiments, and both the predator and the prey were recovered. Recovery of *V. harveyi* CFUs was ~85–fold less in the WT challenge, in comparison to the *ΔvipA* challenge; while recovery of WT *V. cholerae* CFUs was ~4–fold higher (two–tailed t–test, $p < 0.01$; Figure S3.2). We hypothesize that the near elimination of competing *V. harveyi* led to the higher growth yield that was observed, presumably due to a relative increase in nutrient availability from both the media and the prey–lysate.

Collectively, our results demonstrate that the bacterial T6SS enables intraguild predation, increasing predator success through the acquisition of nutrients from prey lysate and reduction of competition. Given the high prevalence of bacteria with contact-dependent growth inhibition systems, such as the T6SS, we suggest that intraguild predation may play an important role in

nutrient cycling in high bacterial density marine habitats such as marine snow, fecal pellets, and sediment. Future work might also consider the impact of intraguild predation in other systems, including animal and human microbiomes.

Acknowledgments

We are grateful to B. Ho and J. Toska for assistance and discussion. We thank B. Stock for help with data analysis. This work was supported by the Gordon and Betty Moore Foundation, Marine Microbial Initiative grant (4827) to (FA) and from the LLNL biofuels Science Focus Area grant #SCW1039 from DOE's Genomic Sciences Program. Parts of this study were performed under the auspices of the US Department of Energy at the Lawrence Livermore National Laboratory under Contract DE-AC52-07NA27344.

Figures

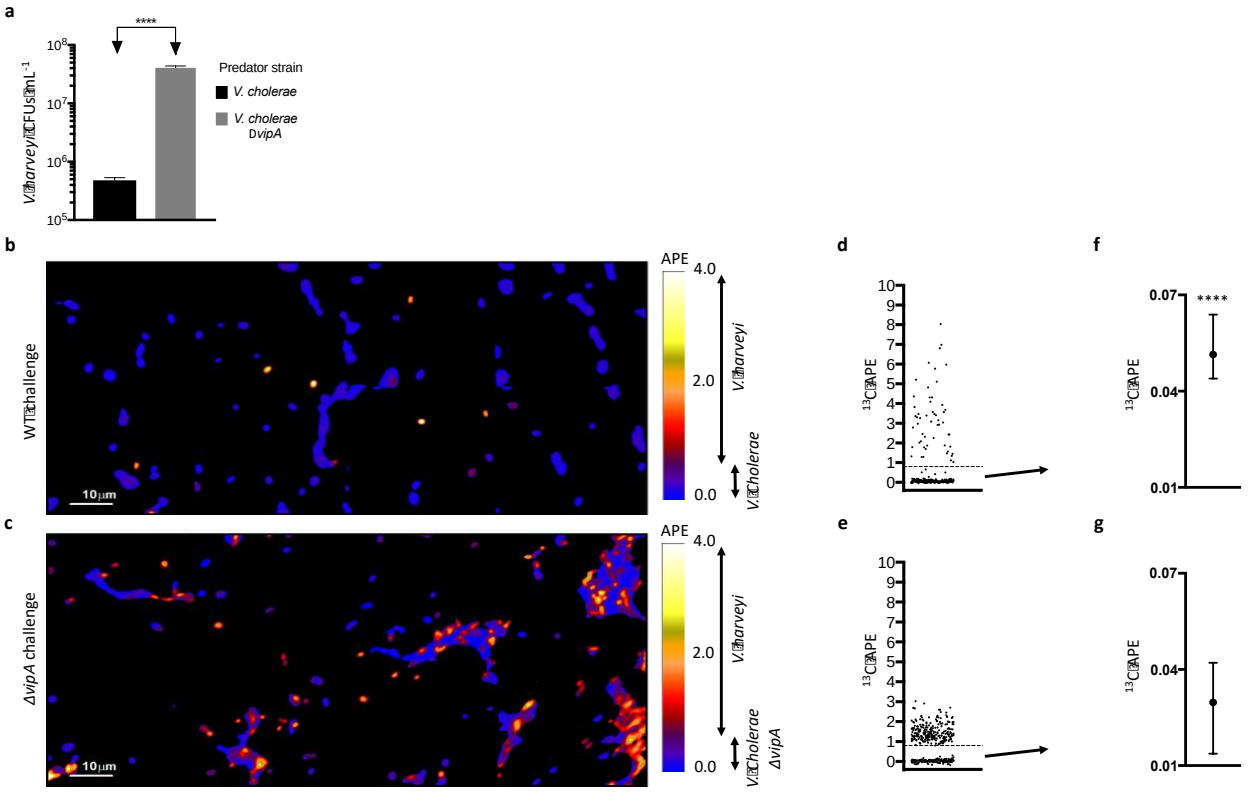

Figure 3.1 *V. harveyi* (prey) versus WT *V. cholerae* or *V. cholerae ΔvipA* (predators). (a) Recovered *V. harveyi* CFUs (y–axis) from the WT challenge (black) and the *ΔvipA* challenge (grey). Error bars represent the mean ± SD of three independent replicates. **** (two–tailed t–test, $p < 0.0001$). (b, c) Representative NanoSIMS images showing ^{13}C atom percent excess (APE) of the predator and prey strains from each challenge. (d, e) Summarized NanoSIMS data showing ^{13}C APE of individual ROIs from the WT challenge (d) and the *ΔvipA* challenge (e). ROIs falling below the analysis cutoff (dashed line, 0.81% ^{13}C APE) were scored as predators, while ROIs above the cutoff were scored as prey. (f, g) Median ± 95% confidence intervals for the ^{13}C APE of WT *V. cholerae* (f) and *V. cholerae ΔvipA* (g). **** (Mann–Whitney U Test, $p < 0.0001$; Kolmogorov–Smirnov Test, $p = 0.0001$).

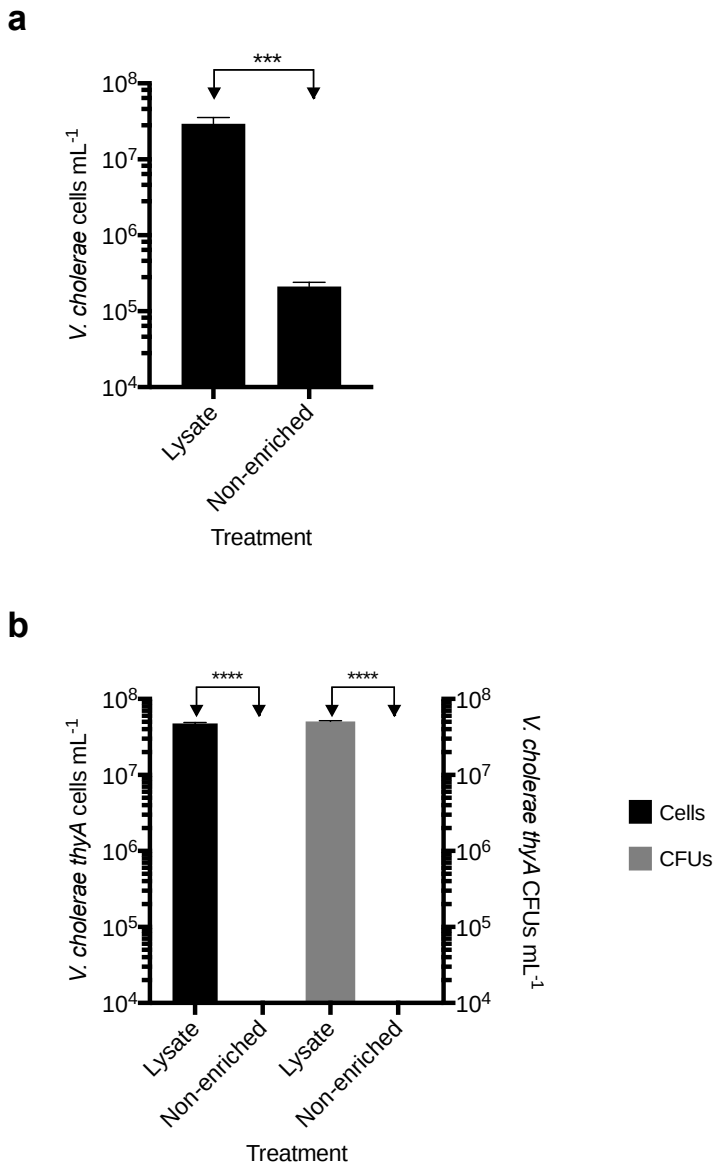

Figure 3.2 Artificial seawater cultures with and without amendment of *V. harveyi*–lysate to WT *V. cholerae* (a) or *V. cholerae thyA*, a thymine auxotroph (b). Incubations took place for 24h. Error bars represent the mean ± SD. Statistical differences between treatments are denoted by asterisks (two–tailed t–test, ***$p < 0.001$; ****$p < 0.0001$). CFUs (grey bars) were enumerated for *V. cholerae thyA* in addition to the microscopy–based cell counts (black bars) to ensure that the recovered cells maintained their antibiotic resistance to trimethoprim, an antibiotic which inhibits bacterial synthesis of thymine.

APPENDIX 3.1: SUPPLEMENTARY INFORMATION

Supplementary Note

This note addresses the identification of WT *V. cholerae* predator cells to calculate ^{13}C incorporation from *V. harveyi* prey lysate. We established a conservative cutoff value (0.81 ^{13}C APE) below which all cells from the challenge assays should be WT *V. cholerae* or *V. cholerae ΔvipA*. This cutoff value was based on both k–means cluster analysis and the lowest *V. harveyi* ^{13}C enrichment observed in the *ΔvipA* challenge. We also discuss the basis for our upper estimate of WT *V. cholerae* enrichment (8.1 ^{13}C APE).

We used k–means cluster analysis in an attempt to distinguish predator from prey based on ^{13}C APE of single cells (selected as regions of interest; ROIs) plotted for each experimental treatment. K–means has been used as an effective method for grouping cells according to their isotope ratios in stable isotope probing and NanoSIMS studies[14]. It is a partitional cluster analysis method that uses a known, fixed number of clusters (k), and a starting configuration of cluster centers[12, 13]. The analysis then assigns each ROI to the clusters and uses an iterative refinement technique to optimize the ROI's membership to that cluster. In this way, the sum of square distance is minimized between the cluster center and the ROI.

Our k–means analysis of the *ΔvipA* challenge resulted in distinct clusters for the predator and prey populations (Figure S3.3a). However, clustering for the WT challenge was less clear, as the plotted ROIs were more dispersed along the y–axis (Figure S3.3b). Therefore, we set a conservative cutoff for the identification of WT *V. cholerae* at 0.81 ^{13}C APE for our statistical analysis and for calculating the lower estimate of prey assimilation. The cutoff was based both on the k–means analysis of the *ΔvipA* challenge, which showed 0.81 ^{13}C APE for the least enriched of the 243 *V. harveyi* cells (Figure S3.31a), and the fact that all *V. harveyi* cells in the

8h control (n = 104) had ^{13}C APE above 0.81 (Figure S3.3d; Table S2). However, we expect that a portion, if not all of the more ^{13}C–enriched cells in the WT challenge were actually *V. cholerae* cells.

To assess the likelihood that a portion of cells in the WT challenge with > 0.81 ^{13}C APE were *V. cholerae*, we considered two issues: (1) the possibility that some of the analyzed cells were residual dead–*V. harveyi*, and (2) the probability that *V. harveyi* survived the WT challenge. The following discussion addresses both of these issues.

(1) Our data do not support the hypothesis that residual dead–*V. harveyi* remained after 8h in the WT challenge. We found that the ^{13}C labeling of *V. harveyi* cells in the *ΔvipA* challenge at 0h (median = 24.4 ^{13}C APE; Figure S3.3c) was diluted ~16–fold to 1.5 ^{13}C APE after the 8h competition assay (Figure S3.3a). Assuming this same exponential dilution rate for *V. harveyi* in the WT challenge and the results of previous work that definitively showed that prey are killed within two hours during T6SS–mediated competition assays[7], the average ^{13}C label of *V. harveyi* in the WT challenge would have been down to 12.2 ^{13}C APE by the time *V. harveyi* was killed. Given the result that no cells in the WT challenge exhibited ^{13}C APE values above 8.1 ^{13}C APE, we conclude it is unlikely that our analysis included residual dead–*V. harveyi*.

(2) We assert that live *V. harveyi* would have been rare after 8h in the WT challenge because our experiments have shown that 98.8% of the *V. harveyi* population was killed (Fig. 3.1a). Based on binomial statistics, we expect that a maximum of 8 out of the 246 analyzed cells in the WT challenge could have been live *V. harveyi* at the 8h experiment termination (Wilson/Brown binomial proportions, lower limit = 0 cells; upper limit = 8 cells; mean = 3 cells). By comparison, we found 54 cells in the WT challenge that

exhibited ^{13}C APE values that were in the range of analyzed *V. harveyi* cells in the 8h control incubation (Figure S3.3d) and the *ΔvipA* challenge (Figure S3.3a). Thus, while up to eight of the analyzed cells in the WT challenge could have been *V. harveyi* survivors, we expect at least 46 of the cells to have been *V. cholerae*.

Based on this analysis, most, if not all of the analyzed cells in the WT challenge were likely *V. cholerae*. Therefore, while we used 0.81 ^{13}C APE as a conservative cutoff for our statistical analysis and for calculating the lower estimate of prey lysate assimilation, there is a sound basis for posing an upper assimilation estimate of up to 8.1 ^{13}C APE for select-single cells of WT *V. cholerae*.

Supplementary Materials and Methods

Bacterial strains

WT *V. cholerae 2740–80*, and its T6SS–inoperable derivative, *V. cholerae ΔvipA*, have been previously described[18]. *V. cholerae thyA*, a thymine auxotroph, was selected for by plating 10^8–10^9 cells of *V. cholerae* on M9 glycerol with 0.01% thymine plus trimethoprim (TMP). TMP–resistant mutants lack ThyA activity and grow at the expense of exogenous thymine[19]. TMP resistant colonies were purified through successive streaking and then plated onto M9 glycerol with TMP and 2 mg mL^{-1} DNA (Salmon testes, Sigma Cat# D1626). Colonies that grew at the expense of exogenous DNA were used in the lysate amendment experiments (described below). Model prey, *Vibrio harveyi* strain B392 has been described previously[20]. The following concentrations of antibiotics were used where indicated: streptomycin, 100 µg mL^{-1}; rifampicin, 50 µg mL^{-1}; trimethoprim, 10 µg mL^{-1}.

Competition assays

V. harveyi was grown in 0.22–µm filtered autoclaved seawater (FASW) that was enriched with $NaNO_3$ (88 µM final), NaH_2PO_4 (3.6 µM final), 0.1 g L^{-1} yeast extract, 0.5 g L^{-1} peptone, and D–glucose–$^{13}C_6$ (0.4% final, Sigma–Aldrich, Cat# 389374). The *V. cholerae* strains were grown in Zobell 2216 E. All cultures were grown for 18h, diluted 1000–fold into fresh media, and then grown overnight. The cultures were then washed, diluted 50–fold into fresh media, and grown for 2–3h until they reached mid–exponential phase. All strains were cultured with shaking at 25C. Centrifugation was conducted at 10,000 x G for 4 minutes.

Once the cultures reached mid–exponential phase they were concentrated to an OD_{600} of 10.0 in Zobell 2216 E. To determine the initial isotopic–label (APE at 0h), aliquots of each strain were immediately fixed with formalin (2% final) and processed as described below. For the experimental treatments, 10 µl volumes of WT *V. cholerae* or *V. cholerae ΔvipA* were mixed 1:1 (v:v) with *V. harveyi*. 5 µl aliquots of the co–cultures were spotted onto Zobell agar plates and allowed to compete for 8h. In parallel, 5 µl aliquots of each strain were also independently plated onto Zobell 2216 E to determine the isotopic–label (%) that remained after 8h incubation (8h control). After incubation, the cells from each treatment were resuspended from the plate into FASW. Aliquots were immediately filtered onto white 0.2 µm pore–size polycarbonate filters (MilliporeSigma, Burlington, MA, USA), rinsed twice with FASW, then fixed with 2% formalin while in the filtration rig. The filters were then washed three times with MilliQ water and air–dried. The dried filters were sectioned with sterile scissors and prepared for NanoSIMS analysis. Aliquots from each treatment were also serial–diluted and plated onto antibiotic selection media to recover and enumerate the surviving *V. cholerae* strains (streptomycin) or *V. harveyi* (rifampicin).

NanoSIMS analysis

The sectioned filters were mounted to analysis substrates with conductive tabs and coated with ~5 nm of gold. NanoSIMS analysis was performed at Lawrence Livermore National Laboratory using a NanoSIMS 50 (Cameca, Gennevilliers, France). Prior to analysis, samples were sputtered to a depth of ~60 nm with 90 pA of Cs^+ current to achieve sputtering equilibrium and to ensure that the analysis was of intracellular material. For each filter, a primary $^{133}Cs^+$ ion beam (2 pA, ~150 nm diameter, 16 keV) was rastered over 30 x 30 μm analysis areas (n= 8–12) with 256 x 256 pixels and a dwell time of 1 ms/pixel, for 19–30 scans (cycles). The secondary ion mass spectrometer was tuned for ~7000 M/ΔM. Secondary electron images and quantitative secondary ion images were simultaneously collected for $^{12}C_2^-$, $^{13}C^{12}C^-$, and $^{12}C^{14}N^-$, on individual electron multipliers in pulse counting mode[21].

The NanoSIMS data were processed using L'Image (http://limagesoftware.net). Ion image data were deadtime and image shift corrected before producing $^{13}C^{12}C^-/^{12}C^{12}C^-$ ratio images, which reflect the level of ^{13}C incorporation into biomass. Regions of interest (ROIs) for isotopic ratio quantification were drawn around each cell. These ratios were extracted by cycle and averaged. Note that $^{13}C^{12}C^-/^{12}C_2^-$ is divided by two to calculate the $^{13}C/^{12}C$ ratio. The data are presented as ^{13}C atom percent excess (APE), which are calculated from the initial (R_i) and final (R_f) $^{13}C/^{12}C$ ratios: $APE = [R_f/(R_f + 1) - R_i/(R_i + 1)] \cdot 100\%$[22]. Cluster analysis of ^{13}C APE was performed in R using the default 'kmeans' function[14, 23]. The fraction of carbon assimilated by the predator from the prey was calculated by subtracting the mean ^{13}C APE of the WT *V. cholerae* population after 8h competition assays (0.07; Table S3.1) by its ^{13}C initial APE (0.0, Table S3.2), divided by the ^{13}C APE of source (17.3, *V. harveyi* at 1 h). The same calculation was also performed to estimate prey assimilation for the most enriched ROI from our cutoff-

defined population (0.66 ^{13}C APE) and for the most enriched of all ROIs in the WT challenge (8.1 ^{13}C APE). The calculation assumes that the ^{13}C of *V. harveyi* in the WT challenge diluted at the same exponential rate as *V. harveyi* in the *ΔvipA* challenge (from 24.4 ^{13}C APE at 0h to 1.5 ^{13}C APE at 8h; Tables S3.1, 2).

Vibrio cholerae growth on lysate

Overnight cultures of the *V. cholerae* strains were grown in liquid Zobell 2216 E, diluted 1: 10,000 in artificial seawater[24], and acclimated for 24h with shaking. The cultures were then diluted ~100–fold into fresh ASW to obtain cell concentrations of 5 x 10^4 mL^{-1} or 2.5 x 10^5 mL^{-1} and incubated for 24h with and without amendment. Each treatment consisted of three independent replicates (10 mL volumes). The treatments included: (1) *V. harveyi* lysate (WT *V. cholerae* was amended with ~6 x 10^7 lysed *V. harveyi* cells mL^{-1}, *V. cholerae thyA* was amended with ~6 x 10^8 lysed *V. harveyi* cells mL^{-1}); (2) DNA (3.3, 33.3, or 333.3 µg mL^{-1}; Salmon testes, MilliporeSigma); or (3) Ribosomes (3.3 µg $mL^{-}1$; *E. coli*, New England BioLabs, Ipswich, MA, USA). WT *V. cholerae* and *V. cholerae thyA* were grown with streptomycin or streptomycin and trimethoprim, respectively. To obtain bacterial lysate, an overnight culture of streptomycin–sensitive *V. harveyi* was washed, re–suspended in ASW plus streptomycin, and subjected to three successive passages through a French press at ~18,000 psi. Microscopic examination confirmed that the *V. harveyi* cells were lysed. In a parallel control, *V. haveyi* lysate was incubated in ASW plus streptomycin and plated on streptomycin containing agar. The lack of cell growth that was observed indicates that no *V. harveyi* cells were included in our *V. cholerae* cell counts.

Samples from each replicate (1–2 mL) were fixed with 2% formalin, filtered onto 0.2 µm pore–size polycarbonate filters, and stained with DAPI Vectashield (Vector Labs., Burlingame,

CA)[25]. At least 200 cells from 10 or more fields of view were counted by epifluorescence microscopy. To ensure that the cultures were bacteriophage–free, one sample from each treatment was also filtered onto a 0.02 µm pore–size Anodisc filter (Whatman, GE Life Sciences, Marlborough, MA, USA) then stained with SYBR Green I (Invitrogen, Carlsbad, CA, USA) to enumerate virus–like–particles (VLPs)[26]. No VLPs were observed on any of the filters. Sub–samples from the *V. cholerae thyA* cultures were also serial diluted and plated onto streptomycin plus trimethoprim containing plates to ensure that the recovered cells maintained their antibiotic resistance to trimethoprim.

Statistics

GraphPad Prism version 7.0 (GraphPad Software, Inc.) was used for statistical analyses.

References

[1]Fuhrman, J. A. & Hagstrom A. In: Kirchman, D (ed). Microbial Ecology of the Oceans. John Wiley & Sons, Inc., 299-334(2008).

[2]Long, R. A. & Azam F. Antagonistic Interactions among Marine Pelagic Bacteria. Appl Environ Microbiol. 2001;67:4975-4983.

[3]Yair, S., Yaacov D., Susan K. & Jurkevitch E. Small eats big: Ecology and diversity of Bdellovibrio and like organisms, and their dynamics in predator–prey interactions. Agronomie. 2003;23:433–439.

[4]Welsh, R. M., Zaneveld J. R., Rosales S. M., Payet J. R. M. P., Burkepile D. E. & Thurber R. V. Bacterial predation in a marine host-associated microbiome. The ISME Journal. 2016;10:1540–1544.

[5]Boyer, F., Fichant G., Berthod J., Vandenbrouck Y. & Attree I. Dissecting the bacterial type VI secretion system by a genome wide in silico analysis: what can be learned from available microbial genomic resources? BMC Genomics. 2009;10:104.

[6]Pukatzki, S., Ma A. T., Sturtevant D., Krastins B., Sarracino D., Nelson W. C., Heidelberg J. F. & Mekalanos J. J. Identification of a conserved bacterial protein secretion system in

Vibrio cholerae using the Dictyostelium host model system. Proc. Natl. Acad. Sci. U S A. 2006;103:1528-1533.

[7]Macintyre, D. L., Miyata S. T., Kitaoka M. & Pukatzki S. The Vibrio cholerae type VI secretion system displays antimicrobial properties. Proc. Natl. Acad. Sci. USA. 2010;107:19520-19524.

[8]M. Basler, Ho B. T. & Mekalanos J. J. Tit-for-tat: type VI secretion system counterattack during bacterial cell-cell interactions. Cell. 2013;152:884-94.

[9]Pukatzki, S. & Provenzano D. Vibrio cholerae as a predator: lessons from evolutionary principles. Front Microbiol. 2013;4:384.

[10]Polis, G. A., Myers C. A. & Holt R. D. The ecology and evolution of intraguild predation: potential competitors that eat each other. Annu Rev Ecol Syst. 1989;20:297-330.

[11]Unterweger, D., Kitaoka M., Miyata S. T., Bachmann V., Brooks T. M., Moloney J., Sosa O., Silva D., Duran-Gonzalez J., Provenzano D. & Pukatzki S. Constitutive type VI secretion system expression gives Vibrio cholerae intra- and interspecific competitive advantages. PLoS One. 2012;7:e48320.

[12]Lance, G. N. & Williams W. T. A general theory of classificatory sorting strategies II. Clustering systems. Comput J. 1967; 10:271–277.

[13]Macqueen, J. Some methods for classification and analysis of multivariate observations. Proc of the fifth Berkeley Symp on Math Statis and Prob. 1967;281–297.

[14]Dawson, K. S., Scheller S., Dillon J. G. & Orphan V. J. Stable Isotope Phenotyping via Cluster Analysis of NanoSIMS Data As a Method for Characterizing Distinct Microbial Ecophysiologies and Sulfur-Cycling in the Environment. Front Microbiol. 2016;7:774.

[15]Borgeaud, S., Metzger L. C., Scrignari T. & Blokesch M. The type VI secretion system of Vibrio cholerae fosters horizontal gene transfer. Science. 2015;347:63-67.

[16]Veening, J. W. & Blokesch M. Interbacterial predation as a strategy for DNA acquisition in naturally competent bacteria. Nat Rev Microbiol. 2017;15:621-629.

[17]Ellison, C. K., Dalia T. N., Ceballos A. V., Wang J. C.-Y., Biais N., Brun Y. V. & Dalia A. B. Retraction of DNA-bound type IV competence pili initiates DNA uptake during natural transformation in Vibrio cholerae. Nat Microbiol. 2018;3:773-780.

[18]Basler, M., Pilhofer M., Henderson G. P., Jensen G. J. & Mekalanos J. J. Type VI secretion requires a dynamic contractile phage tail-like structure. Nature. 2012;483:182-6.

[19]Neuhard, J. & Kelln R. A. In: Neidhardt, FC et al. (eds). Am. Soc. Microbiol.: Washington, DC, 580-599(1996).

[20]Ruby, E. G. & Nealson K. H. Seasonal changes in the species composition of luminous bacteria in nearshore water. Limnol.Oceanogr. 1978;23:530-533.

[21]Pett-Ridge, J. & Weber P. K. In: A., N (ed). Microb. Syst. Biol. Humana Press, Totowa, NJ, 375-408(2012).

[22]Popa, R., Weber P. K., Pett-Ridge J., Finzi J. A., Fallon S. J., Hutcheon I. D., Nealson K. H. & Capone D. G. Carbon and nitrogen fixation and metabolite exchange in and between individual cells of Anabaena oscillarioides. ISME J. 2007;1:354-60.

[23]J. A. Hartigan & Wong M. A. Algorithm AS 136: A K-means clustering algorithm. J. Royal Stat. Soc. 1979;28:100-108.

[24]Cohen, W. D. 1997. Biol. Bull. Comp. Available: http://comm.archive.mbl.edu/publications/biobull_comp.html.

[25]Porter, K. & Feig Y. The use of DAPI for identifying and counting aquatic microflora. Limnology and Oceanography. 1980;25:943-948.

[26]Noble, R. & Fuhrman J. Use of SYBR Green I for rapid epifluorescence counts of marine viruses and bacteria. Aquatic Microbial Ecology. 1998;14:113-118.

Supplementary Figures

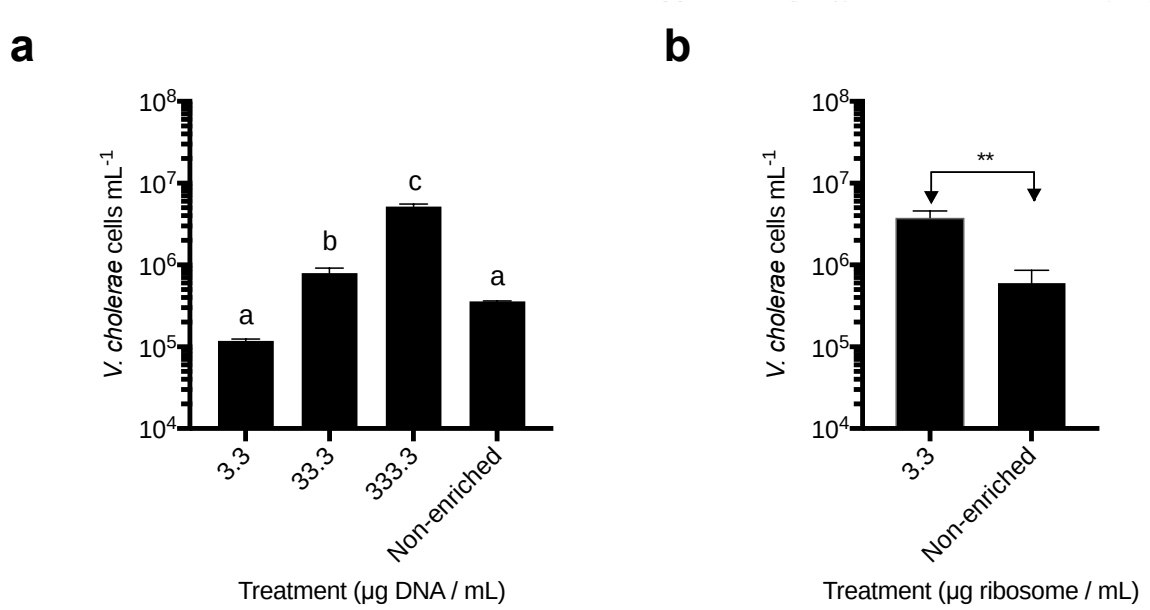

Figure S3.1 WT *V. cholerae* cells mL^{-1} (y–axis) after 24h artificial seawater incubations with and without amendment of DNA (a) or ribosomes (b). Error bars represent the mean ± SD. Statistical differences between treatments are denoted by asterisks (two–tailed t–test, **$p < 0.01$); or letters (ordinary one–way ANOVA, $\alpha = 0.05$) where statistically significant differences among treatments are denoted by different letters (Sidak's multiple comparisons test, a; b; c; d).

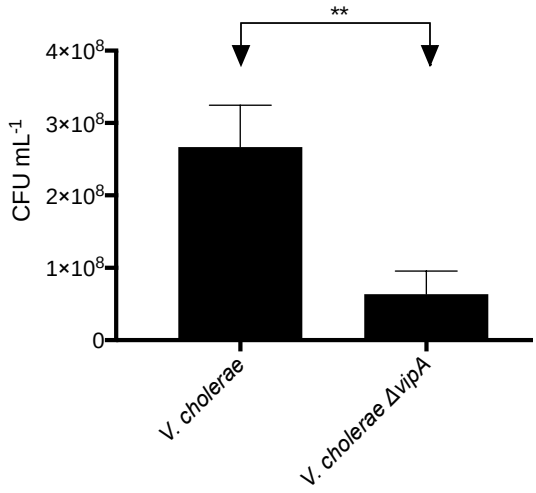

Figure S3.2 Recovery of WT *V. cholerae* and *V. cholerae vipA* CFUs (y–axis) after 8h competition assays versus *V. harveyi*. Error bars represent the mean ± SD of three independent replicates. **(two–tailed t–test, $p < 0.01$).

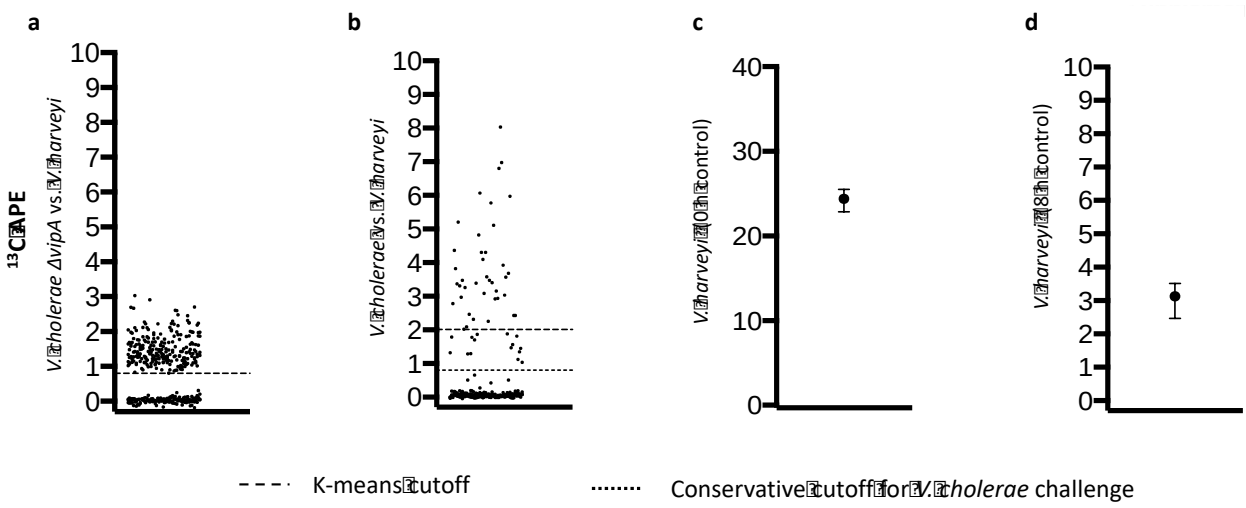

Figure S3.3 Distinction of predator and prey cell populations. The ^{13}C APE calculated from each region of interest (ROI) identified in the Δ*vipA* challenge (a) and the WT challenge (b) were plotted on the y–axis. Each ROI represents a single cell. The x–axis was expanded to show individual ROIs. K-means cluster analysis established cutoffs (dashed–lines) for the identification of the predator strains (below the lines) and prey (above the lines). The dotted–line indicates a conservative cutoff value that was applied for the identification of predator and prey in the WT challenge. The median ± 95% confidence intervals for *V. harveyi* controls at 0h (c) and 8h (d) are shown for comparison. Note the difference in scale (y-axis) between scatter plots a, b, d versus c.

Supplementary Tables

Table S3.1 Summarized data of ^{13}C atom percent excess (APE) for all ROIs respective to their treatment in Figure 3.1b,c.

	V. cholerae vs. *V. harveyi*		*V. cholerae* Δ*vipA* vs. *V. harveyi*	
	V. cholerae	***V. harveyi***	***V. cholerae* Δ*vipA***	***V. harveyi***
Sample size (n)	192	54	141	243
Median ^{13}C APE	0.05	3.06	0.03	1.46
Actual confidence level	96.39%	95.98%	95.71%	96.01%
Lower confidence limit	0.04	2.43	0.01	1.34
Upper confidence limit	0.06	3.47	0.04	1.47
Mean ^{13}C APE	0.07	3.22	0.03	1.50
Std. Error of Mean	0.01	0.22	0.01	0.03
Shapiro-Wilk normality test				
W	0.7133	0.9255	0.979	0.9352
P value	<0.0001	0.0024	0.0289	<0.0001
Passed normality test (alpha=0.(	No	No	No	No
P value summary	****	**	*	****
D'Agostino & Pearson normality test				
K2	170.1	8.865	6.953	35.43
P value	<0.0001	0.0119	0.0309	<0.0001
Passed normality test (alpha=0.(	No	No	No	No
P value summary	****	*	*	****

Mann Whitney test:	
V. cholerae* vs. *V. cholerae* Δ*vipA	
P value	<0.0001
Exact or approximate P value?	Approximate
P value summary	****
Significantly different (P < 0.05	Yes
One- or two-tailed P value?	Two-tailed
Sum of ranks	35762 , 19850
Mann-Whitney U	9839
Difference between medians	
Median of *V. cholerae*	0.0514, n=192
Median of *V. cholerae* Δ*vipA*	0.0297, n=141
Difference: Actual	-0.0217
Difference: Hodges-Lehmann	-0.0296

Kolmogorov-Smirnov test:	
V. cholerae* vs. *V. cholerae* Δ*vipA	
P value	0.0001
Exact or approximate P value?	Approximate
P value summary	***
Significantly different (P < 0.05	Yes
Kolmogorov-Smirnov D	0.2439

*ROIs above the dashed line in Fig. 1b, c were scored as *V. harveyi* , those below as *V. cholerae* or *V. cholerae* Δ*vipA*.

Table S3.2 Summarized data of ^{13}C atom percent excess (APE) for the 0h and 8h controls.

		^{13}C APE					
		V. cholerae		*V. cholerae* Δ*vipA*		*V. harveyi*	
		0 h	8 h	0 h	8 h	0 h	8 h
	n (cells)	15	63	22	85	22	104
	Median	0.00	0.00	0.00	0.00	24.39	3.60
95% CI of median	Actual confidence level	96.5%	95.7%	98.3%	97.1%	98.3%	96.1%
	Lower confidence limit	0.00	0.00	0.00	0.00	22.86	3.50
	Upper confidence limit	0.00	0.00	0.00	0.00	25.52	3.68

Chapter 3, in full, has been submitted for publication of the material. Guillemette, R., Ty J. Samo, Xavier Mayali, Peter K. Weber, John J. Mekalanos, and Farooq Azam. The bacterial Type Six Secretion System enables intraguild predation. The dissertation author was the primary investigator and author of this material.

CHAPTER 4

Insight into the resilience and susceptibility of marine bacteria to T6SS attack by *Vibrio cholerae* and *Vibrio coralliilyticus*

Abstract

The type 6 secretion system (T6SS) is carried by many bacteria and is capable of killing adjacent bacterial cells in a contact-dependent manner. T6SS-mediated killing of prey bacteria can lead to ecological advantages for the bacterial predator, however, relatively little is known about the range of prey bacteria that are susceptible to T6SS attack. In this study, 15 diverse marine bacterial isolates from the phyla Bacteroidetes and ɣ-Proteobacteria were challenged against the marine bacterium and human pathogen, *Vibrio cholerae*, which has a well described T6SS. We found that the T6SS of *V. cholerae* killed a subset of the tested ɣ-Proteobacteria, including members of the orders Vibrionales, Alteromonadales, Oceanospirillales, and Pseudomonadales. *V. cholerae* also co-existed with multiple Bacteroidetes and ɣ-Proteobacteria, and was specifically killed by only one of the isolates, *Vibrio coralliilyticus*. Follow-up experiments revealed that five *V. coralliilyticus* strains, including known coral and shellfish pathogens were not only able to survive the T6SS challenge against *V. cholerae*, but also killed *V. cholerae*. Predicted protein comparisons and mutagenesis strongly suggested that *V. coralliilyticus* may have used its own T6SS to kill *V. cholerae*, and showed that *V. coralliilyticus* was not immune to the *V. cholerae* T6SS. Presumably, *V. coralliilyticus* protected itself from *V. cholerae* T6SS-mediated killing by striking first, or more effectively with its own T6SS. This study provides greater insight into the killing efficacy of the *V. cholerae* T6SS against marine bacteria, while describing a potentially analogous lethal system in *V. coralliilyticus*, both of which have implications for human health, aquaculture, and coral pathogenesis.

Introduction

Bacterial-bacterial antagonism plays a major role in shaping bacterial community structure and function[1-5], however there is only a modest amount of information available regarding the nature and mechanisms of such interactions. The early studies investigating marine bacterial-bacterial antagonism predominantly focused on the production and release of antibiotics by predatory bacteria as a means to inhibit their preys' growth[6-8]. While their findings demonstrated that marine bacteria were in fact capable of killing other bacteria, it has been suggested that the relatively low frequency of killing that was observed may have been due to the common use of non-marine bacteria as model prey[9]. Later, experiments that used more ecologically-relevant bacterial prey species from pelagic seawater, marine particles, and coral found that killing occurred in > 50% of their competition assays[9, 10]. Taken together, these studies highlighted the need for more ecologically relevant predator and prey in laboratory antagonism assays, and also implied that a substantial proportion of the tested marine bacteria were able to defend themselves against bacterial antagonism techniques that had been demonstrated to kill non-marine bacterial types.

In addition to chemical-mediated bacterial growth inhibition, marine bacteria have been shown to possess and use a wide variety of other antibacterial mechanisms. For example, bdellovibrios have long been known to prey upon marine bacteria by invading their prey and digesting them from the inside out[11, 12]. Recent studies have demonstrated that bdellovibrios, such as *Halobacteriovorax,* can influence bacterial communities associated with corals and that they were able to readily consume coral-associated bacteria including known coral pathogens[13, 14]. Another example of predatory marine bacteria is represented by the *Saprospiraceae* family, such as the bacterium *Saprospira grandis*, which traps bacteria on a mucilaginous substance

using a method known as ixotrophy. *S. grandis* then kills its prey via cell-cell contact, presumably through expression of a needle-like rhapidosome, digestive enzymes, or a combination of both mechanisms[15]. Evidence suggests that other killing techniques mediated by cell-cell contact, commonly known as contact-dependent growth inhibition (CDI) are highly prevalent among marine bacteria, however such studies are limited[16-18].

In this work, we focused on one well characterized CDI system that is carried by many gram-negative bacteria, the type 6 secretion system (T6SS)[17, 19]. The T6SS is a nanomachine that is capable of killing eukaryotic and bacterial prey cells by directly injecting toxic effector proteins into them, which carry out a variety of lethal functions[20-23]. Generally, the needle-like apparatus is assembled in stages (as reviewed in Toska et al., 2018)[24] and once complete it resembles an inverted bacteriophage tailspike[25]. Upon assembly initiation, a transmembrane baseplate is formed to anchor the system to the cell envelope[26]. VgrG and PAAR-domain-containing effector proteins are then recruited to the baseplate to form a needle-like tip and serve as the nucleation site for the formation of a Hcp protein shaft[27-29]. A sheath comprised of VipA and VipB subunits then assembles around the shaft and when the sheath contracts the Hcp/VgrG/PAAR complex is propelled into adjacent target cells[30-33]. VasK and VasF proteins are also associated with the extracellular secretions of the effector proteins[34]. The ATPase ClpV then disassembles the sheath, and possibly the entire apparatus, within seconds after "firing"[35]. Bacteria carrying a functional T6SS exhibit a remarkable ability to efficiently kill their bacterial prey, which can apparently lead to the displacement of host associated commensals[36], intraspecific competition during host colonization[37], community phase separation[38], and intraguild predation[39] (Guillemette et al., *submitted*). Conversely, some bacteria have developed mechanisms to resist T6SS attack. For example, a recent study showed that the production of

exopolysaccharide (EPS) by *Vibrio cholerae* can act as a unidirectional barrier to protect itself from T6SS attack. Furthermore, it has been well documented that some bacterial species such as members of the *Bacteroides* contain immunity genes against various effectors. In addition to passive resistance mechanisms, bacteria such as *P. aeruginosa* can sense exogenous T6SS attacks and retaliate with a T6SS of their own[40].

Despite the large increase in recent T6SS studies, relatively little is known about the effectiveness of T6SS expression against different marine bacterial types. It was found that the marine bacterium and human pathogen, *Vibrio cholerae* is capable of using its T6SS to kill species such as *V. communis*, *V. harveyi*, *Pseudoalteromonas phenolica*, and *Aeromonas sp.*[41, 42]. Other vibrio species, such as *V. parahaemolyticus*, *V. alginolyticus*, and *V. fischeri* were also shown to have functional T6SSs, however the known scope of their susceptible marine prey remains limited to three *Vibrio* species: *V. cholerae*, *V. natriegens*, and select strains of *V. fischeri*[37, 43, 44]. We considered that further exploration into the range of T6SS-susceptible prey should increase understanding of the type of bacteria that a T6SS can kill, while also helping to inform microbial ecologists on the type of bacteria, and ultimately the mechanisms, that are resistant to T6SS attack. Such knowledge may prove useful in trying to understand marine microbial community dynamics and has already been posited to be an important consideration for the development of antimicrobials and probiotics[24]. Here, we challenged a number of phylogenetically diverse marine bacterial types, including members of the phyla Proteobacteria and Bacteroidetes against T6SS attack from *V. cholerae* strain 2740-80. Our results included observations that *V. cholerae* exhibited both amensalism and commensalism with many of the isolates, and that *V. cholerae* itself fell prey to select isolates. Interestingly, we discovered that the known coral and shellfish pathogen, *V. coralliilyticus*, likely has a functional T6SS that is

capable of killing *V. cholerae*. The results of this study are broadly discussed in the context of marine ecology, which includes implications for ocean health and human health, aquaculture, and coral pathogenesis.

Materials & Methods

Bacterial strains

The phylogeny, description, and source of each isolate that was used in the challenge assays are contained in Table 4.1 and Table S4.1. Prior to our experiments, each of the marine bacterial challengers listed in Table S4.1 were plated onto rifampicin containing media to generate spontaneous rifampicin mutants (R^r). Single R^r colonies for each isolate were picked, streaked purified, and confirmed resistant to rifampicin before storage in 25% glycerol at -80 °C. For challenge assays, the isolates were grown with Zobell 2216E at 25 °C. The following concentrations of antibiotics were used where appropriate: streptomycin, 100 µg mL^{-1}; rifampicin, 50 µg mL^{-1}; ampicillin 100 µg mL^{-1}.

For mutagenesis, *V. coralliilyticus* strains were grown in a modified glycerol artificial seawater (GASW) media supplemented with 50 mM Tris-Base (GASW-Tris) and the pH adjusted to 8.3 with HCl prior to autoclaving to prevent acidification of the media and incubated at 27 °C[45], unless otherwise stated. For solid media, 15 g/l of agar was added prior to autoclaving. All *E. coli* strains were grown in LB-Miller at 37 °C, unless otherwise stated. Antibiotics for selection with *E. coli* were used at the following concentrations unless otherwise stated: kanamycin, 50 µg/ml; streptomycin, 25 µg/ml; spectinomycin, 50 µg/ml; and chloramphenicol, 15 µg/ml. Antibiotics for selection with *V. coralliilyticus* were used at the following concentrations unless otherwise stated: ampicillin, 200 µg/ml; streptomycin, 50 µg/ml;

spectinomycin, 100 µg/ml; and chloramphenicol, 5 µg/ml. Growth media for *E. coli* auxotrophic strains were supplemented with deoxythymidine (DT) or diaminopimelate (DAP) at a final concentration of 0.3 mM as required. Arabinose-inducible expression of the *ccdB* gene was achieved by the addition of 0.3% L-arabinose to GASW-Tris (GASW-ARA) and expression was repressed by the addition of 1% D-glucose to LB (LB-DEX) or GASW-Tris (GASW-DEX)[46]. Bacterial cultures were washed with either ASW (GASW lacking glycerol, tryptone, or yeast extract) or phosphate buffered saline (PBS) for *Vibrio* and *E. coli* strains, respectively.

Plasmid construction

All of the plasmids that were used are listed in Table S4.2, and the DNA oligonucleotide primers are listed in Table S4.3. The plasmid pBU226 is a suicide vector used to create a clean deletion of the *vtpR* homolog in OCN008 except for the first and last 18 nucleotides. Genomic DNA from OCN008 was used as template for PCR with the primer pairs 008-vtpR-up-EcoRI-F and Vcor-vtpR-up-OEX-R and Vcor-vtpR-down-OEX-F and 008-vtpR-down-XbaI-R to amplify regions up- and downstream of *vtpR*, respectively. The resulting PCR product was cloned as a *Eco*R1/*Xba*I fragment into the same sites in pSW4426T to create pBU226. Unless otherwise stated, all suicide plasmids were screened using PCR and sanger sequencing using the primer pair pSW4426T-MCS-F and pSW4426T-MCS-R to confirm successful cloning.

The plasmid pBU247 is a suicide vector used to create a clean deletion of the *vasK* homolog in OCN008 except for the first and last 18 nucleotides. OCN008 genomic DNA was used as template for PCR with the primer pairs 008vasK-up-EcoR1-F and 008vasK-up-OEX-R and 008vasK-down-OEX-F and 008vasK-down-XbaI-R. The resulting PCR product was cloned as a *Eco*R1/*Xba*I fragment into the same sites in pSW4426T to create pBU247.

The plasmid pBU266 is a suicide vector used to create a clean deletion of the *vtpA* homolog in OCN008 except for the first and last 18 nucleotides. OCN008 genomic DNA was used as template for PCR with the primer pairs vtpA-up-EcoRI-F and vtpA-up-OEX-R and vtpA-down-OEX-F and vtpA-down-SpeI-R. The resulting PCR product was cloned as a *Eco*R1/*Spe*I fragment into the same sites in pSW4426T to create pBU266.

The plasmid pBU267 is a suicide vector used to create a clean deletion of the *vtpB* homolog in OCN008 except for the first and last 18 nucleotides. OCN008 genomic DNA was used as template for PCR with the primer pairs vtpB-up-SpeI-F and vtpB-up-OEX-R and vtpB-down-OEX-F and vtpA-down-SpeI-R. The resulting PCR product was cloned as a *Spe*I fragment into the *Xba*I site in pSW4426T that had been previously dephosphorylated with FastAP Thermosensitive Alkaline Phosphatase (Thermo Fisher Scientific) to create pBU266.

The plasmid pBU270 is a replicative vector used to express a wild type copy of *vasK* to complement the OCN008 *vasK* mutant. OCN008 genomic DNA was used as template for PCR with the primer pair vasK-XbaI-F and vasK-XbaI-R. The resulting PCR product was cloned as a *Xba*I fragment into the same site in pBU246 that had been previously dephosphorylated to create pBU270.

The plasmid pBU271 is a replicative vector used to express a wild type copy of *vtpR* to complement the OCN008 *vtpR* mutant. OCN008 genomic DNA was used as template for PCR with the primer pair 008-vtpR-SacI-F and 008-vtpR-XbaI-R. The resulting PCR product was cloned as a *Sac*I/*Xba*I fragment into the same sites in pBU246 to create pBU271.

Mutant creation

All *V. coralliilyticus* suicide vectors were introduced using tri-parental conjugations with *E. coli* as previously described[45]. Donor and recipient strains were grown overnight with the appropriate antibiotics and DAP or DT as required. Overnight cultures were diluted 1:1000 in fresh culture medium without antibiotics, grown to an optical density measured at 600 nm (OD_{600}) of 0.4, and then one ml washed three times with either ASW or PBS for *Vibrio* or *E. coli* strains, respectively. The strains were then combined, resuspended in ASW to a total volume of 50 µl, and spotted onto GASW-DEX plates supplemented with DAP and DT. Conjugation spots were incubated at 30 °C for 15 h before being resuspended in ASW, washed three times with ASW, diluted, and plated onto GASW-DEX supplemented with chloramphenicol, but lacking DAP or DT, at 27 °C. Chloramphenicol-resistant colonies, were streaked for isolation on GASW-DEX with spectinomycin and streptomycin, the colonies were then screened for the presence of the suicide vector integrated into the chromosome using colony PCR and the primers pSW4499-cat-F and pSW4499-oriT-R. Colonies of *Vibrio* with the integrated plasmid were grown for 15 h in GASW-DEX broth. Cultures were washed with ASW three times, diluted, and plated onto GASW-ARA to isolate mutants with a clean deletion of the target gene. Mutants were confirmed using PCR and primers specific to the gene being mutated.

Challenge assays

Bacterial isolates were grown in liquid culture overnight, washed, diluted 1:10 into fresh media, and grown for ~3 h. The cultures were then concentrated to an OD_{600} of 10. Predator and challenger were mixed 1:1 (v:v; 10 µl total) and 5 µl aliquots of the co–cultures were spotted onto Zobell 2216E agar. Challenge assays were conducted for 4 h at 25 °C. The cells were then

resuspended, serial–diluted, and plated onto antibiotic selection media to recover and enumerate the surviving predator and challenger. Centrifugation was conducted at 8,600 x G for 5 minutes. Each challenge was independently repeated three times (biological replicates, n= 3), and each biological replicate consisted of three technical replicates.

To ensure that our results were consistent and that the data interpretation was standardized, each bacterial challenger was screened against the same batch-culture of the predator. We compared the mean +/- SD of recovered colony forming units (CFUs) for both of the predators and the challenger to their expected recovery, assuming that no killing took place. Isolates were scored as "killed" if their recovery was at least one log-fold less than their expected recovery (p-value < 0.01; two-tailed t-test).

Statistics

GraphPad Prism version 7.0 (GraphPad Software, Inc.) was used for statistical analyses.

Results & Discussion

Select Ɣ-Proteobacteria exhibited susceptibility to T6SS attack by *V. cholerae*

To test the killing efficacy of T6SS expression during interspecific bacterial competition, we challenged a suite of marine isolates from different environmental and phylogenetic backgrounds (Table S4.1) against *V. cholerae* strain 2740-80 with either an active T6SS ($T6SS^+$) or its isogenic T6SS knockout mutant ($T6SS^-$) derivative (Table 4.1). Colony forming unit (CFU) recoveries were reduced by > 90% for 6 out of the 15 isolates in the challenges against $T6SS^+$ *V.*

cholerae ($p < 0.01$, two-tailed t-test), but were fully recovered in the challenges against T6SS$^-$ *V. cholerae,* indicating that those isolates were highly susceptible to T6SS attack (Table 4.2). The six susceptible isolates were all Ɣ-Proteobacteria, including three members of the order Vibrionales (*V. harveyi, Vibrio* sp. SWAT-3, and *V. shilonii,*), an Alteromonadales (*Alteromonas* Alt-SIO), an Oceanospirillales (*Halomonas* sp. 73), and a Pseudomonadales (*Psychrobacter aquimaris*). One obvious insight that is provided by these data is that the susceptible isolates must avoid encounters with T6SS-expressing bacteria in the ocean in order to survive. Avoidance should be relatively easy for free-living, planktonic bacteria such as *Alteromonas* Alt-SIO, and for bacteria that are found at cold temperatures which has been demonstrated to reduce T6SS expression[42], such as *Halomonas* sp. 73 and *Psychrobacter aquimaris*. However, susceptible bacteria that may reside in higher bacterial density environments such as *V. harveyi*, *Vibrio* sp. SWAT-3, and *V. shilonii* might be exposed to T6SS attack more often. It is possible that such taxa are selected for in environments where T6SS-expression is absent or that these taxa are able to avoid cell-cell contact with T6SS-armed predators, however these possibilities were not tested here.

Surprisingly, two of the Bacteroidetes isolates (*Aequorivita* sp. 97 and *Roseivirga* sp. 121), along with one Ɣ-Proteobacteria (*Pseudomonoas* sp. 2) were killed in the presence of both T6SS$^+$ and T6SS$^-$ *V. cholerae* ($p < 0.01$, two-tailed t-test; Table 4.2). These results suggested that the T6SS did not play a role in the killing of these isolates. While the mechanism(s) that led to significantly reduced recovery of these three isolates when co-cultured with T6SS$^-$ *V. cholerae* were not explored here, we offer several possible scenarios that might explain these observations: (1) the challenged isolates went into a viable but not culturable (under these conditions) state, (2) the challenged isolates were outcompeted for resources, and/or (3) T6SS$^-$ *V.*

cholerae used an alternative inhibitory mechanism such as toxic byproducts of metabolism to kill the challenged isolates. Interestingly, we also observed that when T6SS$^+$ and T6SS$^-$ *V. cholerae* were each challenged against *Pseudoalteromonas flavipulchra* it resulted in death for both *V. cholerae* strains and for *P. flavipulchra* itself ($p < 0.01$, two-tailed t-test; Table 4.2). This result may be explained in part by *P. flavipulchra*'s highly antagonistic nature which has been demonstrated to inhibit the growth of a number of marine bacteria via release of inhibitory chemical(s)[10]. This species is also known to produce amino acid (lysine or glycine) oxidase that are capable of hydrolyzing amino acids present within cells or in the growth media to produce hydrogen peroxide[47]. These enzymes are bactericidal to a wide range of isolates and can also be autotoxic[48-50], often resulting in the death of the bacteria that produce them in rich bacterial media such as Zobell 2216E (Ushijima, *unpublished*). Such a scenario which would explain the loss of both the predator and prey cells. Given that challenge assays with T6SS$^-$ *V. cholerae* resulted in the reduced survival (> 90%) of 4 out of the 15 tested isolates ($p < 0.01$, two-tailed t-test; Table 4.2), we suggest that future experiments are warranted to also test if T6SS$^-$ *V. cholerae* also has a bactericidal mechanism of its own.

Multiple challengers were resistant to attack by the *V. cholerae* T6SS

Three out of the 15 challengers were observed to co-exist with *V. cholerae*, as neither the challenged isolate nor T6SS$^+$ or T6SS$^-$ *V. cholerae* were killed in their respective assays (Table 4.2). Two of these isolates were from the phylum Bacteroidetes (*Flavobacteria* sp. BBFL7 and *Salgentibacter* sp. 1). Interestingly, members of the Bacteroidetes have been demonstrated to exhibit immunity against T6SS toxic effector proteins[51]. This is relevant to marine microbial

ecology since Bacteroidetes are commonly found to be the predominant taxa on particles such as marine snow[52], despite an apparently high susceptibility to antagonistic molecules[9]. The other isolates that we observed to co-exist with T6SS$^+$ *V. cholerae* were two closely related ɣ-Proteobacteria (*Pseudoalteromonas* Tw7 and *Pseudoalteromonas* Tw2). *Pseudoalteromonas* Tw2 also exhibited the ability to kill T6SS$^-$ but not T6SS$^+$ *V. cholerae* ($p < 0.01$, two-tailed t-test; Table 4.2). Overall, of the 15 isolates tested only *V. coralliilyticus* displayed the ability to survive the assays and kill both T6SS$^+$ and T6SS$^-$ *V. cholerae* ($p < 0.01$, two-tailed t-test; Table 4.2). Collectively, our results suggest that resistance to *V. cholerae* 2740-80 and similar T6SSs might be common for marine bacteria and we have begun looking into the resistance mechanisms that are used.

Multiple *V. coralliilyticus* strains killed T6SS$^+$ *V. cholerae*

Intrigued by the ability of *V. coralliilyticus* to survive the T6SS challenge assays and to kill *V. cholerae*, we conducted further experiments to determine if these characteristics were strain-specific. Five *V. coralliilyticus* strains were challenged, including known coral and shellfish pathogens (OCN008, OCN014, RE98, RE22, and BAA-450; Table 4.1) against T6SS$^+$ and T6SS$^-$ *V. cholerae*. Consistent with our initial result, we found that all five of the *V. coralliilyticus* strains fully recovered after the assays and that the survival of both T6SS$^+$ and T6SS$^-$ *V. cholerae* was reduced > 99% by all five strains ($p < 0.0001$, two-tailed t-test; Fig. 4.1). This suggested the presence of conserved mechanisms shared between these strains that offered protection to *V. coralliilyticus* and enabled them to kill *V. cholerae*.

Evidence supports the hypothesis that *V. coralliilyticus* killed *V. cholerae* by expressing its own T6SS

We hypothesized that the observed survival of *V. coralliilyticus* when challenged against T6SS$^+$ *V. cholerae* could have been due to (1) *V. coralliilyticus* being resistant to T6SS attack, (2) *V. coralliilyticus* killing *V. cholerae* before itself was killed, or (3) a combination of both scenarios. For the first scenario, we considered that protease production by *V. coralliilyticus* might enable it to resist T6SS attack. Two metalloproteases produced by *V. coralliilyticus*, VtpA and VtpB, are believed to contribute to its virulence towards coral and oyster larvae[53-56], and the purified proteases have been demonstrated to degrade coral tissue and disrupt the photosystem of *Symbiodinium* spp.[54, 55]. Furthermore, these proteases can degrade enzymes in culture[57], and the supernatants of *V. coralliilyticus* cultures containing the proteases are able to substantially degrade 10 µg of BSA within 30 min (data not shown). Additionally, previous studies have demonstrated that the VtpA and VtpB proteases are maximally produced at high cell density[53], similar to the conditions that we used for the T6SS challenge assays. We hypothesized that the proteolytic activity of *V. coralliilyticus* could degrade the *V. cholerae* T6SS apparatus or effector proteins before they are able to function, or that the protease could potentially kill *V. cholerae* directly. To test these hypotheses, knockout mutants were made using strain OCN008 with deletions of the quorum sensing regulator *vtpR*, which regulates protease activity in *V. coralliilyticus*[58], as well as the protease-encoding genes *vtpA* and *vtpB* individually and in combination. These four mutant strains were challenged against T6SS$^+$ and T6SS$^-$ *V. cholerae* in our competition assays. We found that the Δ*vtpR* mutant was more susceptible to T6SS-mediated killing and that it was unable to kill *V. cholerae* ($p < 0.001$, two-tailed t-test; Fig. 4.2). However, all three *V. coralliilyticus* protease mutants (Δ*vtpA*, Δ*vtpB*, and Δ*vtpAB*) survived the assays and

retained their ability to kill *V. cholerae* at levels equivalent to the wild-type strain ($p < 0.0001$, two-tailed t-test; Fig. 2). Therefore, we concluded that while VtpR did play a role in the success of *V. coralliilyticus* survival, the proteases were unlikely to be the main mechanism that protected *V. coralliilyticus* from T6SS attack and were not responsible for the observed killing of *V. cholerae*.

As a homolog of the *V. cholerae* quorum sensing regulator HapR, VtpR is believed to regulate a wide range of physiological functions[58]. Recently, Strutzmann and Blokesch (2016) reported that mutations that inactivated HapR resulted in reduced T6SS activity for *V. cholerae*[59]. At the time of our study, it was not known if *V. coralliilyticus* had a functional T6SS, however T6SS-like needle structures within *V. coralliilyticus* had been observed[60]. We considered that if *V. coralliilyticus* carries a functional T6SS that is regulated in part by VtpR, then the deletion of *vtpR* in OCN008 may have diminished or eliminated T6SS expression in our study, explaining our observation that the Δ*vtpR* strain was unable to kill *V. cholerae*. Further experiments are underway to demonstrate this regulatory link.

To investigate the possibility of *V. coralliilyticus* expressing its own T6SS, we created a *V. coralliilyticus vasK* deletion mutant (Δ*vasK*) and challenged it against $T6SS^+$ or $T6SS^-$ *V. cholerae*. This mutant has a deletion in a gene predicted to encode a homolog of VasK, which is essential for *V. cholerae* T6SS function[34]. In accordance with our hypothesis, we found that both $T6SS^+$ and $T6SS^-$ *V. cholerae* survived the challenge assays (Fig 3), demonstrating that the killing of *V. cholerae* by *V. coralliilyticus* requires the *vasK* gene. Moreover, the $T6SS^-$ *V. coralliilyticus* strain was susceptible to T6SS attack by *V. cholerae* ($p < 0.0001$, two-tailed t-test; Fig. 4.3), demonstrating that *V. coralliilyticus* is not inherently resistant to the *V. cholerae* T6SS. Genetic complementation of the $T6SS^-$ *V. coralliilyticus* strain restored the mutants' ability to

kill *V. cholerae* and to resist T6SS-mediated attacks ($p < 0.0001$, two-tailed t-test; Fig. 4.3). Thus, the inability of the T6SS$^-$ *V. coralliilyticus* strain to kill *V. cholerae,* in combination with its increased susceptibility to T6SS-mediated killing strongly suggests that *V. coralliilyticus* uses its own T6SS to kill *V. cholerae* before *V. cholerae* can strike. Therefore, in T6SS duels with *V. cholerae*, *V. coralliilyticus* may be able to survive by winning in the 'quick draw' or by striking more effectively, as opposed to being resistant to attack. This contrasts with the previously described tit-for-tat interactions between *V. cholerae* and *P. aeruginosa*, in which, *P. aeruginosa* is naturally resistant to *V. cholerae* T6SS-mediated killing, while utilizing its own T6SS only in response to bacterial aggression[40]. Furthermore, given that the T6SS$^-$ *V. coralliilyticus* mutant was found to be susceptible to *V. cholerae* T6SS attack, we were able to rule out the hypothesis that *V. coralliilyticus* employed other natural resistance mechanisms to T6SS attack such as immunity to the toxic effector proteins or protective exopolysaccharide (EPS) "armor" that have been previously described[51, 61]. Interestingly, the Δ*vtpR* strain, which was susceptible to T6SS$^+$ *V. cholerae* was found to produce more EPS in comparison to the wild-type strain ($p < 0.0001$, Tukey's multiple comparisons test; Fig. S4.1), further suggesting that EPS production was not the protective mechanism for *V. coralliilyticus* in our study. In all, these results support the hypothesis that *V. coralliilyticus* has a functional T6SS, which we found to be effective at killing *V. cholerae* and required for resistance to T6SS-mediated killing by *V. cholerae*.

V. coralliilyticus T6SS expression has implications for coral and shellfish health

We surmise that the other four *V. coralliilyticus* strains that were observed to kill T6SS$^+$ and T6SS$^-$ *V. cholerae* (Fig. 4.1) also carried a functional T6SS. While that hypothesis was not

explicitly tested here, we did find that proteins required for a functional T6SS in *V. cholerae* had 24-69% amino acid homology with *V. coralliilyticus* proteins (Table S4.4). Furthermore, the putative OCN008 T6SS proteins were present in the genomes of the four other *V. coralliilyticus* strains (OCN014, RE98, RE22, and BAA-450) sharing 99-100% amino acid homology (Table S4.5). Collectively, our results suggest that each of these strains have functional T6SSs which could have a large impact on the understanding and treatment of coral and shellfish health. For example, *V. coralliilyticus* strains OCN008, OCN014, and BAA-450 have all been described as etiological agents of disease for multiple genera of coral[54, 56, 62], and strains RE98 and RE22 have been implicated in mass shellfish larvae mortalities[63]. It has been suggested that *V. coralliilyticus* is capable of altering the coral microflora which is thought to protect the host from infection[13], however, no mechanisms have been proposed for how the pathogen accomplishes this. Furthermore, Kimes et al. (2011) demonstrated that the *V. coralliilyticus* upregulates expression of T6SS-assocaited proteins at temperatures that correlate with increased virulence, and showed the presence of putative T6SS needle structures using electron microscopy[60]. Therefore, we propose that the T6SS of *V. coralliilyticus* could be an important mechanism for the displacement of, and protection against host-associated bacteria as it attempts to colonize potential hosts. Furthermore, while T6SS-expressing bacteria have been proposed as probiotics to kill aquaculture-associated pathogens such as *V. coralliilyticus*, our results suggest that more work is required to further understand the complexity of bacterial-bacterial antagonism before such probiotic treatments can be rendered effective.

We propose that *V. coralliilyticus* might also use the T6SS to attack other host-associated organisms or the hosts-cells themselves. Studies have suggested that during infections, *V. coralliilyticus* is capable of harming the photosynthetic algal symbionts within coral cells

(*Symbiodinium* spp.), resulting in coral bleaching[54, 55]. Given that the *V. cholerae* T6SS has been shown to kill eukaryotic organisms, such as the amoeba *Dictyostelium discoideum*, it is tempting to speculate that the *V. coralliilyticus* T6SS may be utilized to kill *Symbiodinium* or even attack the host cells directly. While it is still unclear if *V. coralliilyticus* acts as an intracellular pathogen, a recent study has demonstrated that *V. coralliilyticus* can end up within coral cells and vesicles during infection[64]. We suggest that it might be possible for *V. coralliilyticus* to respond in these environments with its T6SS to escape host cells. This scenario would be reminiscent to how the intracellular pathogens *Francisella tularensis* and *Burkholderia pseudomallei* uses their T6SS to escape vesicles and macrophages, or to spread from cell to cell[65, 66]. We propose that further investigations are warranted to better understand the role of T6SS expression by *V. coralliilyticus* in coral and shellfish pathogenesis, which may aid in the protection of these environmentally and economically-important organisms.

Conclusion

The bacterial type 6 secretion system is carried by various bacteria and is capable of efficiently killing susceptible bacterial prey. Here, we challenged diverse marine bacterial isolates against T6SS$^+$ *V. cholerae* and confirmed previously documented high mortality rates for select members of the genus vibrio. We also provided the first documentation of T6SS-mediated killing of marine Alteromonadales (*Alteromonas Alt-SIO*), Oceanospirillales (*Halomonas* sp. 73), and Pseudomonadales (*Psychrobacter aquimaris*). Additionally, we observed that a number of isolates including members of the Bacteroidetes and ϒ-Proteobacteria phyla were resistant to *V. cholerae* T6SS attack, including five *V. coralliilyticus* strains. Furthermore, we found that all of the tested *V. coralliilyticus* strains also killed *V. cholerae*, presumably via the use of their own

T6SS. We propose that bacterial susceptibility and resistance to contact dependent growth inhibition mechanisms, such as the T6SS, might be important for the structuring of marine microbial communities in high bacterial density environments such as marine snow, fecal pellets, sediment, and animal hosts. Future work will be required to test the ecological impacts of such mechanisms *in situ* which should be possible by using conventional imaging techniques.

Acknowledgements

We thank Dr. John Mekalanos for providing the *V. cholerae* 2740-80 strains and Logan Peoples for many of the marine bacterial isolates. We thank Nicholas Lee for assistance. This work was supported by the Gordon & Betty Moore Foundation Grant #4827 to (FA).

References

[1]Fuhrman, J. A. & Hagstrom A. In: Kirchman, D (ed). Microbial Ecology of the Oceans. John Wiley & Sons, Inc., 299-334(2008).

[2]Polz, M. F., Alm E. J. & Hanage W. P. Horizontal gene transfer and the evolution of bacterial and archaeal population structure. Trends in Genetics. 2013.

[3]Cordero, O. X. & Al E. Ecological Populations of Bacteria Act as Socially Cohesive Units of Antibiotic Production and Resistance. Science. 2012;337:1228–1231.

[4]Charlotte, E. & Al. E. Regulation of Bacterial Communities Through Antimicrobial Activity by the Coral Holobiont. Microbial Ecology. 2011;63:605–618.

[5]Hunt, D. E. & Al. E. Resource Partitioning and Sympatric Differentiation Among Closely Related Bacterioplankton. Science. 2008;1081–1085.

[6]Nair, S. & Simidu U. Distribution and significance of heterotrophic marine bacteria with antibacterial activity. Appl Environ Microbiol. 1987;53:2957-2962.

[7]Okami, Y. Marine microorganisms as a source of bioactive agents. Microbial Ecology. 1986;12:65-78.

[8]Rosenfeld, W. D. & Zobell C. E. Antibiotic production by marine microorganisms. Journal of bacteriology. 1947;54:393-398.

[9]Long, R. A. & Azam F. Antagonistic Interactions among Marine Pelagic Bacteria. Appl Environ Microbiol. 2001;67:4975-4983.

[10]Rypien, K., Ward J. & Azam F. Antagonistic interactions among coral-associated bacteria. Environmental Microbiology. 2010;12:28-39.

[11]Stolp, H. & Starr M. P. Bdellovibrio bacteriovorus gen. et sp. n., a predatory, ectoparasitic, and bacteriolytic microorganism. Antonie van Leeuwenhoek. 1963;29:217-248.

[12]Schoeffield, A. & Williams H. Efficiencies of recovery of bdellovibrios from brackish- water environments by using various bacterial species as prey. Appl Environ Microbiol. 1990;56:230-236.

[13]Welsh, R. M., Rosales S. M., Zaneveld J. R., Payet J. P., Mcminds R., Hubbs S. L. & Thurber R. L. V. Alien vs. predator: bacterial challenge alters coral microbiomes unless controlled by Halobacteriovorax predators. PeerJ. 2017;5.

[14]Welsh, R. M., Zaneveld J. R., Rosales S. M., Payet J. P., Burkepile D. E. & Thurber R. V. Bacterial predation in a marine host-associated microbiome. The ISME Journal. 2016;10:1540-1544.

[15]Lewin, R. A. Saprospira grandis: A Flexibacterium That Can Catch Bacterial Prey by ‘‘Ixotrophy’’. Microbial Ecology. 1997;34:232-236.

[16]Moran, M. A., Belas R., Schell M. A., Gonzalez J. M., Sun F., Sun S., Binder B. J., Edmonds J., Ye W., Orcutt B., Howard E. C., Meile C., Palefsky W., Goesmann A., Ren Q., Paulsen I., Ulrich L. E., Thompson L. S., Saunders E. & Buchan A. Ecological genomics of marine roseobacters. App Env Microbiol. 2007;73:4559-4569.

[17]Boyer, F., Fichant G., Berthod J., Vandenbrouck Y. & Attree I. Dissecting the bacterial type VI secretion system by a genome wide in silico analysis: what can be learned from available microbial genomic resources? BMC Genomics. 2009;10:104.

[18]Persson, O. P., Pinhassi J., Riemann L., Marklund B. I., Rhen M., Normark S., Gonzalez J. M. & Hagstrom A. High abundance of virulence gene homologues in marine bacteria. Environ. Microbiol. 2009;11:1348-1357.

[19]Pukatzki, S., Ma A. T., Sturtevant D., Krastins B., Sarracino D., Nelson W. C., Heidelberg J. F. & Mekalanos J. J. Identification of a conserved bacterial protein secretion system in Vibrio cholerae using the Dictyostelium host model system. Proc Natl Acad Sci USA. 2006;103:1528-33.

[20]Hood, R. D., Singh P., Hsu F., Guvener T., Carl M. A., Trinidad R. R., Silverman J. M., Ohlson B. B., Hicks K. G., Plemel R. L., Li M., Schwarz S., Wang W. Y., Merz A. J.,

Goodlett D. R. & Mougous J. D. A type VI secretion system of Pseudomonas aeruginosa targets a toxin to bacteria. Cell Host Microbe. 2010;7:25-37.

[21]Zheng, J., Ho B. & Mekalanos J. J. Genetic analysis of anti-amoebae and anti-bacterial activities of the type VI secretion system in Vibrio cholerae. PLoS One. 2011;6:e23876.

[22]Macintyre, D. L., Miyata S. T., Kitaoka M. & Pukatzki S. The Vibrio cholerae type VI secretion system displays antimicrobial properties. Proc. Natl. Acad. Sci. USA. 2010;107:19520-19524.

[23]Ma, A., Mcauley S., Pukatzki S. & Mekalanos J. Translocation of a Vibrio cholerae type VI secretion effector requires bacterial endocytosis by host cell. Cell Host Microbe. 2009;5:234–243.

[24]Toska, J., Ho B. & Mekalanos J. Exopolysaccharide protects Vibrio cholerae from exogenous attacks by the type 6 secretion system. . Proceedings of the National Academy of Sciences of the United States of America. 2018;115:7997–8002.

[25]Pukatzki, S., Ma A. T., Revel A. T., Sturtevant D. & Mekalanos J. J. Type VI secretion system translocates a phage tail spike-like protein into target cells where it cross-links actin. Proc. Natl. Acad. Sci. 2007;104:15508–15513.

[26]Durand, E. & Al. E. Biogenesis and structure of a type VI secretion membrane core complex. Nature. 2015;523:555–560.

[27]Leiman, P. & Al. E. Type VI secretion apparatus and phage tail-associated protein complexes share a common evolutionary origin. Proc Natl Acad Sci USA. 2009;106:4154–4159.

[28]Shneider, M. & Al. E. PAAR-repeat proteins sharpen and diversify the type VI secretion system spike. Nature. 2013;500:350–353.

[29]Nazarov, S. & Al. E. Cryo-EM reconstruction of type VI secretion system baseplate and sheath distal end. EMBO J. 2018.

[30]Kudryashev, M. & Al. E. Structure of the type VI secretion system contractile sheath. Cell. 2015;160:952–962.

[31]Zoued, A. & Al. E. Priming and polymerization of a bacterial contractile tail structure. Nature. 2016;531:59–63.

[32]Kapitein, N. & Al. E. ClpV recycles VipA/VipB tubules and prevents non-productive tubule formation to ensure efficient type VI protein secretion. Mol Microbiol. 2013;87:1013–1028.

[33]Basler, M., Pilhofer M., Henderson G., Jensen G. & Mekalanos J. Type VI secretion requires a dynamic contractile phage tail-like structure. Nature. 2012;182–186.

[34]Pukatzki, S., Ma A., Sturtevant D., Krastins B., Sarracino D., Nelson W. & Al E. Identification of a conserved bacterial protein secretion system in Vibrio cholerae using the Dictyostelium host model system. Proceedings of the National Academy of Sciences of the United States of America. 2006;103:1528–1533.

[35]Basler, M., Pilhofer M., Henderson P. G., Jensen J. G. & Mekalanos J. J. Type VI secretion requires a dynamic contractile phage tail-like structure. Nature. 2012;483:182-186.

[36]Zhao, W., Caro F., Robins W. & Mekalanos J. Antagonism toward the intestinal microbiota and its effect on Vibrio cholerae virulence. Science. 2018;359:210–213.

[37]Speare, L., Cecere A. G., Guckes K. R., Smith S., Wollenber M. S., Mandel M. J., Miyashiro T. & Septer A. N. Bacterial symbionts use a type VI secretion system to eliminate competitors in their natural host. Proc Natl Acad Sci USA. 2018.

[38]Mcnally, L., Bernardy E., Thomas J., Kalziqi A., Pentz J., Brown S. P., B. K. Hammer, Yunker P. J. & Ratcliff W. C. Killing by Type VI secretion drives genetic phase separation and correlates with increased cooperation. Nat Commun. 2017;8:14371.

[39]Pukatzki, S. & Provenzano D. Vibrio cholerae as a predator: lessons from evolutionary principles. Front Microbiol. 2013;4:384.

[40]Basler, M., Ho B. T. & Mekalanos J. J. Tit-for-tat: type VI secretion system counterattack during bacterial cell-cell interactions. Cell. 2013;152:884-94.

[41]Unterweger, D., Kitaoka M., Miyata S. T., Bachmann V., Brooks T. M., Moloney J., Sosa O., Silva D., Duran-Gonzalez J., Provenzano D. & Pukatzki S. Constitutive type VI secretion system expression gives Vibrio cholerae intra- and interspecific competitive advantages. PLoS One. 2012;7:e48320.

[42]Townsley, L., Sison Mangus M. P., Mehic S. & Yildiz F. H. Response of Vibrio cholerae to Low-Temperature Shifts: CspV Regulation of Type VI Secretion, Biofilm Formation, and Association with Zooplankton. Appl Environ Microbiol. 2016;82:4441-52.

[43]Salomon, D., Gonzalez H., Updegraff B. L. & Orth K. Vibrio parahaemolyticus type VI secretion system 1 is activated in marine conditions to target bacteria, and is differentially regulated from system 2. PLoS One. 2013;8:e61086.

[44]Salomon, D., Klimko J. A., Trudgian D. C., Kinch L. N., Grishin N. V., Mirzaei H. & Orth K. Type VI Secretion System Toxins Horizontally Shared between Marine Bacteria. PLoS Pathog. 2015;11:e1005128.

[45]Ushijima, B. & Häse C. C. The Influence of Chemotaxis and Swimming Patterns on the Virulence of the Coral Pathogen Vibrio coralliilyticus. Journal of bacteriology. 2018.

[46]Ushijima, B. & Al. E. Mutation of the toxR or mshA genes from Vibrio coralliilyticus strain OCN014 reduces infection of the coral Acropora cytherea. Environmental Microbiology. 2016;18:4055–4067.

[47]Yu, M. & Al. E. Purification and characterization of antibacterial compounds of Pseudoalteromonas flavipulchra JG1. Microbiology. 2012;158:835–842.

[48]Lucas-Elio, P., Gomez D., Solano F. & Sanchez-Amat A. The Antimicrobial Activity of Marinocine, Synthesized by Marinomonas mediterranea, Is Due to Hydrogen Peroxide Generated by Its Lysine Oxidase Activity. Journal of bacteriology. 2006;188: 2493–2501.

[49]Campillo-Brocal, J. C., Chacón-Verdú M. D., Lucas-Elío P. & Sánchez-Amat A. Distribution in microbial genomes of genes similar to lodA and goxA which encode a novel family of quinoproteins with amino acid oxidase activity. BMC Genomics. 2015;16.

[50]Bowman, J. P. Bioactive compound synthetic capacity and ecological significance of marine bacterial genus Pseudoalteromonas. Marine drugs. 2007;5.

[51]Wexler, A. & Al E. Human symbionts inject and neutralize antibacterial toxins to persist in the gut. Proc Natl Acad Sci USA. 2016;113:3639–3644.

[52]Delong, E. F., Franks D. G. & Alldredge A. L. Phylogenetic diversity of aggregate-attached vs. free-living marine bacterial assemblages. Limnology and Oceanography. 1993;38:924-934.

[53]Hasegawa, H., Lind E., Boin M. & Hase C. The Extracellular Metalloprotease of Vibrio tubiashii Is a Major Virulence Factor for Pacific Oyster (Crassostrea gigas) Larvae. Applied and Environmental Microbiology. 2008;74:4101–4110.

[54]Ben-Haim, Y., Zicherman-Keren M. & Rosenberg E. Temperature-regulated bleaching and lysis of the coral Pocillopora damicornis by the novel pathogen Vibrio coralliilyticus. Applied and Environmental Microbiology. 2003;69:4236–4242.

[55]Sussman, M., Mieog J., Doyle J., Victor S., Willis B. & Bourne D. Vibrio Zinc-Metalloprotease Causes Photoinactivation of Coral Endosymbionts and Coral Tissue Lesions. PLoS ONE. 2009;4.

[56]Sussman, M., Willis B., Victor S., Bourne D. & Ahmed N. Coral Pathogens Identified for White Syndrome (WS) Epizootics in the Indo-Pacific. PLoS ONE. 2008;3.

[57]Hasegawa, H. & Hase C. The extracellular metalloprotease of Vibrio tubiashii directly inhibits its extracellular haemolysin. Microbiology. 2009;155:2296–2305.

[58]Hasegawa, H. & Hase C. TetR-Type Transcriptional Regulator VtpR Functions as a Global Regulator in Vibrio tubiashii. Applied and Environmental Microbiology. 2009;75:7602–7609.

[59]Stutzmann, S. & Blokesch M. Circulation of a Quorum-Sensing-Impaired Variant of Vibrio cholerae Strain C6706 Masks Important Phenotypes. mSphere. 2016;1.

[60]Kimes, N. E., Grim C. J., Johnson W. R., Hasan N. A., Tall B. D., Kothary M. H., Kiss H., Munk A. C., Tapia R., Green L., Detter C., Bruce D. C., Brettin T. S., Colwell R. R. &

Morris P. J. Temperature regulation of virulence factors in the pathogen Vibrio coralliilyticus. The ISME Journal 2012;6:835–846.

[61]Dong, T., Ho B., Yoder-Himes D. & Mekalanos J. Identification of T6SS-dependent effector and immunity proteins by Tn-seq in Vibrio cholerae. Proc Natl Acad Sci USA. 2013;110:2623–2628.

[62]Ushijima, B., Videau P., Burger A. H., Shore-Maggio A., Runyon C. M., Sudek M., Aeby G. S. & Callahan S. M. Vibrio coralliilyticus Strain OCN008 Is an Etiological Agent of Acute Montipora White Syndrome. Applied and Environmental Microbiology. 2014;80:2102–2109.

[63]Estes, R., Friedman C., Elston R. & Herwig R. Pathogenicity testing of shellfish hatchery bacterial isolates on Pacific oyster Crassostrea gigas larvae. Diseases of aquatic organisms. 2004;58:223–230.

[64]Gibbin, E., Gavish A., Domart-Coulon I., Kramarsky-Winter E., Shapiro O., Meibom A. & Al E. Using NanoSIMS coupled with microfluidics to visualize the early stages of coral infection by Vibrio coralliilyticus. BMC Microbiology. 2018.

[65]Brodmann, M., Dreier R., Broz P. & Basler M. Francisella requires dynamic type VI secretion system and ClpB to deliver effectors for phagosomal escape. Nature Communications. 2017.

[66]Toesca, I., French C. & Miller J. The Type VI Secretion System Spike Protein VgrG5 Mediates Membrane Fusion during Intercellular Spread by Pseudomallei Group Burkholderia Species. Infection and Immunity. 2014;1436–1444.

[67]Goldberg, S. & Murphy J. Molecular epidemiological studies of United States Gulf Coast Vibrio cholerae strains: integration site of mutator vibriophage VcA-3. Infection and Immunity. 1983;42:224-230.

[68]Ben-Haim, Y. & Rosenberg E. A novel Vibrio sp. pathogen of the coral Pocillopora damicornis. Marine Biology. 2002;141:47-55.

[69]Kushmaro, A., Loya Y., Fine M. & Rosenberg E. Bacterial infection and coral bleaching. Nature. 1996;380:396.

[70]Byers, D. M. & Meighen E. A. Acyl-acylcarrierproteinasasourceoffattyacidsfor bacterialbioluminescence. Proc Natl Acad Sci USA. 1985;82:6085-6089.

[71]Bidle, K. D. & Azam F. Bacterial control of silicon regeneration from diatom detritus: Significance of bacterialectohydrolases and species identity. Limnology and Oceanography. 2001;46:1606–1623.

[72]Pedler, B. E., Aluwihare L. I. & Azam F. Single bacterial strain capable of significant contribution to carbon cycling in the surface ocean. Proceedings of the Academy of Natural Sciences. 2014;111:7202–7207.

[73]Peoples, L. M., Donaldson S., Osuntokun O., Xia Q., Nelson A., Blanton J., Allen E. E., Church M. J. & Bartlett D. H. Vertically distinct microbial communities in the Mariana and Kermadec trenches. PLoS ONE. 2018.

[74]Yoon, J.-H., Lee C.-H., Yeo S.-H. & Oh T.-K. Psychrobacter aquimaris sp. nov. and Psychrobacter namhaensis sp. nov., isolated from sea water of the South Sea in Korea. International Journal of Systematic and Evolutionary Microbiology. 2005;55:1007-1013.

[75]Roux, F. L., Binesse J., Saulnier D. & Mazel D. Construction of a Vibrio splendidus Mutant Lacking the Metalloprotease Gene vsm by Use of a Novel Counterselectable Suicide Vector. App Env Microbiol. 2007;73:777-784.

Figures

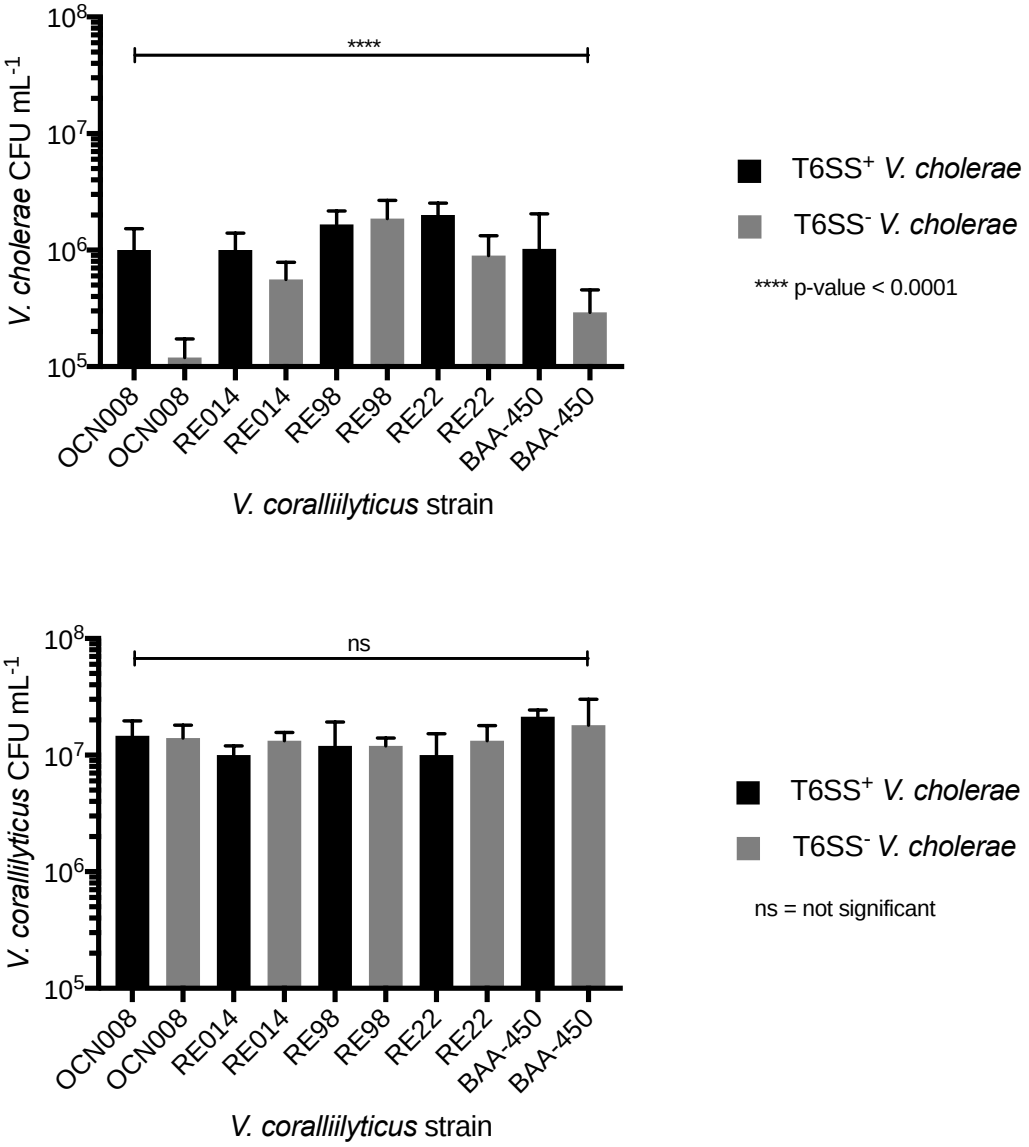

Figure 4.1 *V. coralliilyticus* challenge assays. Five *V. coralliilyticus* strains (OCN008, RE014, RE98, RE22, and BAA-450) were challenged against T6SS$^+$ *V. cholerae* (black bars) and T6SS$^-$ *V. cholerae* (grey bars). (a) *V. cholerae* CFU recovery; (b) *V. coralliilyticus* CFU recovery. Error bars represent the mean ±SD of three biological replicates. Statistical difference was determined by comparing the data to fully recovered CFUs for each strain (2.5 x 10^7 CFU mL^{-1}).

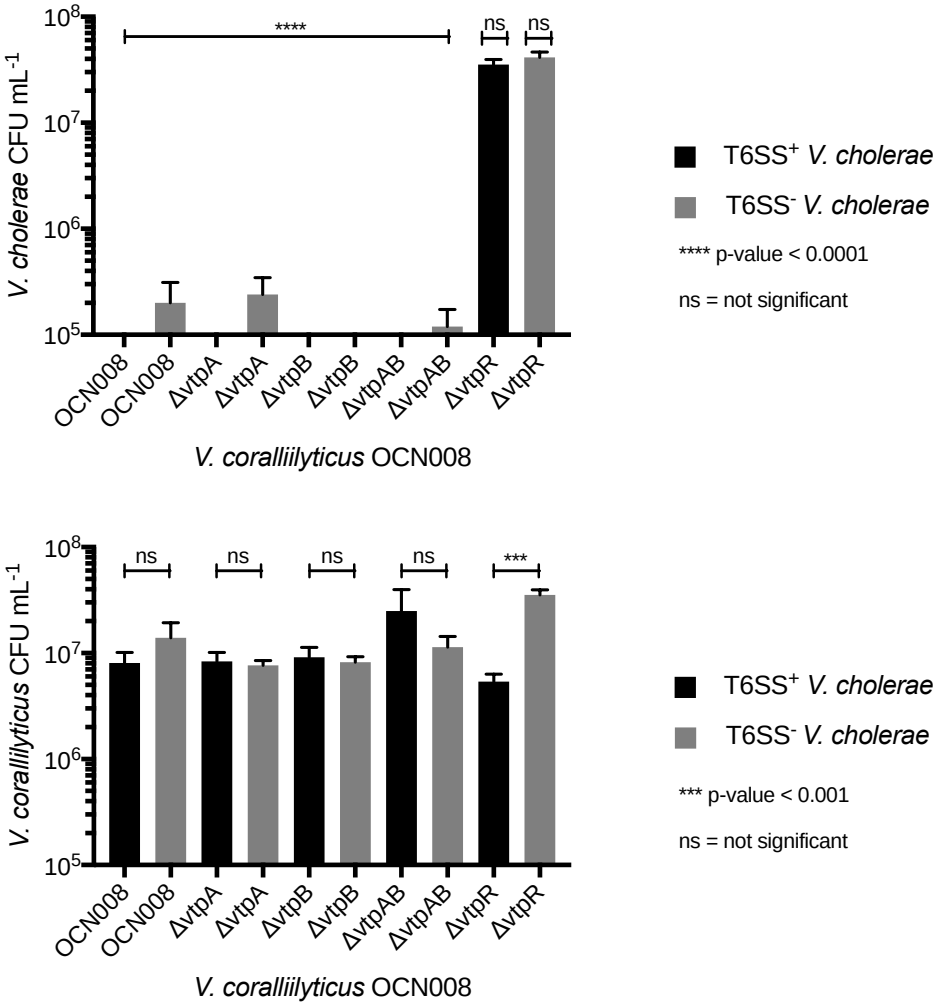

Figure 4.2 *V. coralliilyticus* protease-mutant challenge assays. *V. coralliilyticus* OCN008, protease-mutant derivatives (Δ*vtpA,* Δ*vtpB,* and Δ*vtpAB*), and the Δ*vtpR* mutant were challenged against T6SS^{+} *V. cholerae* (black bars) and T6SS^{-} *V. cholerae* (grey bars). (a) *V. cholerae* CFU recovery; (b) *V. coralliilyticus* CFU recovery. Error bars represent the mean ±SD of three biological replicates. Statistical difference was determined by comparing the data to fully recovered CFUs for each strain (2.5 x 10^7 CFU mL^{-1}).

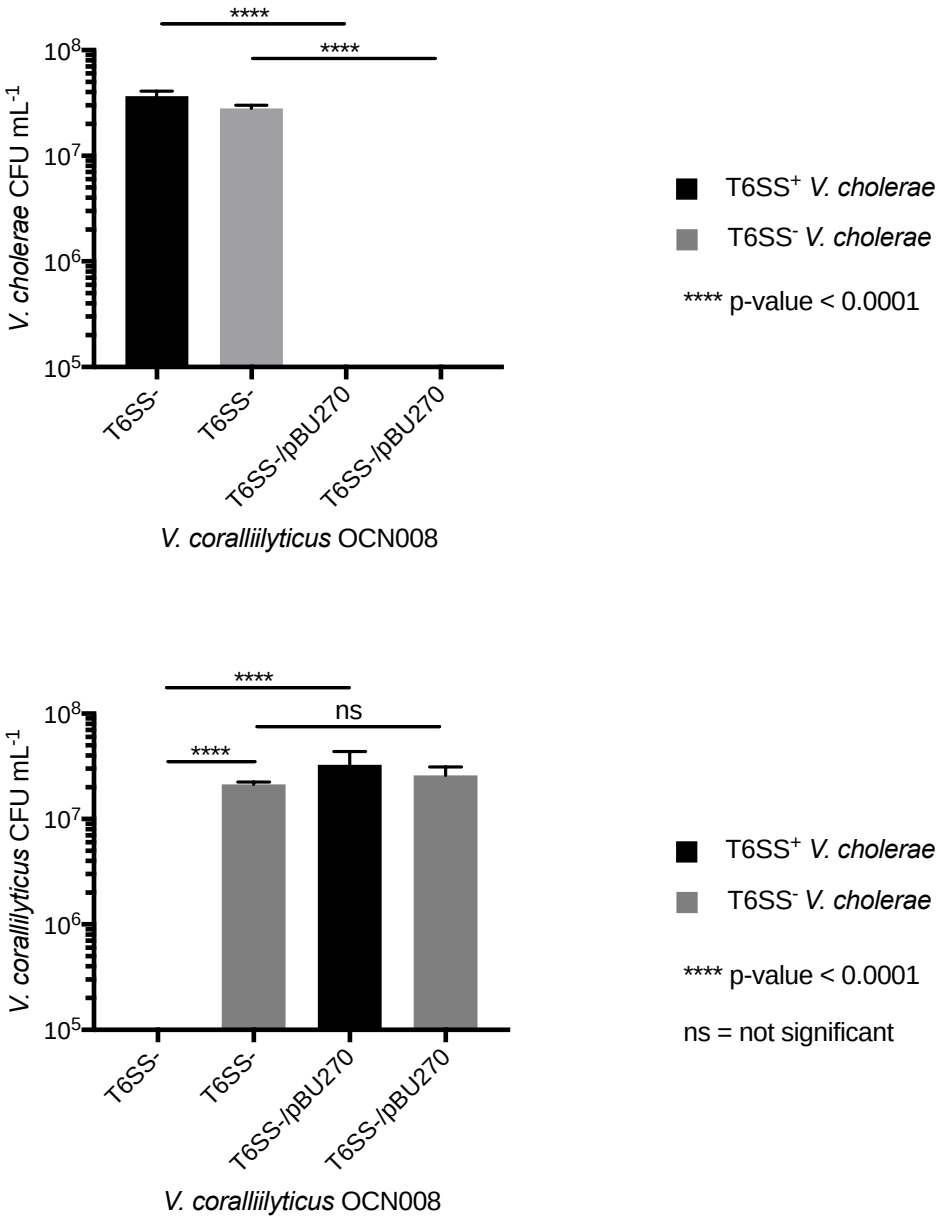

Figure 4.3 Genetically complemented *V. coralliilyticus* T6SS mutant challenge assay. The *V. coralliilyticus* OCN008 Δ*vasK* strain (T6SS$^-$) and the Δ*vasK* strain carrying a plasmid expressing a wild-type copy of *vasK* (pBU270) were challenged against T6SS$^+$ *V. cholerae* (black bars) and T6SS$^+$ *V. cholerae* (grey bars). (a) *V. cholerae* CFU recovery; (b) *V. coralliilyticus* CFU recovery. Error bars represent the mean ±SD of three biological replicates.

Tables

Table 4.1 *V. cholerae* and *V. coralliilyticus* strains used in this study.

Genus, species, strain		Description	Source/citation
Wild type	*V. cholerae* 2740-80	Nontoxinogenic El Tor strain isolated from a patient in Florida, United States; Sm^R, Rf^R	(Goldberg & Murphy 1983)[67]
	V. coralliilyticus ATCC BAA-450	Type strain of *V. coralliilyticus*; coral pathogen isolate off the coast of Zanzibar; Ap^R	(Ben-Haim & Rosenberg 2002)[68]
	V. coralliilyticus OCN008	Coral pathogen isolated from Kaneohe Bay, HI; Ap^R	(Ushijima et al. 2014)[62]
	V. coralliilyticus OCN014	Coral pathogen isolated from Palmyra Atoll; Ap^R, Sm^R	(Ushijima et al. 2016)[46]
	V. coralliilyticus RE22	Oyster larvae pathogen isolated from Netarts Bay, OR; Ap^R, Sm^R	(Estes et al. 2004)[63]
	V. coralliilyticus RE98	Oyster larvae pathogen isolated from Netarts Bay, OR; Ap^R	(Estes et al. 2004)[63]
Mutant	*V. cholerae* 2740-80 Δ*vipA*	*V. cholerae* 2740-80 with an in-frame deletion of *vipA*; Sm^R, Rf^R	(Basler et al. 2012)[35]
	V. coralliilyticus OCN008 Δ*vtpR*	OCN008 with an in-frame deletion of the quorum sensing regulatory protein-encoding gene *vtpR*; Ap^R	This study
	V. coralliilyticus OCN008 Δ*vtpA*	OCN008 with an in-frame deletion of the metalloprotease-encoding gene *vtpA*; Ap^R	This study
	V. coralliilyticus OCN008 Δ*vtpB*	OCN008 with an in-frame deletion of the metalloprotease-encoding gene *vtpB*; Ap^R	This study
	V. coralliilyticus OCN008 Δ*vtpAB*	An OCN008 double deletion mutant with in-frame deletions of *vtpA* and *vtpB*; Ap^R	This study
	V. coralliilyticus OCN008 Δ*vasK*	OCN008 with an in-frame deletion of a *vasK* homolog predicted to encode a T6SS-associated protein; Ap^R	This study

*Abbreviations: Ap^R = resistant to ampicillin, Sm^R = resistant to streptomycin, Rf^R = resistant to rifampicin, Km^R = resistant to kanamycin, Em^R = resistant to erythromycin, Tc^R = resistant to tetracycline.

Table 4.2 Summary of *V. cholerae* challenge assays.

	T6SS+ assay		T6SS- assay	
Challenger isolate	Predator	Challenger	Predator	Challenger
Vibrio coralliilyticus				
Vibrio shilonii				
Vibrio harveyi B392				
Vibrio sp. SWAT3				
Pseudoalteromonas sp. Tw7				
Pseudoalteromonas sp. Tw2				
Alteromonas Alt-SIO				
Pseudoalteromonas flavipulchra				
Halomonoas sp.				
Pseudomonoas sp.				
Psychrobacter aquimaris				
Flavobacterium sp. BBFL7				
Salgentibacter sp.				
Aequorivita sp.				
Roseivirga sp.				

*Predators, T6SS$^+$ or T6SS$^-$ *V. cholerae* were challenged against marine bacterial isolates in 4 h competition assays. Predator and challenger were both recovered. Isolates that yielded at least one log-fold less ($p < 0.01$) of recovered colony forming units after the assays were scored as "killed" (grey boxes).

= Killed

Supplementary information

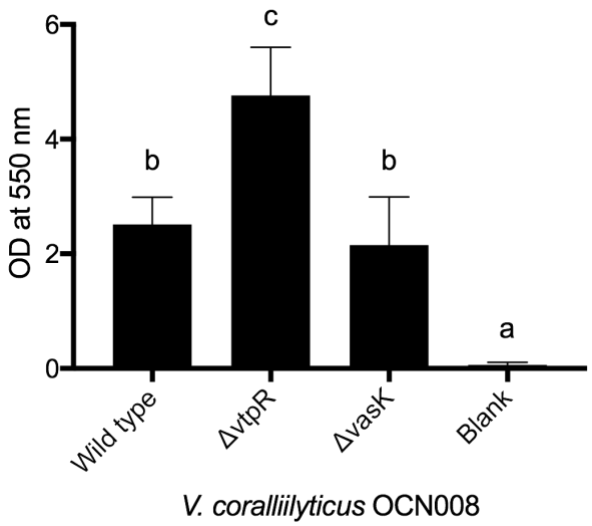

Figure S4.1 *V. coralliilyticus* OCN008 biofilm assay. A crystal violet assay was run to measure the amount of biofilm mass produced by wild type *V. coralliilyticus* and the ΔvtpR and ΔvasK mutant strains. Blank = marine broth with no *V. coralliilyticus* cells. Higher optical density (OD) values at 550nm indicates more biofilm (extracellular polysaccharide) production. Statistical differences between treatments are denoted by different letters (ordinary one–way ANOVA, $\alpha = 0.05$; $p < 0.0001$, Tukey's multiple comparison test, a, b, c).

Table S4.1 Marine bacterial challenger strains used in this study.

Phylum, class	Order	Genus, species, strain	Description	Source/citation
Ɣ-Proteobacteia	Vibrionales	*V. coralliilyticus*	Coral pathogen; Rf^R	(Rypien et al. 2010)[10]
		Vibrio shilonii AK1	Coral pathogen; Rf^R	(Kushmaro et al. 1996)[69]
		Vibrio harveyi B392	Free-living and marine organism associated bacterium; Rf^R	(Byers & Meighen 1985)[70]
		Vibrio sp. SWAT3	Particle-attached bacterium, isolated from Scripps Pier, CA; Rf^R	(Long & Azam 2001)[9]
	Alteromonadales	*Pseudoalteromonas* sp. Tw7	Particle-attached bacterium, isolated from Scripps Pier, CA; Rf^R	(Bidle & Azam 2001)[71]
		Pseudoalteromonas sp. Tw2	Particle-attached bacterium, isolated from Scripps Pier, CA; Rf^R	(Bidle & Azam 2001)[71]
		Alteromonas Alt-SIO	Free-living bacterium, isolated from Scripps Pier, CA; Rf^R	(Pedler et al. 2014)[72]
		Pseudoalteromonas flavipulchra 2ta6	Coral associated bacterium that exhibits high antagonism towards other bacteria; Rf^R	(Rypien et al. 2010)[10]
	Oceanospirillales	*Halomonoas* sp. 73	Isolated from Mariana Trench benthic boundary water; Rf^R	(Peoples et al. 2018)[73]
	Pseudomonadales	*Pseudomonoas* sp. 28	Isolated from Mariana Trench sediment; Rf^R	(Peoples et al. 2018)[73]
		Psychrobacter aquimaris	Isolated from the South Sea in Korea; Rf^R	(Yoon et al. 2005)[74]
Bacteroidetes	Flavobacteriales	*Flavobacteria* sp. BBFL7	Isolated from Scripps Pier, CA; Rf^R	(Bidle & Azam 2001)[71]
		Salgentibacter sp. 1	Mariana trench water column; Rf^R	(Peoples et al. 2018)[73]
		Aequorivita sp. 97	Mariana trench sediment; Rf^R	(Peoples et al. 2018)[73]
	Flammeovirgacea	*Roseivirga* sp. 121	Mariana trench sediment; Rf^R	(Peoples et al. 2018)[73]

*Abbreviations: Rf^R = resistant to rifampicin.

Table S4.2 Conjugation strains and plasmids used in this study.

ID	Description	Citation or source
E. coli β3916	Conjugation strain; Δ*dapA*::(*erm-pir*); Km^R, Em^R, Tc^R	(Le Roux et al. 2007)[75]
E. coli π3813	Conjugation strain; Δ*thyA*::(*erm-pir*); Em^R	(Le Roux et al. 2007)[75]
pSW4436T	Base plasmid for suicide vectors that carries an inducible *ccdB* selectable marker; Cm^R, Sp^R, Sm^R	(Le Roux et al. 2007)[75]
pBU226	Suicide vector used to delete the *vtpR* homolog in OCN008; Cm^R, Sp^R, Sm^R	This study
pBU246	Base plasmid for inducible expression plasmids used to complement *V. coralliilyticus* deletion mutants; Cm^R, Sp^R, Sm^R	(Ushijima et al. 2018)[45]
pBU247	Suicide vector used to delete the *vasK* homolog in OCN008; Cm^R, Sp^R, Sm^R	This study
pBU266	Suicide vector used to delete the *vtpA* homolog in OCN008; Cm^R, Sp^R, Sm^R	This study
pBU267	Suicide vector used to delete the *vtpB* homolog in OCN008; Cm^R, Sp^R, Sm^R	This study
pBU270	Inducible expression plasmid used to express a wild type copy of *vasK* in OCN008; Cm^R, Sp^R, Sm^R	This study
pBU271	Inducible expression plasmid used to express a wild type copy of *vtpR* in OCN008; Cm^R, Sp^R, Sm^R	This study

Table 4.3 DNA oligonucleotide primers used in this study.

Primer name	DNA sequence (5' → 3')	Source or citation
pSW4426T-MCS-F	CTCAACGGGAATCCTGCTCTGCGAG	(Ushijima et al. 2016)[46]
pSW4426T-MCS-R	ACTGCTTGGTGCCAGCCAATGAG	(Ushijima et al. 2016)[46]
008-vtpR-up-EcoRI-F	ATATATGAATTCACGAGAAGGCTTATCAAGCAGCGTA	This study
Vcor-vtpR-up-OEX-R	ACTTGTAGATGCAAAGCTTAGCTATAGAATCCATAGTTATATTTCCTTG	This study
Vcor-vtpR-down-OEX-F	GGATTCTATAGCTAAGCTTTGCATCTACAAGTAGATTAACCAGTGTCAT	This study
008-vtpR-down-XbaI-R	ATGGTGAGAAAGCAGGTCTAGAAATTGATGAG	This study
008vasK-up-EcoR1-F	ATATATGAATTCTCCTTCCGTACCGGGTGGTAT	This study
008vasK-up-OEX-R	ATAGGTCGATGGTTTCTATAATATTTTTTAGCATAGTTATTCAGCCA	This study
008vasK-down-OEX-F	GCTAAAAAATATTATAGAAACCATCGACCTATAAAAAAGTAAACTTA	This study
008vasK-down-XbaI-R	ATATATTCTAGATCCACGCCGAGCAAACTACAAG	This study
vtpA-up-EcoRI-F	ATATATCGAATTCATTCGGCAATCATAAAGGCACAGGCTGT	This study
vtpA-up-OEX-R	AGTCTAATCTTAGTGTCATTTGACGTTGTTTCATTTTACTTTCCTGTT	This study
vtpA-down-OEX-F	GAAACAACGTCAAATGACACTAAGATTAGACTAATAAAAAAACACAAC	This study
vtpA-down-SpeI-R	ATATATACTAGTCTGGTTCTCTGCGGCCTTGCCATCTCTTTT	This study
vtpB-up-SpeI-F	ATATATACTAGTTACGTACCAAGTTTGGTTTAGGCCAGTTATT	This study
vtpB-up-OEX-R	AGTTGGCTTTGATGAAACGCTTGGCTATTTTCATTATGATTCTCCTT	This study
vtpB-down-OEX-F	GAAAATAGCCAAGCGTTTCATCAAAGCCAACTAATCCATTCTAA	This study
vtpB-down-SpeI-R	ATATATACTAGTTTGATGGTGCGATCTGGCTGGATACC	This study
vasK-XbaI-F	ATATATTCTAGAAGTCGTGGCTGAATAACTATGCTAAAAAATATTAT	This study
vasK-XbaI-R	ATATATTCTAGATTATAGGTCGATGGTTTCGGGTAGAGAGAAGTTAT	This study

Table S4.4 Comparison of *V. coralliilyticus* T6SS-associated proteins to select *V. cholerae* proteins.

V. cholerae T6SS protein	OCN008 homolog	OCN014 homolog	BAA-450 homolog	RE22 homolog	RE98 homolog	General protein function
VasA (VCA0110)	ERB64088 (43%)	AIS57250 (43%)	EEX32046 (43%)	KPH23943 (43%)	AIW21233 (43%)	Structural
VasK (VCA0120)	MH794511 (24%)	AIS57248 (24%)	WP_039952112 (24%)	KPH23940 (24%)	AIW21236 (24%)	Structural
VipA (VCA0107)	ERB64085 (55%)	AIS57253 (55%)	EEX32049 (55%)	KPH23946 (55%)	AIW21230 (55%)	Structural
VipB (VCA0108)	ERB64086 (69%)	AIS57252 (69%)	EEX32048 (69%)	KPH23945 (69%)	AIW21231 (69%)	Structural
Hcp-1* (VC1415)	ERB62208 (55%)	AIS57260 (55%)	EEX32057 (55%)	KPH23954 (55%)	AIW21222 (55%)	Structural
Hcp-2* (VCA0017)	ERB62208 (55%)	AIS57260 (55%)	EEX32057 (55%)	KPH23954 (55%)	AIW21222 (55%)	Structural
VasH (VCA0117)	ERB65234 (42%)	AIS57262 (42%)	EEX32059 (42%)	KPH23956 (42%)	AIW21220 (42%)	σ^{54} activator
VasF (VCA0115)	ERB64099 (37%)	AIS57243 (37%)	EEX32037 (37%)	KPH23935 (37%)	AIW21241 (37%)	Effector translocation
VgrG-2* (VCA0018)	ERB64077 (34%)	AIS57259 (34%)	EEX32056 (34%)	KPH23953 (34%)	AIW21223 (34%)	Effector
VgrG-3* (VCA0123)	ERB64077 (32%)	AIS57259 (32%)	EEX32056 (32%)	KPH23953 (32%)	AIW21223 (32%)	Effector

More than one *V. cholerae* homolog is most similar to multiple homologs in *V. coralliilyticus

Table S4.5 Comparison of *V. coralliilyticus* T6SS-related proteins to OCN008 proteins.

OCN008 protein	OCN014 homolog	BAA-450 homolog	RE22 homolog	RE98 homolog
VasA (ERB64088)	AIS57250 (99%)	EEX32046 (100%)	KPH23943 (99%)	AIW21233 (100%)
VasK (MH794511)	AIS57248 (99%)	WP_039952112 (99%)	KPH23940 (99%)	AIW21236 (99%)
VipA (ERB64085)	AIS57253 (100%)	EEX32049 (100%)	KPH23946 (100%)	AIW21230 (99%)
VipB (ERB64086)	AIS57252 (100%)	EEX32048 (100%)	KPH23945 (100%)	AIW21231 (99%)
Hcp (ERB62208)	AIS57260 (100%)	EEX32057 (100%)	KPH23954 (100%)	AIW21222 (100%)
VasH (ERB65234)	AIS57262 (99%)	EEX32059 (99%)	KPH23956 (99%)	AIW21220 (99%)
VasF (ERB64099)	AIS57243 (100%)	EEX32037 (100%)	KPH23935 (100%)	AIW21241 (100%)
VgrG (ERB64077)	AIS57259 (100%)	EEX32056 (99%)	KPH23953 (99%)	AIW21223 (99%)

Chapter 4, in full, has been submitted for publication of the material. Guillemette, R., Ushijima B., Jalan M., Hase C., and Farooq Azam. Insight into the resilience and susceptibility of marine bacteria to T6SS attack by *Vibrio cholerae* and *Vibrio coralliilyticus.* The dissertation author was the primary investigator and author of this material.